INTERGRATED WATER RESOURCE MANAGEMENT FOR BUNG BORAPHET

INTRODUCTION

Bung Boraphet is located in Nakhon Sawan Province and covers the area of around 212 km^2. It is considered as the largest fresh water lake and wetland system in Thailand. According to its significant biodiversity value, Bung Boraphet was therefore registered as an important international wetland for ecological system and biodiversity in 1999 by the Office of Natural Resources and Environmental Policy and Planning (ONEP, 2002). At present there are around 30,000 people living in the conservation zone (Rural Development Information Center, 2005) and using its resoureces as the main source of income. Natural resources of the lake are therefore deteriorated dramatically. This is especially for water resource that has been over-use for paddy farm in the dry seasons and has the effect on ecological system of the wetland. Water quality of the lake has been also degraded by the over use of pesticide, insecticide, and chemical fertilizer by people who live in its basin as well as sedimentation occurring in the lake. Moreover, there are many stakeholders - such as Fisheries Department (FD), The Royal Irrigation Department (RID), Department of Water Resources (DWR), Natural Park, Wildlife and Plants Conservation Department (DNP), Local Government Agencies, and local people – have been using and managing the lake without integrated policy for its sustainability. To overcome these problems, the efficient water resource and water quality management is urgently needed. Profound investigation for an understanding of changes in water quantity and water quality from past to present of the lake is therefore one of the main objectives in this dissertation and will bring useful information to identify the future of the lake. A daily water budget model, a two dimensional depth averaged water quality model, and changes of physical characteristics using remote sensing technique will be provided as the useful tools and information for finding the suitable guidelines for water resource and water quality management of the lake.

OBJECTIVES

1. To make an understanding about the problems facing Bung Boraphet, especially for water resource situation.

2. To prepare daily water budget model to be used for water resource management of Bung Boraphet.

3. To evaluate the present water quality situation and to identify the critical water quality parameters in Bung Boraphet.

4. To investigate changes of physical characteristics in Bung Boraphet and its surroundings correlating water quantity and quality of the lake.

5. To apply the water budget and water quality models for demonstrating and identifying advantages and disadvantages of management operations carrying out by different government agencies.

SCOPES

1. Secondary data relating the problems and situations - especially for water resource - of Bung Boraphet will be collected from reports, database, internet, dissertations, and publications.

2. Primary data of hydrological budget parameters for daily water budget analysis will be collected in and around Bung Boraphet during study period. These parameters include inflow, outflow, direct rainfall over the lake surface, and seepage loss. Rating curves for inflow and outflow points of the lake will be prepared to provide inflow and outflow data using water level data that will be also collected.

3. Secondary data of hydrological budget parameters for daily water budget analysis will be collected from related government agencies. These data comprise daily lake level collected at the regulator carried out by the Local Fisheries Department, and daily pan evaporation collected at Muang Nakhon Sawan carried out by the Meteorological Department.

4. Since physical characteristics in Bung Boraphet and its surroundings correlates closely to its water quantity and quality, changes of the lake's physical characteristics will be therefore investigated using Landsat5 images collected at a specific lake level in the last 10 years. Correlation between physical characteristics, and water quantity and quality of the lake, will be clarified and used to set appropriated recommended measures.

5. To collect primary water quality parameters - such as DO, BOD, suspended sediment, and nutrient - that can be used to specify the situation of Bung Boraphet during study period. Historical secondary data of these parameters will also be collected from the Pollution Control Department to investigate water quality trend. Primary and secondary water quality parameters that have been collected will be investigated for their situations and trends. The critical parameters that would significantly affect the well being and sustainability of the lake will be chosen for further investigations.

6. According to a large area of the lake surface, the critical parameters at each location for particular time can be different. Spatial and temporal variation of the critical parameters will be therefore investigated using primary data of water quality parameters as well as hydraulic parameters which are discharges at inflow and outflow points of the lake, lake levels, and flow velocity at some observed locations in the lake. This study was carried out using the hydrodynamic model (RMA2) and the water quality model (RMA11), which are the two-dimensional depth averaged models without considering vertical variations of hydraulic and water quality changes according to shallow lake levels within 5 m in the usual wet seasons. The models will

be also used to simulate possible scenarios of future changes in the critical parameters of the lake and then control measures will be therefore recommended.

7. Results gained in this study will be used to prepare suitable and practical measures for controlling water quantity and quality for sustainability of the lake.

LITERATURE REVIEW

1. Study Area

1.1 Physiography and background

Bung Boraphet is Thailand's largest freshwater wetland. It is located in Nakhon Sawan Province between the latitude 15^0 40' N and 15^0 45' N and between the longitude 100^0 10' E to 100^0 23' E. The location and catchment area of the lake are shown in Figure 1. The catchment area of the lake of around 4,288 km^2 is located in the provinces of Nakhon Sawan, Pichit and Lopburi. Klong Tatako and Klong Bon are the two main tributaries which have the catchment areas of 3,141 and 1,124 km^2, respectively (RID, 2003). The principal water surface inflows to Bung Boraphet can be separated into 3 sources, which are:

a. Runoff from watershed area via the main tributaries consisting of Klong Bon, Klong Tatako and the irrigation canals,

b. Direct rainfall on the lake surface,

c. Diversion or overland flow from the Nan River during flooding period.

The water level records in the lake show that there are 11 years within 13 years of the record (1993-2006) that the water levels above the weir crest. Flood waters, mainly originated from the inflow of its catchment, were spread to the eastern and northern parts of the lake (Ponvilai, 1982). In some years when extreme floods occurred in the Nan River, flood waters were diverted to the lake and caused severe floods in its surrounding areas (RID, 2003).

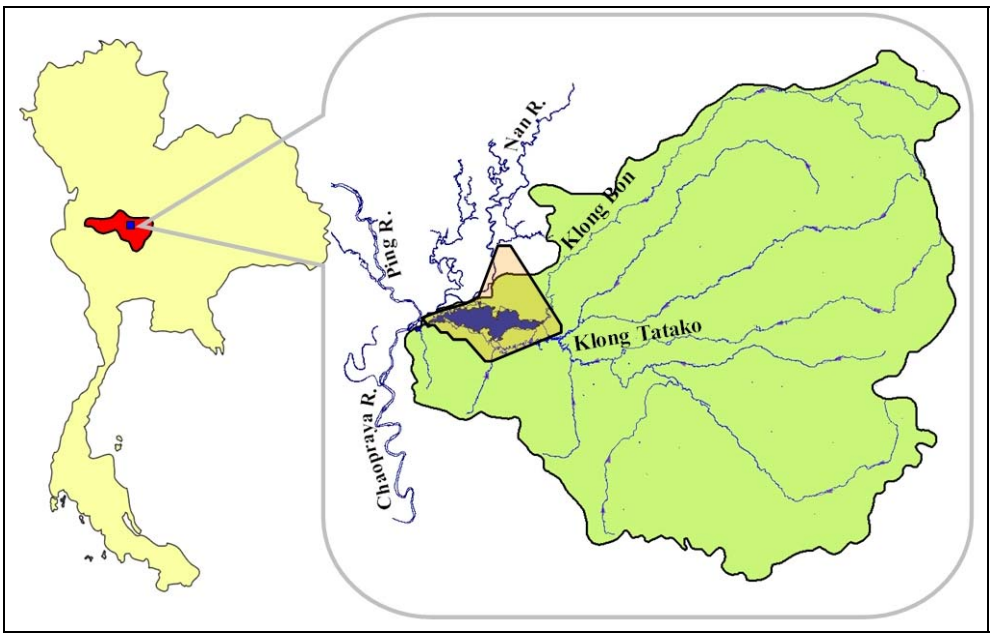

Figure 1 Bung Boraphet Wetland in Nakhon Sawan Province, Thailand

Bung Boraphet development was originated in 1927 by the constructions of a weir and a regulator to provide fish habitat and conservation area for birds and wildlife. However, these constructions have caused permanently flooded some of the wetland. In 1937, Thai Government announced the area of 212 km^2 in Bung Boraphet and its surroundings to be a conservation zone. In 1947, the Agricultural Ministry separated the fish conservation area into two zones. Fishing was prohibited in the first zone of around 62 km^2. However, it was allowed, using appropriate equipment, in the second zone, which has an area of around 150 km^2. The weir was raised a further 0.20 meter in 1993 to the current level of +24.00 m (MSL). At full storage, Bung Boraphet now has a surface area of 148 km^2 and a storage volume of 178 MCM (RID, 2003).

Presently, Bung Boraphet and its catchment have been managing by many government agencies that have been using different regulatory approaches to protect the well-being of the lake such as creating non-hunting zones, announcing the fish conservation areas (FD), and recommending the minimum level (+23.00 m. MSL) (FD). However the distinct evidences of lake deterioration, such as reduced of fish

and bird species, diminished fishery yield, and poor water quality (RID, 2004), show the failure in these management method.

An illegal settlement in the conservation area by more than 30,000 local people (Rural Development Information Centre, 2005) is considered as the most impact causing the lake degradation, especially in water resource issue. Local farmers usually produce two rice crops by using stored water from the lake during the dry season. Therefore, abstraction of water from the lake to irrigate rice farms has drawn the lake water below the recommended minimum level recommended by the Fisheries Department for sustaining fishery resource. The historical record of the lake level show that average annual minimum level between 1993 and 2001 was +22.35 m (MSL) but between 2002 and 2006 the water level fell to +21.41 m (MSL) (FD, 2005). Not only this problem has brought the conflict between the stakeholders, but also threatens the biodiversity and ecosystem integrity of lake.

1.2 Meteorological characteristics

The meteorological data used for this study have been continuously recorded at the nearest meteorological station located at Muang Nakorn Sawan, that is approximately 10 km west of Bung Boraphet. Monthly historical data of important meteorological variables within the 30 years (between 1971 and 2000) are summarized in Table 1 and can be described in the followings.

1.2.1 Temperature: Average monthly temperature varied between 24.6^{o}C and 31.5^{o}C. The minimum and maximum average monthly temperatures occurred in December and April, respectively. Average annual temperature was 28.2^{o}C; while the minimum and maximum averages annual temperatures were 23.3^{o}C and 34.1 ^{o}C, respectively.

1.2.2 Humidity: Average monthly humidity varied between 60% and 82%. The minimum and maximum average monthly humidity occurred in September

and February, respectively. Average annual humidity was 70%; while the minimum and maximum averages annual humidity were 36% and 23 %, respectively.

1.2.3 Pan evaporation: Average annual pan evaporation was 2,018 mm. The minimum and maximum average monthly pan evaporation occurred in October and April with the values of around 126.5 and 243.5 mm, respectively.

1.2.4 Wind speed: Average annual wind speed was 3 knots. The minimum and maximum average monthly wind speed occurred in October and April with the values of around 1.5 and 3.8 knots, respectively.

1.2.5 Rainfall: Average annual rainfall was 1,077 mm. The minimum and maximum average monthly rainfall occurred in January and September with the rainfall depth of around 5.4 and 218 mm, respectively.

1.2 Hydrological characteristics

1.2.1 Rainfall

Historical rainfall data were collected from 3 rainfall stations in Bung Boraphet catchment (station numbers 26102, 26112, and 26032) and 9 stations in nearby areas. The locations of rainfall station and the summary of rainfall data of these 12 stations are shown in Figure 2 and Table 2, respectively. Average annual rainfall depth of these stations during recording periods was around 1,080 mm. The maximum and minimum average annual rainfalls within these 12 stations were recorded at the station numbers 36052 and 19392 with the rainfall depths of around 1,281 and 1,080 mm, respectively. The average rainfall depth during the wet season (May – October) of these stations was around 86.5% of their annual rainfalls. The maximum and minimum average annual rainfall within 3 stations, located in the catchment, were recorded at the station numbers 26102 and 26122 with the rainfall depths of around 1,153 and 1,054 mm, respectively.

Table 1

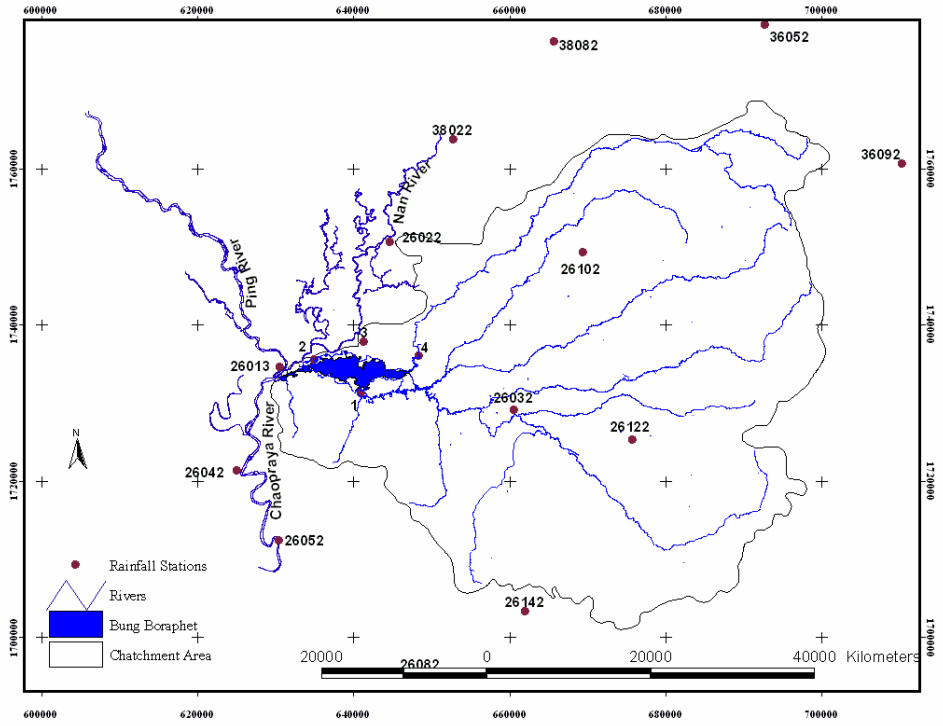

Figure 2 Locations of rainfall stations in Bung Boraphet catchment and nearby areas

Table 2

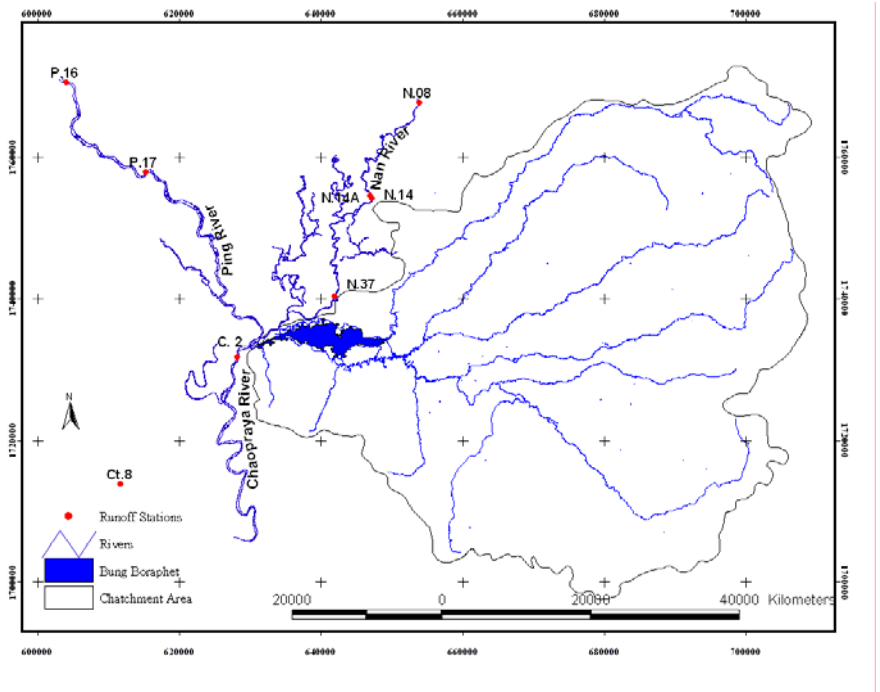

Figure 3 Location of runoff stations in nearby areas of Bung Boraphet catchment

1.2.2 Runoff

Since there is no runoff station located in Bung Boraphet catchment, historical runoff data of 14 stations in nearby catchments, including Ping, Nan, Sakae Krang and Chao Phraya, were therefore collected. The locations of runoff station and the summary of runoff data of these 14 stations are shown in Figure 3 and Table 3, respectively. Average annual runoff and specific yield of the nearest station to Bung Boraphet, N.37, are around 11,341 MCM and 7.53 l/sec/km^2, respectively. However the data collection at the station N.37 was terminated since 1996. After that period, the nearest runoff station has been therefore at the station N.14A, which has an average annual runoff and specific yield around 11,253 MCM and 10.75 l/sec/ km^2, respectively. Average monthly runoff of three stations in the Nan River Basin nearby Bung Boraphet catchment is shown in Table 4. The high flows of these stations normally occur in September and October.

Table 3 Annual runoff data located in Bung Boraphet catchment and nearby areas

Catcht. name	Station Code	Catch. area (km^2)	Range of recorded data	Annual runoff (MCM)			Annual Specific Yield (litre/second/ km^2)
				Average	Maximum	Minimum	
1.Ping	P.16	45,677	1979-1999	6,851.5	11,360.4	4,407.2	4.76
2.Ping	P.17	45,851	1965-1999	7,391.49	12,134.6	4,380.3	5.11
3.Nan	N.53	111	1979-1999	53.52	104.48	23.54	15.29
4.Nan	N.8	32,878	1965-1999	10,287.5	16,313.8	4,785.2	9.92
5.Nan	N.14	33,197	1954-1979	8,978.67	13,266.1	5,142.8	8.58
6.Nan	N.14A	33,182	1978-1995	11,252.7	17,389.9	4,951.80	10.75
7.Nan	N.37	56,214	1968-1996	13,341.4	19,171.9	8,213.3	7.53
8.Sakae Krang	Ct.5A	979	1969-1999	349.56	827.40	72.45	11.32
9.Sakae Krang	Ct.5B	930	1988-1999	408.78	776.67	151.83	13.93
10.Sakae Krang	Ct.4	1,246	1971-1988	307.98	642.48	102.17	7.84
11.Sakae Krang	Ct.7	457	1975-1999	122.39	365.60	3.42	8.49
12.Sakae Krang	Ct.8	3,410	1975-1978	332.25	594.69	38.87	3.09
13.Sakae Krang	Ct.9	522	1977-1999	128.65	397.40	17.67	7.82
14.Chao Phraya	C.2	110,569	1956-1999	22,092.7	37,585.4	10,349.9	6.34

Source: RID (2004)

Table 4

1.3 Land use

Land use patterns within Bung Boraphet catchment can be classified into 5 major different types as summarized in Table 5. Agricultural land covers most of the overall area (around 87%), while the forest areas has only 4.99%. This evidence reveals that land use management of the catchment should be adjusted for the sustainability of the catchment.

Table 5 Land use patterns in Bung Boraphet catchment

No.	Land use	Area	
		km^2	%
1	Agricultural land	3,734	87.08
2	Forest area	214	4.99
3	Residential area	140	3.27
4	Open waters	62	1.44
5	Others	138	3.22
	Total	4,288	100

Source: RID (2004)

2. Related Previous Research

2.1 Water resource and ecological system of Bung Boraphet

Popitak (1970) investigated fish consumption in Bung Boraphet by analyzing the remaining food in their stomach. The data collection was carried out in every 2 months for 1 year period by collecting fish samples from fishermen at every port. The research showed that 22 fish species, such as Sweetlip, Black Shark, Snake Skin Gourami, and Three-spot Gourami, consumed phyto-plankton, and 11 fish species, such as Striped Snaked Head, Giant Snaked Head, and Siamese Tiger, consumed meat.

Nimsomboon (1972) carried out the study on the biodiversity of fish species in Bung Boraphet by investigating fish samples collected from fishermen at every port. The study was carried out every month for 1 year period. Fish species investigated under this study was compared with fish species surveyed by Pinyoying (1969). The comparison showed that fish species had decreased caused by several reasons such as an illegal fishery, water quality contamination by pesticide and insecticide, and an unbalancing food chain.

Office of National Economic and Social Development Board (1983) carried out the study on an aquatic ecological system and fishing in Bung Boraphet. The field data were collected 2 times in the dry and wet seasons for 1 year period. The results showed that the species of aquatic plants, phyto-plankton, zoo-plankton, and fish were 48, 64, 20, and 43 species, respectively. Fish yield at that period was around 5.65 kilogram per rai. The complexity of an ecological system in Bung Boraphet was suitable for biodiversity conservation and eco-tourism promotion.

Promprot (1983) investigated a situation of water quality parameters in Bung Boraphet. Water quality parameters consideration in this study were water temperature, dissolved oxygen, pH, conductivity, and water transparency. Water quality samples were collected every 2 months for 1 year period at 4 locations. These locations were (1) the middle of the lake, (2) Klong Bon inlet (3) Klong Tatako inlet and (4) weir. The results showed that the average values of DO, pH, water temperature, conductivity, and water transparency were 5.6 mg/l, 7.3, 30.3^{o}C, 215.3 umhs/cm, and 121 cm, respectively. Therefore, water quality in Bung Boraphet was suitable for fish and other aquatic animals.

ONEP (1994) developed an environmental and natural resources conservation plan, based on Ramsar wise use criteria, for Bung Bung Boraphet. This study was carried out by a consideration of the situation in Bung Boraphet in term of physical characteristics, biodiversity, and most appropriate conditions for bird habitat. Bung Boraphet was shown to be a complex and dynamic equilibrium ecological system, especially around the lake shoreline. This is because this zone had a particular

characteristic of the transition zone between truly terrestrial ecosystem and truly aquatic ecosystem with complicated food chain that needs to be conserved. The plan that had been developed can be categorized into six different issues which comprised (1) environmental protection zoning (2) land use controlling (3) water resource management (4) lake sustainability management (5) biodiversity management (6) land visualization management and (7) administrative management.

RID (2003) carried out the study on "A Study of Bung Boraphet Development" and prepared the master plan for Bung Boraphet. Planning formulation followed the following steps.

a. To review the related literature and information.

b. To study and analyze the information related to Bung Boraphet for an understanding of its background and problems, and for finding different alternatives to solve the problems.

c. To compare the suitability of each alternative by considering the criteria in engineering, social, environment and economy issues.

d. To develop the project planning for each alternative including cost estimation and Environmental Impact Assessment (EIA).

e. To prepare the master plan for the short-, medium-, and long-term development for Bung Boraphet.

One of the most suitable alternatives is to increase the storage of Bung Boraphet and to stop more settlement in the conservation zone by raising the weir crest for 1 metre (from +24.00 m.MSL to +25 m.MSL) and constructing the dike around the lake.

2.2 Two-dimensional depth averaged hydrodynamic model

Leendertse (1967) used the concept of Hanson (1965) to develop two-dimensional depth averaged hydrodynamic model that can compute flow distribution varying with time around estuaries and coastal area. In this model, the eddy viscosity

is neglected and the velocity distribution in vertical plain is constant. Alternating Direction Implicit Finite Difference Method (ADI) is used to solve the equation system of this model. By using this method for solving the equation system, the model was found to be stable and can be used to simulate the hydraulic characteristics effectively.

Ponce and Yabusaki (1981) adopted the two-dimensional depth averaged hydrodynamic model to investigate the flow patterns in reservoir and extension of cross section in open channel. The effects of wind and earth rotation are neglected in this model and an effective shear stress term is considered in the form $\alpha\left(\partial^2 u/\partial x^2 + \partial^2 v/\partial y^2\right)$, where α is a constant depending on a weighting factor and the grid size. The ADI method is applied in this model. The model simulation was compared with the direct analytical method. The results showed that boundary conditions that have "no-slip" velocity distribution were not significant for vorticity.

Chirananont (1983) adopted the two-dimensional depth averaged hydrodynamic model, that is similar to the model developed by Ponce and Yabusaki (1981), to investigate flow distributions around the area connecting between Songkhla Lake and its tributaries. The model parameters were adjusted until the results which are flow velocity and water depth closed to the measurement in the physical hydraulic model. It was found that the effective shear stress had most effect on the model simulation of flow characteristic.

Stoscheck and Matheja (2000) studied the sensitivity of numerical solving techniques in the MIKE21 model and RMA2/SED2DWES model for simulating the hydrodynamics and sediment transport in tidal environments of the Bremen habour. Model calibration and validation were based on velocity and water level data attained at 2 locations during three week flood event. The model results show only slight difference of simulating water levels (max ±2 cm) for both the RMA2 and MIKE21 models. The differences of velocity distribution between recorded data and both two models are distinct visible around slack water area where

has low momentum and mass transport. For sediment transport simulation, both models show extreme influence of model boundaries. Therefore, the distance between boundaries and interested area should be more than 2 times the range of tidal sediment movement. By applying these two models for hydrodynamic and sedimentation transport investigations, it can be concluded that both models are difficult to use, however they can provide necessary functionality to handle the systems. For the model usages, the MIKE21 model seems to be more stable than the RMA2 model. However the RMA2 model has shown its flexibility to handle flow simulation around hydraulic structures better than the MIKE21 model.

Finnie *et al.* (1999) claimed that curving flow in a river usually develops the secondary flow which is considered as a small flow superimposed on a primary or larger flow. The secondary flow is responsible for deposition and eroding sediment on the inside and outside of the curve, respectively. When applied the depth average model, RMA2, to this flow pattern, the model predicted unrealistically high velocity on the inside of the curve. In this study, the effect of secondary flow was therefore solved by converting the vorticity term in the transport equation to acceleration term according to secondary current. After the secondary flow was added into RMA2 model, the model was compared with experimental data from the Riprap Test Facility at the U.S Army Engineering WES. It was found that the secondary flow correction improved simulation results of flow velocity. However, the improvements were smaller in the first 90°c of the curve. Therefore, the additional work is required to improve the model efficiency.

Srithongsom (2003) applied the two-dimensional depth averaged hydrodynamic and water quality model developed by Jirananon (2001) to investigate BOD and DO for Bung Boraphet. The governing equations of the model base on Navier-Stoke equations of the continuity and mass balance equations. The Alternating Direction Implicit Finite Difference Method (ADI) was used to solve the equation system. In model application, Bung Boraphet shape was simplified using 200x200 m grid size and the overall 39x99 grids. The results of model calibration showed that the roughness coefficient (Manning's n) of Bung Boraphet was between

0.025 and 0.035, while the diffusion coefficient in the vertical and horizontal direction is 90 sq m/sec. The overall results are not highly satisfied for predicting flow velocity, and water quality parameters. Prediction errors mainly caused by an accuracy of flow velocity recorded data, simulating difficulties of various lake characteristics, and the model assumption with neglecting some processes affecting the oxygen concentration (e.g. photosynthesis and respiration of macrophyte and phytoplankton, nutrient decomposition, and sediment oxygen demand).

2.3 Two-dimensional depth averaged water quality model

Liengcharernsit (1979) developed the finite element model of two-dimensional hydrodynamic and water quality and applied for the Upper Gulf of Thailand. The governing of hydrodynamic model is based on the conservation of mass and momentum equations, while the water quality model is based on the mass balance in the vertical direction. The considered water quality parameters in this model consist of salinity, coliform bacteria, mercury, phyto-plankton, BOD and DO. In the model application, averaged flow and concentration of constituents at the Chao-Phraya estuary were used as the boundary condition of the model. The results showed that the maximum flow velocity in the study area is approximately 0.5 m/sec, while the distribution of water quality parameters is more depended on the influence of current and tidal than the influence of internal reaction.

Falconer and Lin (1997) developed the three dimensional layer integrated model and applied the model to predict water surface elevation, layer averaged velocity components, and water quality - consisting of DO, BOD, salinity, and faecal coliform - in the Hamber estuary, England. Finite difference technique was used to solve the conservation of mass, momentum, and transport equations in this model. Field data measurements consisting of the water surface elevation and flow velocity in three different sites were collected for various tidal ranges to calibrate the hydrodynamic model. Water quality parameters - that were collected at several sites along the estuary for calibrating the water quality model - comprised the concentration of DO, BOD, salinity, organic, ammonia, and nitrate nitrogen. The

study area was simulated using finite element mesh 118x56x8 grid volume with equal horizontal spacing of 500 m in both width and long. The result of hydrodynamic model showed an encouraging compatibility between calculated and measured flow velocity at all observed locations. For the water quality model, the calculated water quality parameters also closed with field measured data for all considered parameters. The model was then applied to investigate the efficiency of the constructed new sewage treatment plant at Hull harbor. The results indicated that this new treatment plant can only reduce faecal coliform along the estuary significantly but it only can improve the quality of DO, BOD, and salinity marginally.

Pinthong (1998) developed the numerical model, including hydrodynamic and water quality models, for predicting the distribution of salinity and water quality parameters in a shallow lake where an influence of tidal occurs. The hydrodynamic model bases on the two dimensional depth averaged momentum and continuity equations, while the water quality model, which was used to predict salinity, DO, and BOD, bases on the conservative of mass equation. The governing equations of the model were transformed into numerical forms by a finite difference scheme. The Alternating-Direction-Implicit (ADI) method was used to solve the equation system. The models were then calibrated and validated by using the data of Songkla Lake. The results showed that calculated velocity is slightly different with the measured data. Meanwhile, root mean square error between calculated and measured data of salinity, DO, and BOD were 0.68, 0.72, and 0.63, respectively. The models were then acceptable and could be used as a useful tool for lake environmental management.

Klashefipour *et al.* (2002) studied the impact of various bacterial inputs into the estuary and surrounding coastal waters on the bathing water quality using faecal coliform as the main water quality indicator. For this kind of the study area, one and two dimensional models should be applied to carry out the problems. The DIVAST (two dimensional hydrodynamic and water quality model) was therefore linked to the FASTER (one dimensional hydrodynamic and water quality model) for conducting this study. These two models were developed by the UK Environment Agency in

1994 and 1999, respectively. The hydrodynamic model was calibrated using water level and velocity measurements observed at three observation points. The simulated water surface elevations and velocities showed good compatibility with the measured values. The average error between the simulated and measured water elevation was about 0.15 m. The average error was less than 0.15 m/s, which was around 20% of the average velocity. For feacal coliform calibration process, the maximum decay rate in the dry season of 2.32/day and the minimum decay rate in the wet season of 0.71/day were applied. The calibrated model was therefore suitable to be applied to investigate the efficiency of the proposed sewage treatment plant and the results showed that the plant can reduce 30% of the overall faecal coliform occurring.

Deas *et al.* (2003) studied the alternatives for controlling flow patterns and water quality in Klamath River that usually have been facing water quality problems of eutophication, nutrient loading accumulation, and low dissolved oxygen. In this study, the RMA2 and RMA11 models were used to simulate the flow velocity and changes of water quality parameters (DO), respectively. The results of hydrodynamic model (RMA2) calibration showed that the range of Manning's n along the river was between 0.025 and 0.055. These values are within the recommended range applied for the sandy streams, cobbles, and boulders (Chow, 1959). For calibrating DO concentration, it was relied on an estimation of BOD concentrations by varying the algal growth and respiration rates. In this study, an initial BOD concentration was set as 2.0 mg/l; while algal growth and respiration rates were set as 2.0 per day and 1.0 per day, respectively. The calibration results showed that the average difference between calculated and measured flow velocity for the RMA2 model was within 20%; while the average difference between calculated and measured DO concentrations for the RMA11 model was within 25%. These models were therefore suitable to be used for setting up the management plan to reduce the impacts of the return flow from agricultural areas along the Klamath River.

2.4 The Water Budget Study

Basso (2000) investigated the effectiveness of evaporation rate reduction by applying the mono-molecular layer on some parts of the Lake Managua, Nicaraguan. The water balance study was therefore conducted for evaluating each hydrological component. The hydrologic components of inflows in this water balance study included the followings: 1) discharge measurements at three main tributaries covering 90% of the total catchment area, 2) computed discharges for non-recording areas (10% of the total catchment area) using the average unit flow (discharge per km^2) of the measured discharge areas, 3) direct rainfall on the lake surface, and 4) groundwater discharge into the lake. However, the groundwater component was neglected because of the flat nature of the basin. The hydrologic component of outflows included the following: 1) regulated surface outflow, 2) ground water outflow (assumed to be zero), and 3) evaporation from the lake. In order to evaluate the accuracy of the water balance computation, calculated and observed lake levels were compared over the study period of 6 years. The comparison results showed a corresponding between calculated and observed water levels with the correlation coefficient of around 0.91. The water balance was then re-computed when a thin chemical film was applied to create mono-molecular layer for retard evaporation from the lake surface. The results of re-calculated water balance showed that a mono-molecular layer can reduce evaporation loss of around 15%.

The U.S. Geological Survey (USGS) (2001) developed the TWDB model to estimate the effects of different fresh water inflow volumes on circulation and salinity in the Nueces Estuary. While the daily inflows of the Nueces Estuary were measured, the daily net outflow was not measured and cannot be computed directly from the data collected at the Nueces estuary exit. Therefore, a daily water budget study of Nueces Estuary, as explained in the following equation, was conducted to estimate the net tidal outflow.

Net tidal outflow = Rainfall + Measured inflow – Evaporation – Volume change

In this study, the daily water budget was carried out during July and October 1998. Inflows from the 2 main tributaries that are the Nueces River and the Rincon Bayou Channel were measured at the stream gauging station numbers 08211500 and 08211503, respectively. Discharges through the Rincon Bayou Channel and Nueces River were affected not only by the freshwater inflows but also by the tidal influences. However, during July and October most inflows are mainly from the inflows of their catchments. Direct rainfall volumes over the Nueces Estuary, with the surface area of around 38 km^2, were computed by the product of its surface area and rainfall depth collected at the same location of runoff gauging station at Rincon Bayou Channel, about 4.8 km upstream of the estuary. In this study, evaporation loss was estimated by two methods. The first method was calculated by using pan evaporation data, collected at the nearest station of the estuary (about 13 mi northwest of Nueces Bay), and then multiplied by a coefficient of 0.7. The second method was calculated using the Penman equation to estimate the potential evaporation. It was found that both methods produced similar monthly evaporation. Total evaporation computed from the pan evaporation method was about 3 percent higher than that computed from the Penman equation. The results of water budget calculation during the study period showed that the average monthly net outflows from the Nueces Bay was around 71,875 acre-feet; while the maximum and minimum values were around 112,700 and 39,100 acre-feet, respectively.

Chekol and Egger (2004) developed the daily water balance model to investigate the hydrologic components of the Lake Ziway located at the Ethiopian Rift Valley, Central Ethiopia. The water balance study was then used as a tool to find out the suitable abstracted water from the lake without disturbing its ecological system. In this study, monthly evaporation was estimated by a multiplication between pan evaporation and the pan coefficients which are varied between 0.7 and 0.85. Areal rainfalls were estimated using the Isohyetal method. Besides analysis of the river flow data from gauging station at Meki town was made and the result showed that the river will actually dry up at some time during the period December to March. The outflows mainly occurred at the several irrigation canals were estimated from the irrigation demand model (Halcrow, 1999). In the model calibration procedure, the

predicted and observed lake water levels were compared. The calibration results were satisfied with a high correlation coefficient of around 0.87. The water balance study revealed that the evaporation from the lake surface was around 85% of the total water coming into the Lake Ziway. Therefore this lake is really needed a suitable technology to reduce its evaporation rate. Alternative sources of water for the irrigated areas around the lake need to be explored.

Hammer (2006) studied the daily water balance of the BiGi Pan Wetland in Suriname, South Africa. During the study period between October 2004 and July 2005, four observation stations were installed. Daily discharges at each location were calculated using measured daily water levels and its rating curve. Rainfalls and evaporations were estimated using the rainfall and pan evaporation data observed at the nearest meteorological station in Nieuw Nickerie. The pan evaporation data was then multiplied by the pan coefficient of 0.7 to be the evaporation rates estimating for the study area. Since clay is the soil material in the Bigi Pan Wetland, the permeability rate is therefore very low. Groundwater exchange is then neglected. The water level was then simulated using a quantitative model, which incorporated the daily datasets of water balance components. Because the lack of rainfall network, the measured data indicated a significantly lower water level at the end of wet season (October and November) compared to the simulated results. However, outside this period, the simulated results correspond to the measured data. The water balance model was applied when it is assumed that the evaporation rate in the wetland increase by 30 percent. It was found that the average water level will be lower 60 cm than the current situation. Therefore, the restoration of mangrove forest should be applied to reduce the evaporation loss.

Tanakamaru *et al.* (1999) studied the water balance of the Lake Toba, North Sumatra, to be used for managing the water resources of the lake. Evaporation rates were estimated by the multiplication between the pan evaporations - observed at the meteorological station located at Medan, about 20 km north of the lake - and the pan coefficients which were varied between 0.72 and 0.85. Mean areal rainfalls were estimated from the rainfall data collected at three rain gauge stations located at the

Siguragura Dam, Tangga Dam, and Janji Matogu. The amounts of rainfalls at the Siguragura Dam and the Tangga Dam, which are located in the steep mountainous areas, were around 2,379 and 2,928 mm/year, respectively. They are a lot higher than the rainfalls of around 1,663 mm/year that was measured at Janji Matogu located near the lake. The monthly mean areal precipitation was obtained by the monthly arithmetic mean precipitation of these three stations and then multiplied by the modification coefficient of 0.839. Secondly, the runoff from the main tributaries, Asahan River, is calculated by the variable infiltration capacity (VIC) water balance model. The regulated outflow of the lake was operated and observed at the Lake's regulating dam. The long-term water levels were then simulated using time series of estimated lake evaporation, areal precipitation and inflow and observed outflow. The accuracy of simulated lake water level was not sufficient due to the inadequacy in quality of estimated areal precipitation and the lack of meteorological data near the lake, but the overall variation of water level including recent declines were represented.

3. Theories

3.1 The theory of the water budget study

3.1.1 The continuity equation of water budget study

A study of daily water budget is a basic procedure for managing reservoir in a sustainable way. The principal of water budget is continuity rule (Warren and Claire, 1985). The continuity equation of water budget study for Bung Bong Boraphet can be expressed in the following equation;

$$\frac{\Delta S}{\Delta t} = \sum I(t) - \sum O(t) + (I_r - ET - SL)A_s \quad (1)$$

where, ΔS is a difference of lake's water volume in one day interval (Δt), $\sum I(t)$ is the total inflow varying in one day, $\sum O(t)$ is the total

outflow varying in one day, I_r is a variation of rainfall depth on the lake surface in one day, ET is a variation of the depth of evaporation from the lake's surface in one day, SL is a variation of the depth of seepage loss in one day, and A_S is the surface area of the lake at a specific water level

3.1.2 An evaluation of average rainfall depth using Thiessen Polygon Method

A rainfall gauging station can measure rainfall depth at one location (point rainfall) and cannot be used as the representative of the rainfall depth over a larger area (normally not more than 14 km^2). However, the equivalent uniform depth (EUD) to be used as the representative of the rainfall depth over a larger area can be calculated using rainfall depths that have been measured at different rainfall stations. The simplest method to determine the EUD is the arithmetic averaging. However this approach will be effective if the rainfall gauging stations are uniformly distributed and the topography of the catchment area is flat. For the catchment area with non-uniform distribution of the rainfall gauging stations, the Thiessen Polygon Method is usually be applied.

Thiessen Polygon method assumes that the recorded rainfall depth at a given rainfall station is applied out to a halfway of distance to the next station in any direction. The weight factor of each rainfall station is determined from the corresponding area of application in a Theissen Polygon network, which is formed by perpendicular bisectors of the straight lines joining adjacent gauging stations (see Figure 4). The equation for determining average rainfall depth by applying Thiessen Polygon method can be shown as the following;

$$\overline{P} = \frac{1}{A}\sum_{n=1}^{n} A_n P_n \qquad (2)$$

where

$\overline{P}$ = Average rainfall depth on the watershed

A = Watershed area

A_n = Subarea of station n created from Thiessen Polygon network

P_n = Recorded rainfall depth at station n

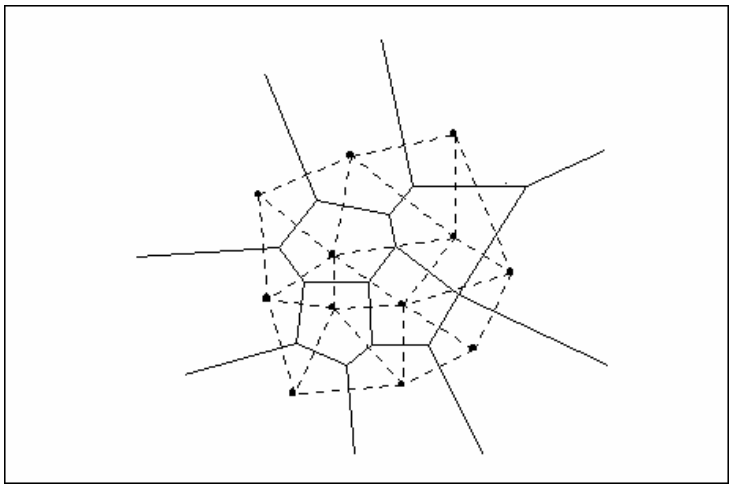

Figure 4. Thiessen Polygon network
Source: Chow *et al.* (1988)

3.1.3 Evaporation

Evaporation is the amount of water that is returned to the atmosphere from the water surface and moist soil. There are several methods used to estimate the amount of evaporation from the free surface. These methods can be grouped into 5 categories including: 1) an energy-budget method, a mass-transfer method, 3) a water budget, 4) an empirical formulae, and 5) evaporation measurement using a pan evaporation (Mutreja, 1986). For this dissertation, the pan evaporation collected from the nearest meteorological station was applied to estimate the evaporation from the lake's surface.

The common type of an evaporation pan is the standard US Weather Bureau Class A pan, which has 1.22 m diameter and 255 mm hdepth (Mutreja, 1986). The water is kept between 50-75 mm below the rim of the pan. Pan

evaporation is evaluated from the change of water level in the pan. To estimate an evaporation rate from the pan evaporation, observed value of pan evaporation has to be multiplied by a pan coefficient which varies with season and location. However, the usual value is around 0.7 (Chow *et al.*, 1988).

3.1.4 A relationship between stage and discharge

According to discharges cannot be measured every day because of economic limitation, the stage-discharge relationship at a particular runoff station is normally produced for discharge estimations. The stage - discharge relationship usually called as "Rating Curve" is developed by measuring the stage simultaneously with measuring of discharge. The coordinates of stages and discharges are then plotted to create a rating curve. Thus, if the stage is known, the discharge can be evaluated from this curve. Generally, if the measured discharge is plotted against the stage, the data will define a parabolic curve as shown in Figure 5 (Mutreja, 1986).

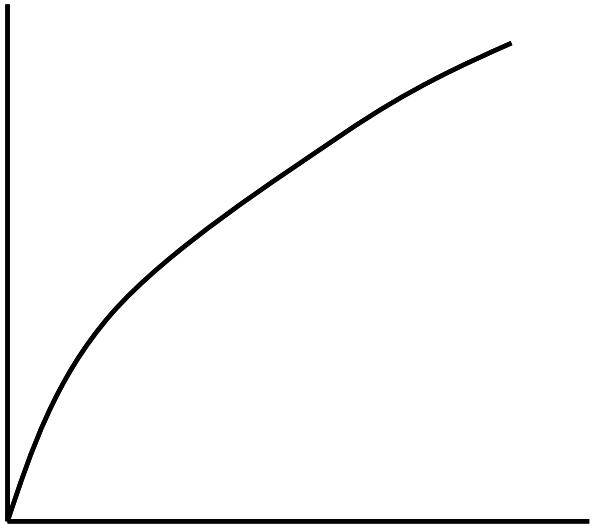

Figure 5 A rating curve

Source: Mutreja (1986)

3.2 Theory and concept of remote sensing technique

Remote sensing is science and art to obtain information of an object, area and phenomena on the earth surface without contacting the object, area, or phenomena under analysis. This technique uses electromagnetic sensors that emit and reflect electromagnetic energy on various earth surface features and these data are analyzed to provide information of investigated resources.

There are two basic processes - data acquisition and data analysis - involved in remote sensing technique. These processes as shown in Figure 6 are explained in the followings.

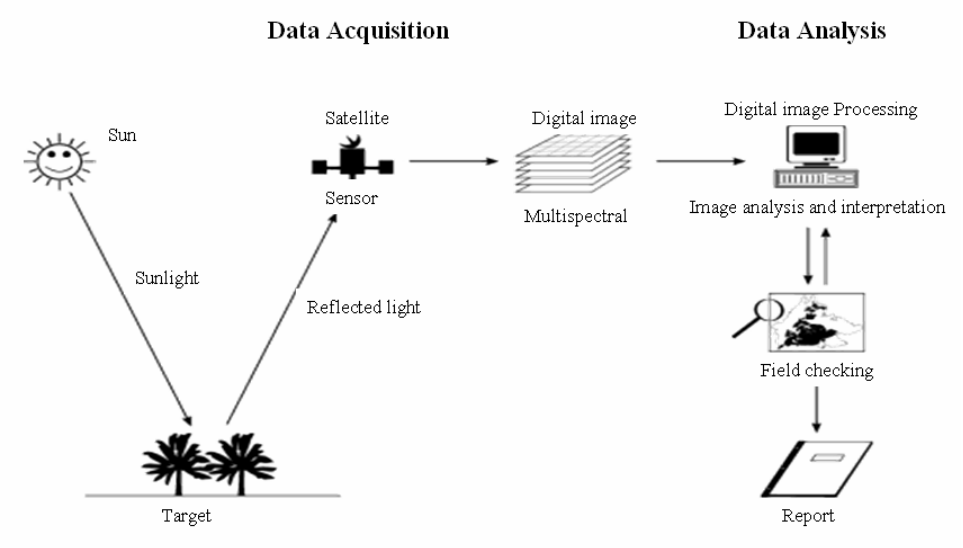

Figure 6 Remote sensing processes
Source: Lillesand and Ralph (2000)

3.2.1 Data acquisition

Data acquisition is the process to obtain data either analog or digital form. The process elements of data acquisition are energy source, propagation of energy through the atmosphere, energy interactions with the earth surface features,

re-transmission in the atmosphere, sending data in analog, and digital form to station ground base station.

Energy source of passive remote sensing is sunlight that is continuous energy in electromagnetic wave form. In remote sensing, it is most common to categorize electromagnetic wave by their wavelength with electromagnetic spectrum (Figure 7). The unit used to measure wavelength is micrometer (μm) that equals $1x10^{-6}$ m.

Electromagnetic spectrum used in remote sensing lies along a continuum characterized by magnitude changes of many power of 10 (Figure 7). The "visible" is an extremely small one, that is sensitive to human eye and extends only from 0.4 μm to approximately 0.7 μm. The color "blue" is approximately range of 0.4 to 05 μm, "green" to 0.5 to 0.6 μm, and "red" to 0.6-0.7 μm. Ultraviolet (UV) adjoins the blue end of visible wavelength. Infrared (IR) waves that have three different categories adjoin the red end of visible region. The three different categories of infrared wave are near IR (from 0.7-1.3 μm), mid IR (from 1.3 to 3 μm), and thermal IR (beyond 3 to 14 μm). A much longer wavelength in spectrum is microwave portion (1 mm to 1 m).

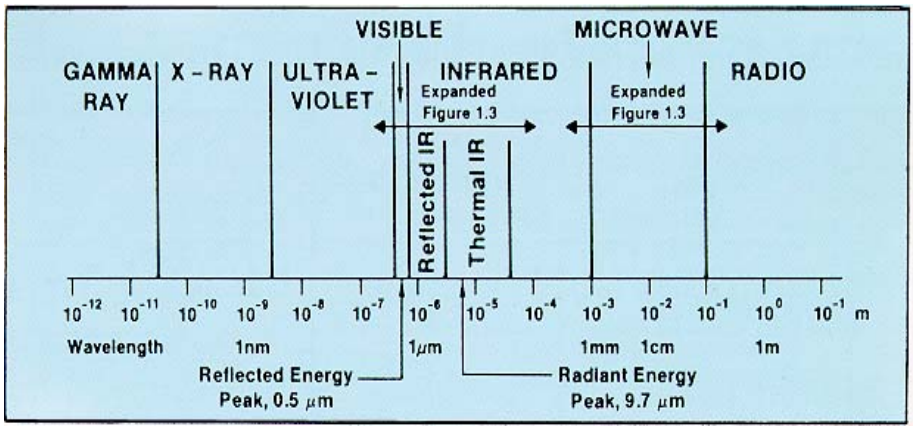

Figure 7 The electromagnetic spectrum
Source: Lillesand and Ralph (2000)

Most remote sensing systems operate in one or several of visible, IR, and microwave portions of the spectrum.

Once Electromagnetic energy is incident on any earth surface features, three energy interactions with that feature are possible. The energy incidents, which are reflected, adsorbed and transmitted, will vary for different earth features, depending on their material type and condition. These differences permit us to identify different feature on an image. Within the visible wavelengths, these variations result in the visual effect called color. For example, the "blue" objects reflect more highly in the blue portion of the spectrum, "green" objects reflect more highly in the green portion of the spectrum. Figure 8 shows typical spectral reflectance curves for three basic types of earth feature: green vegetation, soil, and clear water. The description of reflectance on vegetation, soil and water can be shown as the followings.

1) Vegetation: The pigments in plant leave (Chlorophyll) strongly absorb energy in the wavelength bands centered at about 0.45 and 0.67 μm. Therefore, our eyes perceive vegetation as green color because of very high absorption of blue and red energy and very high reflection of green energy. If a plant is interrupted its normal growth and productivity, it may decrease chlorophyll production. The result is therefore less chlorophyll absorption in blue and red bands. According to this result, the red reflectance will increase and we can see the plant turn yellow.

In near infrared portion (0.7 to 1.3 μm), a plant leaf typically reflects 40 to 50 percent of energy incident upon it. Plant reflectance in this range results from the internal structure of plant leaves. Because this structure is highly variable with plant species, therefore reflectance measurement in this range allow us to identify plant species.

2) Soil: The soil curve in Figure 8 shows less peak and variation in reflectance. The factors affecting soil reflectance are moisture content, soil texture,

surface roughness, presence of iron oxide and organic matter content. The characteristics of soil reflectance depend on these factors. For example, moisture content will decrease its reflectance. Moreover, soil moisture content is strongly related to soil texture. Other two factors that reduce soil reflectance are surface roughness and organic matter content. The iron oxide in soil also decreases reflectance, especially in the visible band.

3) Water: The distinctive characteristic of water is the energy absorption at near IR wavelengths. Therefore, locating water bodies such as lake or river are done most easily in near IR wavelength. However, various contaminations in water bodies manifest themselves primarily in visible wavelengths. For example, turbid water containing large of suspended sediment has much higher reflectance than clear water. Likewise, the reflectance of water changes with the chlorophyll concentration involved. Increasing of chlorophyll tends to decrease water reflectance in blue wavelengths and increase it in green wavelengths. These properties have been used to monitor or estimate the concentration of algae in water bodies via remote sensing data.

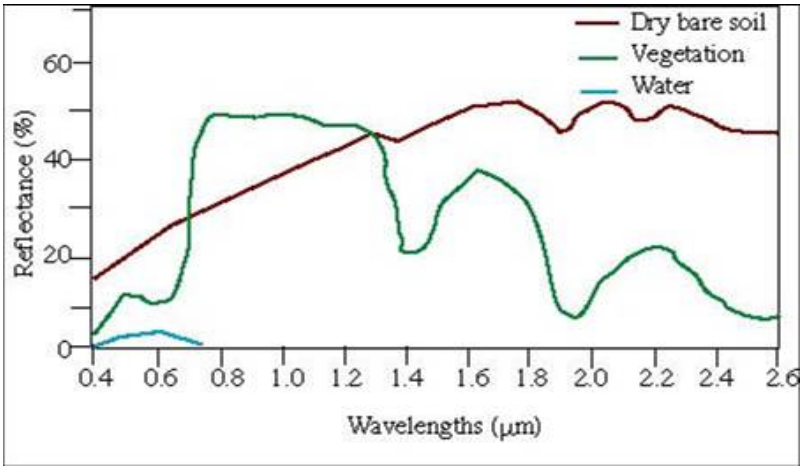

Figure 8 Spectral reflectance curves for vegetation, soil, and water
Source: Swain and Davis (1978)

3.2.2 Data analysis

Data analysis is the process that involves manipulation and interpretation of digital images by using a computer. The processes of data analysis include the computer operation technique that can be described in the followings.

1) Data Preparing

The process involved in data preparing are:

1.1) Wavelengths or bands selection

Hence, any earth surface features have different properties to adsorb and transmit energy incident. Thus, wavelength used for image processing should be related to the objective of the study. For example, wavelengths in green, blue, and near IR portion of spectrum recorded in band 2, 3 and 4 of Landsat5 image are typically used for land use study.

1.2) Image display

Image display is the process to collect data from Computer Compatible Tape (CCT). The data are typically stored in digital format. Before manipulating, these data are therefore changed into hue format for each band. Single color in each band can be overlaid to generate composite color that can help to identify the characteristic of interested objects.

2) Pre-processing

The operations in this process aim to provide and prepare data to more faithful before analytical process. Pre-processing involves the following procedures.

2.1) Radiometric correction

The measurement over the interested objects on the earth surface is usually effected by several factors such as changes in scene illumination, atmospheric conditions, viewing geometry, and instrument response characteristics. In case of satellite image, it is typically needful to generate mosaics of images taken at different times and location. In radiometric correction process, digital image data obtained from different solar illumination angles are adjusted by computing pixel brightness values. Then, pixel values in a scene are divided by the sine of the solar elevation angle for particular time and location to correct the image.

2.2) Geometric correction

Raw digital images normally contain geometric distortions. Therefore they cannot be used as a map base without adjustment process. The geometric correction aims to compensate for the distortions generated from many sources such as variation of altitude, velocity of sensor platform, earth curvature, atmospheric reflection, relief displacement, and nonlinear in the sweep of sensor.

Geometric correction is usually implemented as a two-step, i.e. systematic or predicable distortions, and random or unpredictable distortions.

Systematic distortions are easily corrected by applying formulas derived by modeling the sources of distortions.

Random distortions are corrected by investigating well-distribution of ground control points (GCPs) in an image. GCPs are known location that can be located on the digital imaginary such as highway intersections and distinct shoreline or river features. In the correction process, GCPs are located both in two image coordinates that are on the distortions image and ground coordinate (typically measured form map, in term of UTM coordinates). The distortions images are then corrected by statistical adjustment from the differences of these two coordinate systems.

2.3) Image Enhancement

The aim of image enhancement is to improve the visual of an image for interpretability by increasing the apparent distinction between features in the scene. Enhancement techniques can be categorized as point and local operations. Point operation is the process to independently improve the brightness value of each pixel in an image. Local operation improves the value of brightness of each pixel based on neighboring brightness value. Enhancement operations can be implemented on single band or multi-image composition bands. The resulting of this process may be recorded or display in black and white or in color. Enhancement operations normally applied to image data after the geometric and radiometric correction.

3) Image Classification

The aim of image classification is to categorize all pixels in an image into land cover classes. Generally, multispectral data (multi bands) are used to perform the classification. The two basic processes involved to classify the land covers from multispectral image are supervised classification and unsupervised classification. The descriptions of these procedures can be shown in the followings.

3.1) Supervised classification

In this procedure, the pixels are categorized by specify the algorithm and numerical data according to various land cover types present in a scene. Normally there are three steps, as shown in the following descriptions, involved in supervised classification.

3.1.1) Training stage

In this stage, the analyst can identify the representative known land cover types as sample site called training area. These areas

are used to compile the numerical data in of spectral attributes for each interested land cover types in the scene.

3.1.2) Classification stage

After the training areas have been identified, each pixel in the image data is categorized to land cover types. If some pixels are not similar to any training area set, they are usually labeled as “unknown” or “null” area. Every pixels categorized by this process are then recorded in the interpreted section called “output stage”.

3.1.3) Output stage

The results of image classification procedure may be recorded in the several forms. Normally output products presented in three forms are thematic map, table of statistics for various land cover classes, and digital data file.

3.2) Unsupervised Classification

Unsupervised classification procedures do not need the training stage operation for classification. In this process, unknown pixels are aggregated into a number of classes based on natural grouping in the image values. According to the category based on natural grouping, the identification of spectral classes can not be initially known. Therefore the analyst has to compare the classified data with reference data to identify the land cover types of the spectral classes.

3.2.1) Classification strategies

a. Minimum distance to means classifier

The mean spectral values in each band are computed for each category. These values comprise the mean vector for each category. The unknown pixel can be classified by computing the distance (vector) between the unknown value and each of the category means. After computing the distances, the unknown pixel is identified to the closest category mean. If the pixel value is farther than any defined distances of these category means, it will be classified as unknown value.

However, this strategy is insensitive to different degrees of variance in the response data, therefore it is not favorable used in application that spectral classes are close to one and other and have high variance.

b. Parallelepiped classifier

Each category can be defined by the highest and lowest digital vales in each band and show as a rectangular in scatter diagram. An unknown pixel can be classified by category range or decision region. If the unknown pixel lies outside all ranges or decision regions, it will be classified as unknown. The advantage of the strategy is very fast and efficiently for computation.

However, if unknown pixel lies in the overlap region of any two categories, it will be classified as “not sure” or be arbitrarily placed in one of the two overlapping classes.

c. Gaussian maximum likelihood classifier

Maximum likelihood classifier determines both the variance and covariance of the category when classifying an unknown pixel. In this process, the distribution of point values forming the category is assumed to be Gaussian or normal distribution. For this assumption, the distribution of a category can be described by the both mean vector and covariance matrix. The unknown pixel is classified by probability density function. After computing the probability of each

category, unknown pixel will be assigned to the most likely class. If the unknown pixel values are all below threshold sets of category, it will be labeled as unknown.

3.3 Theory and concept of the RMA2 Model

RMA2 was developed by Norton, King and Orlob in 1973 (U.S. Army Crop of Engineers, 1997). It is a two-dimensional depth averaged hydrodynamic model and can be used to compute water surface elevations and horizontal velocity components for sub-critical and free-surface two-dimensional flow fields.

3.2.1 Governing Equation

The computations of water surface elevation and horizontal velocity component are solving the depth-integrated equations of mass and momentum conservation in two horizontal directions. The forms of the solved equations are shown in the following equations.

Conservation of momentum

$$h\frac{\partial u}{\partial t} + hu\frac{\partial u}{\partial x} + hv\frac{\partial u}{\partial y} - \frac{h}{\rho}\left(E_{xx}\frac{\partial^2 u}{\partial x^2} + E_{xy}\frac{\partial^2 u}{\partial y^2}\right) + gh\left(\frac{\partial a}{\partial x} + \frac{\partial h}{\partial x}\right) + \frac{gu\,n^2}{\left(h^{1/6}\right)^2} + \left(u^2 + v^2\right)^{1/2} - \zeta V_a^2 \cos\psi - 2h\omega v \sin\phi = 0 \quad (2)$$

$$h\frac{\partial v}{\partial t} + hu\frac{\partial v}{\partial x} + hv\frac{\partial v}{\partial y} - \frac{h}{\rho}\left(E_{yx}\frac{\partial^2 v}{\partial x^2} + E_{yy}\frac{\partial^2 v}{\partial y^2}\right) + gh\left(\frac{\partial a}{\partial y} + \frac{\partial h}{\partial y}\right) + \frac{gv\,n^2}{\left(h^{1/6}\right)^2} + \left(u^2 + v^2\right)^{1/2} - \zeta V_a^2 \sin\psi - 2h\omega v \sin\phi = 0 \quad (3)$$

Conservation of mass

$$\frac{\partial h}{\partial t} + h\left(\frac{\partial u}{\partial x} + \frac{\partial v}{\partial y}\right) + u\frac{\partial h}{\partial x} + v\frac{\partial h}{\partial y} = 0 \quad (4)$$

where

h	=	Water depth,
u, v	=	Velocities in the Cartesian directions,
x, y, t	=	Cartesian coordinates and time,
ρ	=	Density of fluid,
E	=	Eddy viscosity coefficient,
		for xx = normal direction on x axis surface,
		for yy = normal direction on y axis surface,
		for xy and yx = shear direction on each surface,
g	=	Acceleration due to gravity,
a	=	Elevation of bottom,
n	=	Manning's roughness n-value,
1.486	=	Conversion from SI (metric) to non-SI units,
ζ	=	Empirical wind shear coefficient,
V_a	=	Wind speed,
ψ	=	Wind direction,
ω	=	Rate of earth's angular rotation,
Φ	=	Local latitude.

Equations (2), (3), and (4) are solved by the finite element method using the Galerkin Method of weighted residuals. The elements may be one-dimensional channel reaches, or two-dimensional quadrilaterals or triangles, and may have curved (parabolic) sides. The shape (or basis) functions are quadratic for velocity and linear for depth. Integration in space is performed by Gaussian integration.

3.2.2 Element Types in RMA2

RMA2 has a capability of supporting different types of basis elements within the same computational finite element mesh. The types of elements which fit into three basic categories consist of two-dimensional elements, one-dimensional elements, and special elements. Details of each element type are explained in the followings.

1) Two dimensional element

Two-dimensional elements, as shown in Figure 9, are the primary type used in RMA2 and may be either triangular or rectangular in shape. A two-dimensional element possesses a length and a width, determined by the positions of the corner nodes which define the element. The water depth at any location within a two-dimensional element is obtained by interpolating among the depths of the corner nodes which define the element.

a. rectangular element b. triangular element

Figure 9 Two dimensional element used with RMA2 model
Source: US. Army Crop of Engineer (1997)

2) One dimensional element

The one-dimensional element is composed of two corner nodes and one midside node, and may be either straight or curved. The Governing Equations for one-dimensional elements are based on a trapezoidal cross-section (Figure 10) with side slopes and off-channel storage. For each one-dimensional

corner node, a bottom elevation, a bottom width (when the depth=0), a left and right bank slope (SL and SR) have to be assigned to describe the trapezoidal cross-section. If the values of SL, SR, and the off channel storage width are zero, the total trapezoidal shape reduces to a rectangle.

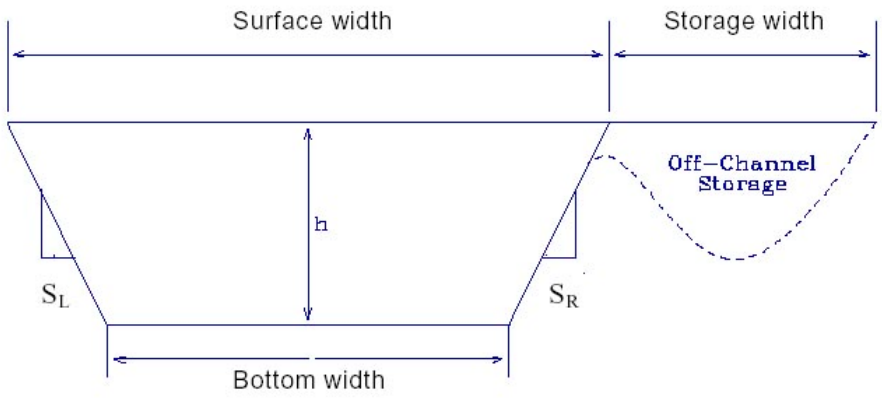

Figure 10 Assumption of one dimensional element cross section
Source: US. Army Crop of Engineer (1997)

The one-dimensional elements can have a different width at each corner node. A basic straight sided element with zero side slopes, but different width assignments at each corner (on the left of figure 11) will have a shape that looks like the figure 11.

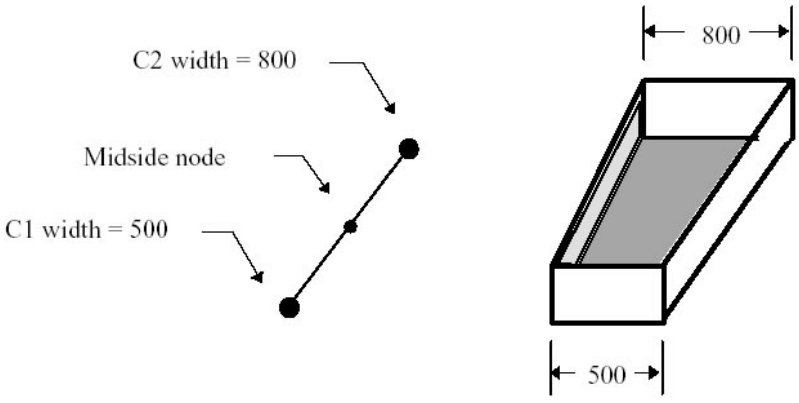

Figure 11 One dimensional element with different width at each corner node
Source: US. Army Crop of Engineer (1997)

3) Special element

The special element is one-dimensional element which serves special purposes. This element can be categorized into 3 types described in the followings.

3.1) Transition element

A transition element is required anytime when using both one dimensional and two dimensional elements in the mesh. This *"*T-*shaped"* type of one-dimensional element, as shown in figure 12, makes the transition between the two-dimensional elements and the one dimensional elements.

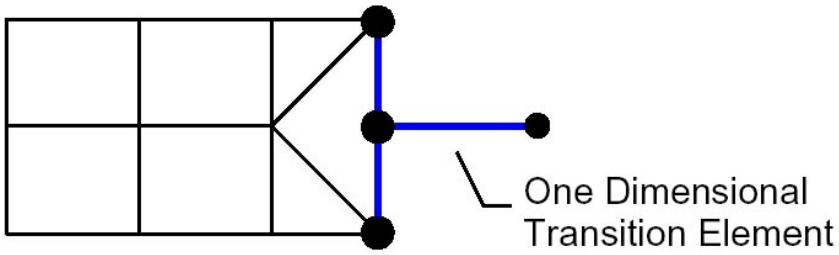

Figure 12 Concept of transition element in RMA2
Source: US. Army Crop of Engineer (1997)

3.2) Junction element

A Junction element (Figure 13) is a special one-dimensional element used to describe the proper characteristics where three or more one-dimensional elements intersect. The junction element is the point where the other one-dimensional elements connect. There are as many nodes defining this junction element as there are one-dimensional elements connecting to it.

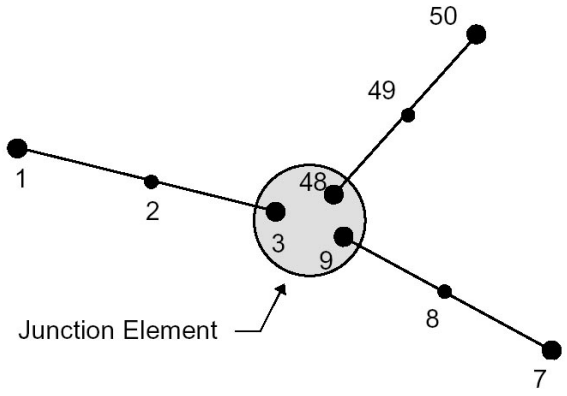

Figure 13 Concept of junction element in RMA2
Source: US. Army Crop of Engineer (1997)

3.3) Control structure element

A control structure element is used when there is the simulation of obstructions in the flow path, such as weirs, dams, flood gates, etc. A one-dimensional can be assigned a control structure element by a single point which contains two nodes and has an IMAT value equals 904 (figure 14). The order of the node numbering at a control structure element should be that the side with higher elevation comes before the side with the lower elevation. This is generally the "upstream" side of the structure followed by the "downstream" side.

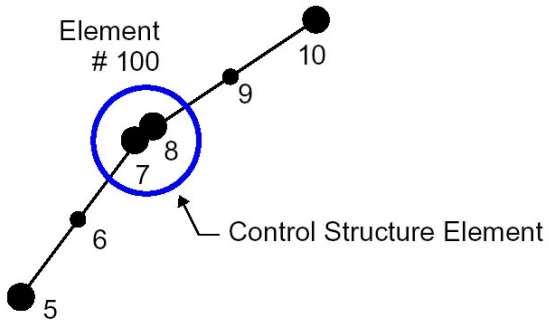

Figure 14 Concept of control structure element in RMA2
Source: US. Army Crop of Engineer (1997)

3.2.3 A Solution Technique in RMA2

Newton-Raphson convergence scheme is used in RMA2 for obtaining a solution. The concept of this method is shown in figure 15. The simplistic example is presented to illustrate the problem of solving the root of a typical quadratic equation. The idea is to find a solution to the equation as close to the root as possible.

On the *x* axis, *x1* is the initial guess at a solution (initial solution). A line (line 1) which is tangent to the curve at *x1* is computed. *x2* is the place which line 1 cross the x axis, then the second guess used to solve the problem.

A new solution is calculated from *x2*, and another tangent line (line 2) is computed. To repeat the solution step, the point where this tangent line crosses the *x* axis becomes the next guess, *x3*. And so on, until the difference in value along the *x* axis, between two successive solutions, becomes less than a pre-defined convergence criterion. At this point, the solution has converged.

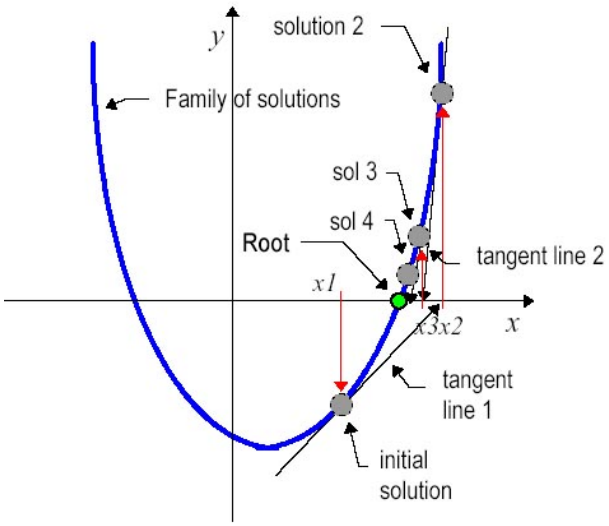

Figure 15 The concept of Newton-Raphson scheme to obtain the solution in RMA2
Source: US. Army Crop of Engineer (1997)

Number of iteration control in RMA2 for each time step can be assigned by different 2 methods.

1) Providing a convergence criterion

The criterion for convergence in RMA2 is the maximum change in calculated depth of all nodes from one iteration to the next. The value typically varies between 0.005 and 0.0001 for steady state, and between 0.05 and 0.001 for dynamic simulation. A more stringent criterion is required for true steady state simulations, and/or wetting and drying simulations. RMA2 will continue the Newton-Raphson iteration process until either the maximum number of iterations, or the depth convergence criterion, has been satisfied

2) Directly specifying the maximum number of iterations

The maximum number of iterations for both steady state and dynamic simulations should be large enough to allow the model to sufficiently converge with the given conditions. The required number of iterations must be larger for complex hydrodynamic studies, such as simulations where wetting and drying occur and the hydrodynamics change from one iteration to the next.

3.3 Theory and concept of RMA11 Model

RMA11 is a three-dimensional model for simulating water quality of estuaries, bays, lakes and rivers (King, 1996). It is also capable of simulating one and two-dimensional approximations. RMA11 model is designed to accept input of velocities and depths, either from an ASCII data file or from binary files produced by RMA2 (two-dimensional hydrodynamic model) or RMA10 (three-dimensional stratified flow model).

3.3.1 Governing Equations for two dimensional depth averaged transport

The governing equations comprise of two principal equations; Continuity and Constituent transport. In depth average condition, all derivatives in vertical direction are eliminated. In RMA11, these equations can be written as equation (5) and (6).

Continuity equation

$$(h\frac{\partial u}{\partial x}+\frac{\partial v}{\partial y})+u\frac{\partial h}{\partial x}+v\frac{\partial h}{\partial y}+\frac{\partial h}{\partial t}-q_1=0 \qquad (5)$$

where q_1 = inflow per unit area

Constituent equation

$$\frac{\partial(hC)}{\partial t}+u\frac{\partial(hC)}{\partial x}+v\frac{\partial(hC)}{\partial y}-\frac{\partial}{\partial x}\left(D_x h\frac{\partial C}{\partial x}+D_{xy}h\frac{\partial C}{\partial y}\right)$$
$$-\frac{\partial}{\partial y}\left(D_{xy}h\frac{\partial C}{\partial x}+D_y h\frac{\partial C}{\partial y}\right)-KhC-h\theta_s=0 \qquad (6)$$

The Continuity equation can be substituted in Constituent equation, therefore equation (6) can be written as:

$$h\left(\frac{\partial C}{\partial t}+u\frac{\partial C}{\partial x}+v\frac{\partial C}{\partial y}\right)-\frac{\partial}{\partial x}\left(D_x h\frac{\partial C}{\partial x}+D_{xy}h\frac{\partial C}{\partial y}\right)-\frac{\partial}{\partial y}\left(D_{xy}h\frac{\partial C}{\partial x}+D_y h\frac{\partial C}{\partial y}\right)$$
$$+(q_1-Kh)C-h\theta_s=0 \qquad (7)$$

For finite element formulation, partial integration is applied to the diffusive terms. Equation (7) can then be written as:

$$f_c = \int_{A_h}^{N^T} [h\left(\frac{\partial C}{\partial t} + u\frac{\partial C}{\partial x} + v\frac{\partial C}{\partial y}\right) + (q_1 - Kh)C - h\theta_s] + N_X^T [h(D_x \frac{\partial C}{\partial x} + D_{xy}\frac{\partial C}{\partial y})]$$

$$+ N_y^T [h(D_{xy}\frac{\partial C}{\partial x} + D_y \frac{\partial C}{\partial y})] dA \quad (8)$$

Water depth (r-a) is multiplied in equation 8**,** the element residual contribution can be written as shown in equation (9):

$$f_{ct} = \int_{A_h}^{N^T} [h(r-a)\left(\frac{\partial C}{\partial t} + u\frac{\partial C}{\partial x} + v\frac{\partial C}{\partial y}\right) - h\frac{\partial a}{\partial x}(D_x\frac{\partial C}{\partial x} + D_{xy}\frac{\partial C}{\partial y}) - h\frac{\partial a}{\partial y}(D_{xy}\frac{\partial C}{\partial x} + D_y\frac{\partial C}{\partial y})$$

$$+ (r-a)\{(q_1 - Kh)C - h\theta_s\}] + N_x^T[(r-a)h(D_x\frac{\partial C}{\partial x} + D_{xy}\frac{\partial C}{\partial y}]$$

$$+ N_y^T [(r-a)h(D_{xy}\frac{\partial C}{\partial x} + D_y\frac{\partial C}{\partial y}] dA \quad (9)$$

where r = water surface elevation

A = bottom elevation

Then, the Newton Raphson derivative can be written as:

$$\frac{\partial f_c}{\partial C} = \int_{A_h}^{N^T} [\{h\frac{\alpha}{\Delta t} + (q_1 - Kh)\}]N + N^T huN_x + N^T hvN_y + N_x^T D_x hN_x$$

$$+ N_x^T D_{xy} hN_y + N_y^T D_{xy} hN_x + N_y^T D_y hN_y dA \quad (10)$$

When Newton Raphson is applied, equation (10) then becomes:

$$\frac{\partial f_{ct}}{\partial C} = \int_{A_h}^{N^T} [(r-a)\{h\frac{\alpha}{\Delta t} + (q_1 - Kh)\}]N + N^T[h(r-a)u - h\frac{\partial a}{\partial x}D_x - h\frac{\partial a}{\partial y}D_{xy}]N_x$$

$$+ N^T[h(r-a)v - h\frac{\partial a}{\partial x}D_{xy} - h\frac{\partial a}{\partial y}D_y]N_y + N_x^T D_x h(r-a)N_x + N_x^T D_{xy}h(r-a)N_y$$

$$+ N_y^T D_{xy} h(r-a)N_x + N_y^T D_y h(r-a)N_y dA \quad (11)$$

3.3.2 Governing Equations for Water Quality parameters

The concept of water quality relationships in RMA-11 are refered from QUAL2E which is three dimensional water quality model developed by Brown and Barnwell (1987). The principal equations for each parameter can be described in the followings (King, 1996).

1) Temperature dependence of rate coefficients

The computations of temperature in RMA-11 are adjustment the rate coefficients in the source / sink terms. These coefficients are input at 20^0C and then Streeter-Phelps formulation as shown in equation (12) is used to correct the actual temperature using:

$$X_t = X_{20}\,\theta^{(T-20)} \tag{12}$$

where

X_t = the value of the coefficient at the local computed temperature,

X_{20} = the value of the coefficient at 20^0C,

θ* = an empirical constant for each reaction coefficient.

2) Chlorophyll <u>a</u> and Algae Growth and Settling Rates

For this model, chlorophyll <u>a</u> is assumed to be directly proportional the algal biomass of phytoplankton. Therefore it can be computed by the following equation.

$$Chl\ \underline{a} = \alpha_0 A \tag{13}$$

Where

$Chl\ \underline{a}$ = chlorophyll a concentration (μg-Chl a/L),

A = algal biomass concentration (mg/L),

α_0 = a conversion factor (μg-Chl a/mg A).

The net growth rate term for algae G_a can be written as equation (14).

$$G_a = \mu A - \rho A \tag{14}$$

where

μ = local specific growth rate of algae with temperature adjusted (1/day),

ρ = local respiration rate of algae with temperature adjusted (1/day).

The settling rate for algae V_a is given by:

$$V_a = \sigma_1 \tag{15}$$

where

σ_1 = settling rate of algae - temperature adjusted (m/day)

A growth rate formula that is limited by lowest nutrients factor can be shown below:

$$\mu = \mu_{\max} (FL) Min (FN, FP) \tag{16}$$

where

μ_{max} = maximum specific growth rate with temperature adjusted (1/day),

FL = algal growth rate limitation factor for light,

FN = algal growth rate limitation factor for nitrogen,

FP = algal growth rate limitation factor for phosphorous.

3) Nitrogen cycle

In RMA11 model, nitrogen cycle is assumed to consist of four nitrogen species that transform cyclically from organic nitrogen to ammonia to nitrite and to nitrate.

3.1) Organic nitrogen

In the model assumption, respiration of algae creates organic nitrogen while it is lost by settling to the bottom and transforming to ammonia. The equations for growth (G_{N4}) and settling (V_{N4}) of organic nitrogen are shown below:

$$G_{N4} = \alpha_1 \rho A - \beta_3 N_4 \quad (17)$$

$$V_{N4} = \sigma_4 \quad (18)$$

where

N_4 = concentration of organic nitrogen (mg-N/L),

α_1 = fraction of algal biomass that is nitrogen (mg-N /mg-A),

β_3 = rate constant for hydrolysis of organic nitrogen to ammonia nitrogen with temperature adjusted (1/day),

σ_4 = rate coefficient for settling of organic nitrogen usually expressed in m/day units with temperature adjusted (m/day). Note that in QUAL2E this rate is expressed in 1/day units.

3.2) Ammonia nitrogen

Hydrolysis of organic nitrogen and release from benthic sources at the bottom create ammonia nitrogen. It is lost by biological oxidation and algal grazing.

The equation for growth (G_{N1}) of ammonia nitrogen is thus given by:

$$G_{N1} = \beta_3 N_4 - \beta_1 N_1 + \sigma_3 / d^{++} - F_1 \alpha_1 \mu A \qquad (19)$$

where

N_1 = the concentration of ammonia nitrogen (mg-N/L),

β_1 = rate constant of biological oxidation of ammonia nitrogen with temperature adjusted (1/day),

σ_3 = the benthos source rate of ammonia nitrogen with temperature adjusted (mg-N/m^2-day),

F_1 = fraction of algal nitrogen uptake from ammonia pool.

3.3) Nitrite

Nitrite is created by oxidation from ammonia and lost by oxidation to nitrate nitrogen.

The equation for growth of nitrite nitrogen (G_{N2}) is shown below:

$$G_{N2} = \beta_1 N_1 - \beta_2 N_2 \qquad (20)$$

Where

N_2 = the concentration of nitrite nitrogen (mg-N/L),

β_2 = rate constant of oxidation of nitrite nitrogen with temperature adjusted (1/day).

3.4) Nitrate

Nitrate nitrogen is created by oxidation from nitrite nitrogen and lost by uptake of algal grazing. The equation for growth of nitrite nitrogen (G_{N3}) is shown below:

$$G_{N3} = \beta_2 N_2 - [1 - F_1]\alpha_1 \mu A \quad (21)$$

where all terms have been previously defined.

4) Phosphorus Cycle

In RMA11, phosphorous cycle is assumed to consist of two phosphorous forms that are organic phosphorous and dissolved phosphorous.

4.1) Organic phosphorus

Organic phosphorous is created by respiration of algae and lost by transformation to the dissolved phosphorus and settling to the bottom.

The equations for growth G_{P1} and settling V_{P1} of organic phosphorous are shown below:

$$G_{P1} = \alpha_2 \rho A - \beta_4 P_1 \quad (22)$$

$$V_{P1} = \sigma_5 \tag{23}$$

where

P_1 = concentration of organic phosphorous (mg-P/L),

α_2 = fraction of algal biomass that is phosphorous (mg-P /mg-A),

β_4 = rate constant for transformation of organic phosphorous to dissolved phosphorous - temperature adjusted (1/day),

σ_5 = rate coefficient for settling of organic phosphorous usually expressed in m/day units with temperature adjusted (m/day). Note that in QUAL2E this rate is expressed in 1/day units.

4.2) Dissolved phosphorus

Dissolved phosphorous is created by transformation from the organic form and from benthic bottom sources. It is lost by uptake as a nutrient by algae and by attachment to suspended sediment.

The equation for growth G_{P2} of dissolved phosphorous is shown below:

$$G_{P2} = \beta_4 P_1 + \sigma_2 / d^{++} - \alpha_2 \mu A \tag{24}$$

where

P_2 = the concentration of dissolved phosphorous (mg-P/L),

σ_2 = the benthos source rate of dissolved phosphorous with temperature adjusted (mg-P/m^2-day).

5) Oxygen cycle

In RMA11, oxygen cycle consists of dissolved oxygen (DO) and carbonaceous BOD, the other nutrient cycles which demand oxygen. Processes in the cycle are completed by re-aeration and algal generation during growth and depletion during respiration.

5.1) CBOD (Carbonaceous Biochemical Oxygen Demand)

CBOD is carbonaceous demand for oxygen in the system. Settling and flocculation of the particles exerting the demand are potential factors which influence to CBOD.

The equations for growth G_L and settling V_L of BOD are given below.

$$G_L = -K_1 L \tag{25}$$

$$V_L = K_3 \tag{26}$$

where

L = the concentration of ultimate carbonaceous BOD, (mg/L)

K_1 = deoxygenation rate coefficient - temperature adjusted, (1/day).

K_3 = rate coefficient for settling of - temperature adjusted, (m/day). Note that in QUAL2E this rate is expressed in 1/day units. This term also incorporates the loss rate due to flocculation converted to an effective settling rate, see Thomas (1948)

5.2) Dissolved oxygen

Dissolved oxygen is a complex parameter relating with many interactions of the constituents in the model. In RMA11, sources of dissolved oxygen are re-aeration and oxygen from photosynthesis during algal growth. The oxygen sinks are: 1) oxygen uptake due to algal respiration, 2) oxidation of ammonia

nitrogen to nitrite nitrogen, 3) oxidation of nitrite nitrogen to nitrate nitrogen, 4) carbonaceous BOD decay, and 5) sediment oxygen demand.

The equation for growth G_O of dissolved oxygen is shown below:

$$G_o = K_2 (O_s - O) + (\alpha_3 \mu - \alpha_4 \rho) A_1 - K_1 L - \alpha_5 \beta_1 N_1 - \alpha_6 \beta_2 N_2 - K_4 / d^{++} \quad (27)$$

where

O = concentration of dissolved oxygen (mg/L),

O_S = saturation concentration of dissolved oxygen at the local temperature and pressure (mg/L),

K_2 = reaeration rate with temperature adjusted (1/day),

α_3 = the rate of oxygen production per unit of algal photosynthesis (mg-O/mg-A),

α_4 = the rate of oxygen uptake per unit of algae respired (mg-O/mg-A),

α_5 = the rate of oxygen uptake per unit of ammonia nitrogen oxidation (mg-O/mg-N),

α_6 = the rate of oxygen uptake per unit of nitrite nitrogen oxidation, (mg-O/mg-N).

μ = local specific growth rate of algae with temperature adjusted (1/day),

ρ = local respiration rate of algae with temperature adjusted (1/day),

A = algal biomass concentration (mg/L),

L = the concentration of ultimate carbonaceous BOD (mg/L),

d = water depth (m),

K_1 = deoxygenation rate coefficient - temperature adjusted (1/day),

K_4 = sediment oxygen demand rate with temperature adjusted, (mg/m^2/day),

β_1 = rate constant of biological oxidation of ammonia nitrogen with temperature adjusted (1/day),

β_2 = rate constant of oxidation of nitrite nitrogen with temperature adjusted (1/day),

N_1 = the concentration of ammonia nitrogen (mg-N/L),

N_2 = the concentration of nitrite nitrogen (mg-N/L).

5.3) Dissolved Oxygen Saturation Concentration

Solubility of dissolved oxygen depends on temperature, atmospheric pressure and concentration of dissolved solids. In RMA-11, dissolved oxygen is limited by temperature and atmospheric pressure.

Saturation concentration of dissolved oxygen can be computed by the following equation.

$$\begin{aligned} \log_e O_{sn} = & -139.34410 + 1.575701E+05/T - 6.642308E+7/T_{k^2} + 1.243800E+10/T_{k^3} \\ & - 8.621949E+11/T_{k^4} - (1./1.80655)\ S_{al}\ ((3.1929E-2) \\ & - (1.9428\ \ E+1/T_k) + (3.8673\ \ E+3/T_{k^2}\ )) \end{aligned} \tag{28}$$

where

O_{sn} = equilibrium oxygen concentration at 1.00 atm (mg/L),

T_k = water temperature in ° K, within the range 0.0 to 40.0 ° C,

S_{al} = salinity (if active in the simulation),

and

$$O_s = O_{sn} P \frac{\{1 - P_{wv}/P\}\{1 - \varphi P\}}{\{1 - P_{wv}\}\{1 - \varphi\}} \tag{29}$$

where

O_S = equilibrium oxygen concentration at non standard pressure (mg/L),

P = atmospheric pressure (atm),

P_{wv} = partial pressure of water vapour (atm) which may be computed from:

$log_e P_{wv}$ = 11.8571 - 3840.70 / T_k - 216961 /T_k

and

φ = 0.000975 - 1.426E-5 T + 6.436E-8 T^2

T = temperature in ° C.

5.4) Atmospheric re-aeration

RMA-11 allows three option which are Churchill formula (1962), Liss and Merlivat formula (1986) and a constant rate input by the user , to compute atmospheric re-aeration.

The equation of Churchill to compute re-areation can be shown as the following.

$$K_2^{20} = 5.026\, u_s^{0.969}\, d^{-0.673} \qquad (30)$$

where

K_2^{20} = reaeration coefficient at 20° C (m/day),

d = average stream depth (m),

u_s = water velocity at the surface (m/sec).

Liss and Merlivat formula which is based on wind speed and suitable for ocean environments is given by:

$$K_2^{20} = 0.048 * u_w \qquad u_w < 3.6 \text{ m/sec}$$
$$K_2^{20} = 0.773 * u_w - 2.61 \qquad 3.6 < u_w < 13.0 \text{ m/sec} \qquad (34)$$
$$K_2^{20} = 1.600 * u_w - 13.3 \qquad 13.0 < u_w$$

where

u_w = wind speed in m/sec.

6) Cohesive suspended sediment

RMA-11 can simulate transport of fine cohesive sediment or mud as an option of the model. The process of cohesive sediment consists of three transport deposition through settling, erosion, and the development history of the bed layer. Erosion and/or deposition depend on the bed shear stress developed by flowing water, and the shear strength of surface layer of the bed. The methodology of this computation is based on Ariathurai and Krone formula (1976).

6.1) Cohesive Sediment Bed Shear Stress

RMA-11 provides two options for computation of bed shear stress, one based on a law of the wall that is assumed smooth. In this case bed shear stress is computed using the following equation.

$$\tau_b = \rho_w u_*^2 \qquad (35)$$

where

u_* = shear velocity (m/sec),

ρ_W = water density (kg/m^3),

then

$$u_m = u_* \log_e \left(\frac{3.32\ u_* d}{\upsilon} \right) / V_k \qquad (36)$$

where

u_m = mean flow velocity (m/sec),

d = water depth (m),

υ = kinematic viscosity of water (m^2/sec),

V_k = Von Karman's Constant

For the case of a rough bed, flow velocity can be computed as the following equation.

$$u_* = \frac{V_k u_m}{\log_e (12.27\ d / r)} \qquad (37)$$

where

r = roughness height (m).

6.2) Cohesive sediment settling rate

In RMA11, particle settling rate is defined as a function of the suspended sediment concentration. The equation for settling velocity (V_S) is written as:

$$\begin{aligned} V_s &= V_1 && \text{for} && S<S_1 \\ V_s &= V_{sk} S^{pc} && \text{for} && S_1<S<S_2 \\ V_s &= V_{sk} S_2^{pc} && \text{for} && S_2<S \end{aligned} \qquad (38)$$

where

V_1, S_1, S_2 and p_c are all input parameters and V_{sk} is derived as matching condition.

6.3) Cohesive sediment erosion

Above a critical level of shear stress erosion of the bed will occur. Resistance of cohesive sediment to erosion by flowing water depends on many factors such as: the type of clay minerals, structure of the bed, the chemical composition of eroding fluids, and the presence of organic matter and its state of oxidation.

In RMA11, the erosion rate for surface erosion can be written as the following equation:

$$E_s = M \frac{\{\tau_b - \tau_{ce}\}}{\tau_{ce}} \tag{39}$$

Where

τ_{ce} = critical shear stress for erosion (N/m^2),

M = erodibility constant.

The equation of erosion rate over a time step can be written as:

$$E_m = \frac{\Delta m}{\Delta t} \tag{40}$$

where

Δm = Mass eroded per unit bed area (gm/m^2),

Δt = time step (s),

τ_l = critical shear stress for mass erosion for layer l (N/m^2),

7) Sand transport

According to the different between sand and cohesive sediment transport, therefore sand transport is modelled using the concept of sand transport potential. A sand transport formulation is assumed to depend on sand and flow parameters. The equation for sand transport computation in RMA11 is given by:

$$S = \frac{C_{eq} - C}{t_c} \tag{41}$$

where

S = source term (gm/s/m^2/meter of depth),

C_{eq} = equilibrium concentration (transport potential) (mg/l),

C = sand concentration in the water,

t_c = characteristic time for effecting the transition, this depends on whether deposition or erosion is occurring (s).

MATERIALS AND METHODS

Materials

1. A personal Computer (PC)
2. Topographic map (scale 1:50,000 and 1:10,000) of Bung Boraphet and the surrounding areas
3. Microsoft Excel Software, XP version
4. RMA2 Model (two-dimensional depth average hydrodynamic model)
5. RMA11 Model (two-dimensional depth average water quality model)
6. PCI Geomatica Software, version 9.1

Methods

1. The study of water budget for Bung Boraphet

The daily water budget study of Bung Boraphet was carried out for an understanding of hydrologic-budget components of the lake. A conceptual model describing Bung Boraphet flow characteristics during the inflow and outflow periods has been developed as shown in Figure 16, to distinguish simply the flow directions of the two seasons. The two principal sources of water to the lake are rain falling on its surface and runoff from the watershed. Water losses are mainly through evaporation and regulated outflows for agriculture. Minor losses are through soil seepage and aquaculture.

The inflow periods occur in the wet season between July and November. During these periods, inflows normally occur at Bung Boraphet tributaries and irrigation canals and outflows occur at the weir and regulator. At the beginning of the wet season mostly around July, net runoffs from Bung Boraphet catchment area flow into Bung Boraphet via Klong Bon, Klong Tatako, and two irrigation canals. Bung Boraphet water level is increasing resulting from net inflow to the lake from the average minimum water level of +22.50 m MSL to the weir crest and regulator crest

at +24.00 m MSL happening around August to September. At this stage, the lake water storages start flowing out from weir and regulator. However, runoffs from tributaries and irrigation canals are still flowing in Bung Boraphet more than lake water storages flowing out from the weir and regulator. Bung Boraphet water levels are therefore continuously increasing to the average maximum water level of around +24.47 m MSL that usually occurs in November when rainfall stops. Bung Boraphet water levels are then continuously decreasing from the maximum water level to the weir crest level at around the end of November when the dry season starts.

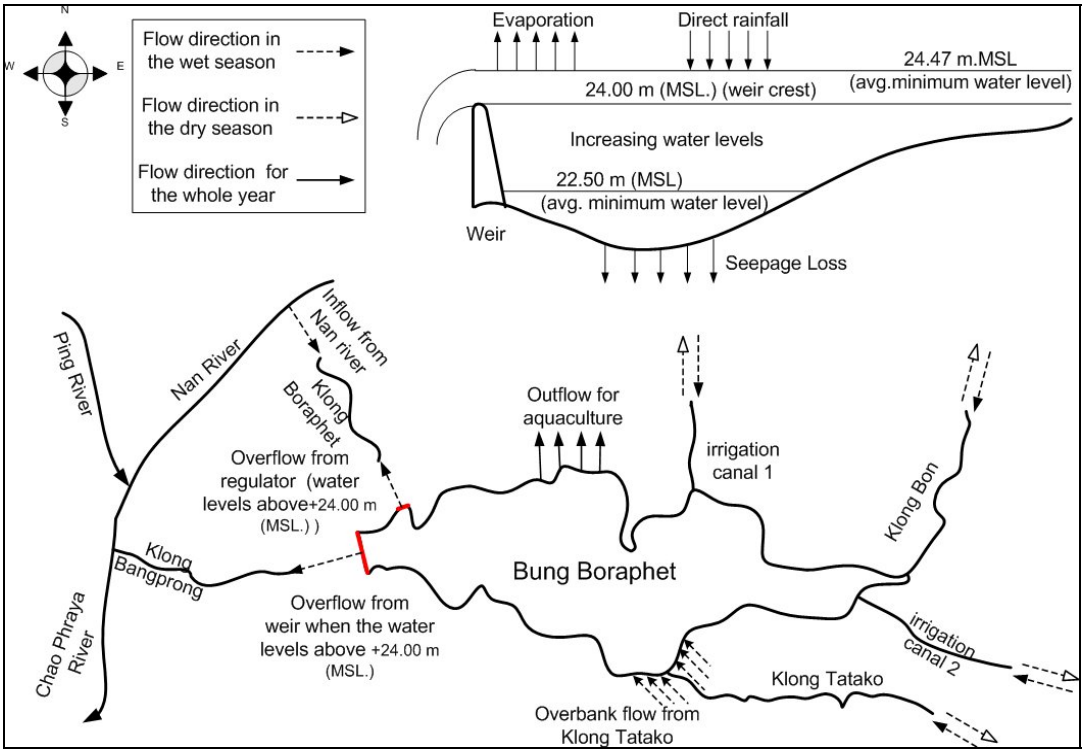

Figure 16 Conceptual model of Bung Boraphet water budget

The water budget study of Bung Boraphet based on Eq. (1) can be schematized as a conceptual model water budget analysis shown in Figure 17. The hydrologic components and calculation methodology are expressed in the conceptual model. There are 9 blocks of hydrologic components that have the effects on daily water balance study of Bung Boraphet. Block 1 explains daily water volume variation (ΔS) in one day intervals (Δt). An investigation of daily inflow summation from

lake tributaries ($\sum I(t)$) is shown in block 2. Inflow from Nan River can be estimated using its rating curve and water level data at the regulator. Daily lake outflows ($\sum O(t)$) can be calculated by a summation of the outflow from lake tributaries (block 4), outflow for water supply and aquaculture (block 5), and outflow from the weir and regulator (block 6). Approximation methodology for daily direct rainfall, daily evaporation, and daily seepage loss are described in blocks 7, 8, and 9, respectively. Details of data collection and methodology used for an approximation of each parameter are explained in the following sections.

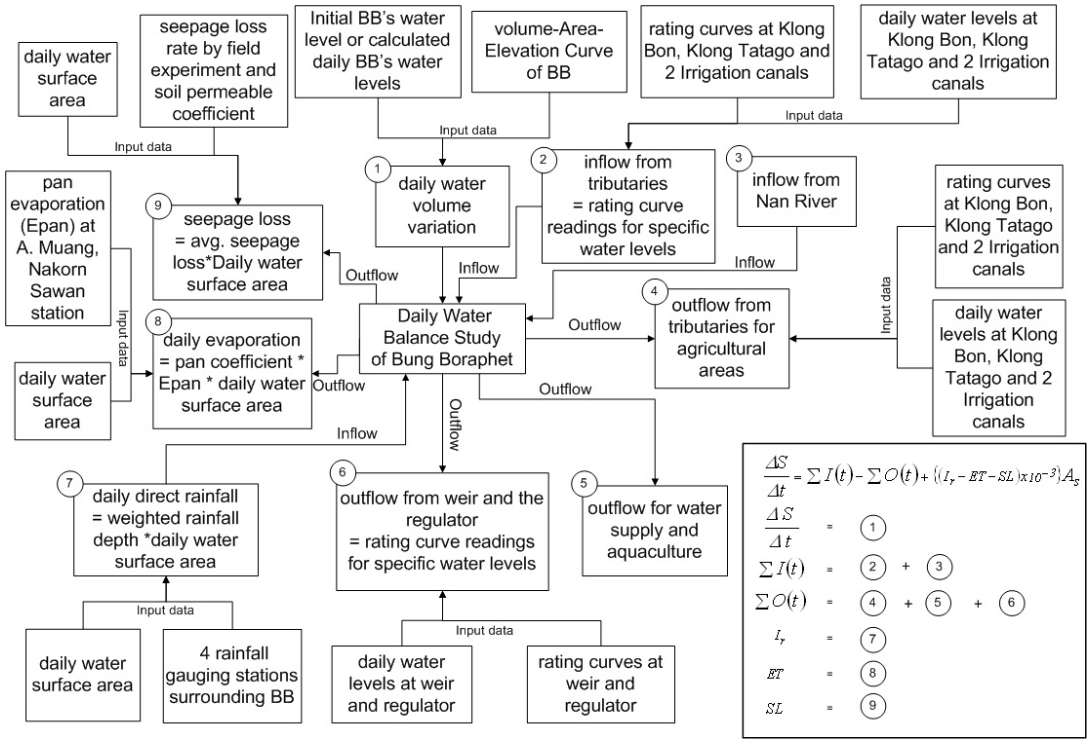

Figure 17 Conceptual model of Bung Boraphet water budget analysis

1.1 Daily Water Volume Variation

The daily water volume variation (ΔS) in one day intervals (Δt) as shown in Eq. (1) can be calculated using the volume-area-elevation curve of Bung

Boraphet and the daily variations of lake water level. The details of the volume-area-elevation curve and lake water levels are explained below.

1.1.1 Volume-Area-Elevation Curve of Bung Boraphet

A survey for Bung Boraphet's bathymetry was carried out by RID in 2003. The volume-area-elevation curve of the lake preparing from Bung Boraphet's bathymetry is shown in Figure 18. The lake water level at +20 m (MSL) has a surface area and water storage of approximately 2.93 square kilometers and 4.62 MCM, respectively. The level of +23 m (MSL), which is the minimum water level recommended for sustainable flora and fauna biodiversity, has a surface area and water storage of around 65.63 square kilometers and 75.15 MCM, respectively. The weir crest level of +24.00 m (MSL), which has a surface area of approximately 147.53 square kilometers, can store water up to 177.50 MCM.

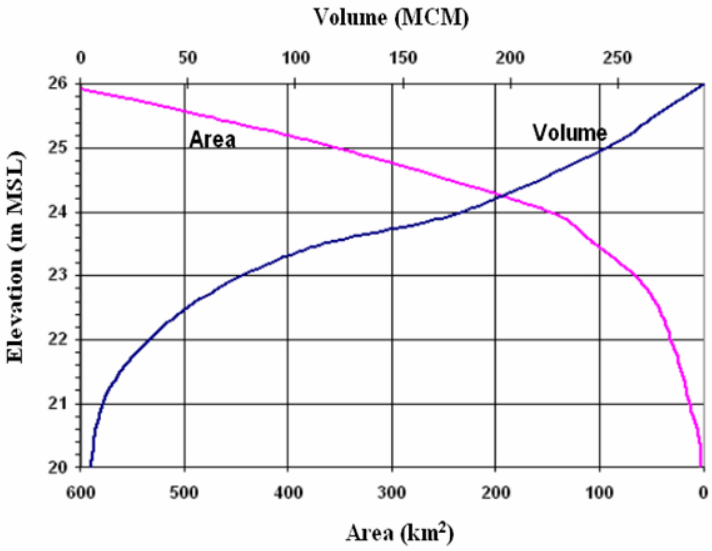

Elevation (m MSL)	Volume (MCM)	Area (km²)
20.0	2.93	4.62
20.2	4.32	4.99
20.4	5.71	5.36
20.6	7.10	6.03
20.8	8.45	7.57
21.0	10.30	13.27
21.2	13.19	15.55
21.4	16.59	18.32
21.6	20.80	24.54
21.8	25.95	27.39
22.0	31.76	31.55
22.2	38.46	35.02
22.4	45.78	38.03
22.6	54.37	47.38
22.8	64.16	50.32
23.0	75.15	65.63
23.2	89.01	72.32
23.4	104.01	78.21
23.6	124.23	115.45
23.8	149.46	134.25
24.0	177.50	147.53
24.2	191.00	188.64
24.4	204.50	229.75
24.6	218.00	270.86
24.8	231.50	311.97
25.0	245.00	353.08
25.2	254.03	406.56
25.4	263.06	460.04
25.6	272.09	513.52
25.8	281.12	567.00
26.0	290.14	620.47

Figure 18 Volume-area-elevation curve of Bung Boraphet

1.1.2 Lake Water Levels

The water levels of Bung Boraphet were measured at the regulator, situated on the Boraphet Canal connecting Bung Boraphet and the Nan River, by FD since April 1993. The daily water levels of the lake between 1994 and 2006 are shown in Figure 19. The wet season is between July and November and the dry season is from December until June. The average maximum water level is around 24.47 m (MSL) occurring mostly in November. The average minimum water level is around 22.50 m (MSL) mostly occurring between May and June. However, in some years the minimum water levels occurred earlier in April and later in July. The average water depth at the weir crest level (+24.00 m (MSL)) is around 2.3 m compared with the average bed level of the lake of approximately 21.70 m (MSL). In the wet season, the maximum water levels are usually beyond the weir crest level and the average depth at the maximum water levels during the flood period is approximately 2.77 m (without consideration of the extreme levels happening in the year 1995, 1996 and 2002). During the dry season, the average depth at the minimum water levels is around 0.80 m. Therefore, the fluctuation of the water level between the maximum and minimum water levels is around 1.97 meters. As mentioned earlier, the suitable water level recommended by FD is at the level of 23.00 m (MSL) to be suitable for a sustainable fishery and the maintenance of biodiversity and ecosystem integrity in the wetlands. However, there is up to 22 percent of the time (1,269 days out of the total 4,473 days) that water levels are below the recommended level.

1.2 Inflow and Outflow Investigations

The daily inflows and outflows from the tributaries were calculated from rating curves and daily water level records at gauging stations in 5 locations. The details of water level measurements of the lake and its tributaries during the study period, the rating curves of all tributaries, and inflow and outflow investigation are described in the sections below.

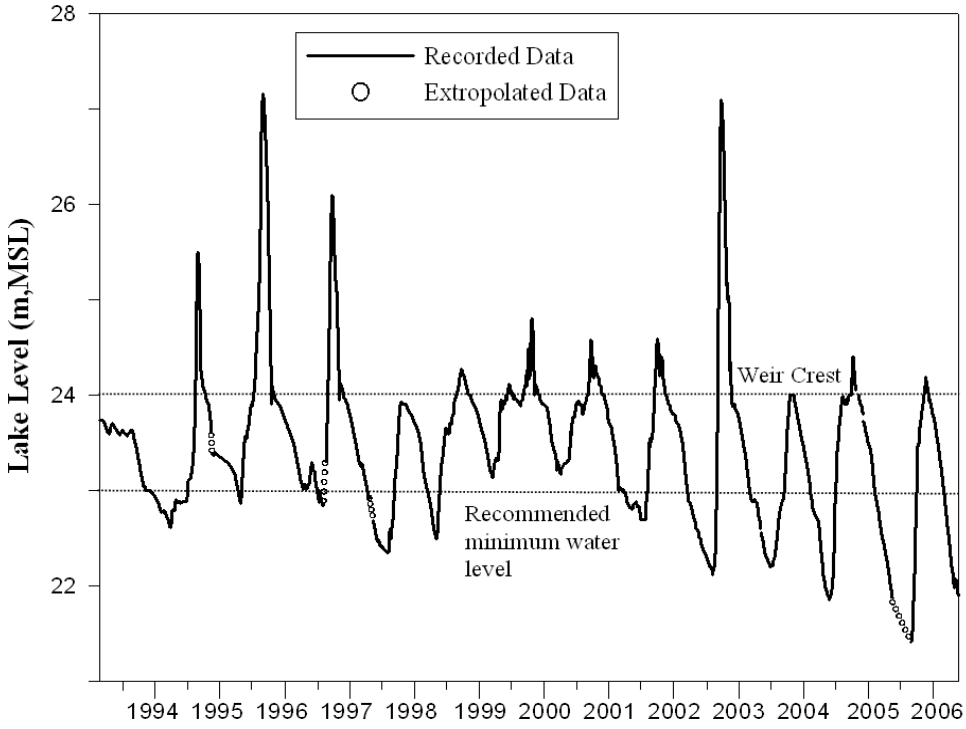

Figure 19 Daily water levels of Bung Boraphet

1.2.1 Water Level Measurements

There was no gauging station installed in the catchment of Bung Boraphet before this study was carried out besides staff gauges at the regulator situated on the Boraphet Canal. Four staff gauges were installed in canals and streams around Bung Boraphet to monitor the drainage from 99.4 % of the Bung Boraphet catchment area (Figure 20 and Table 6). The gauge heights were recorded daily (precision of ±1cm).

Table 6 Locations of 5 gauge height recording station

Point	Location	Coordinate	
		N	E
1	Regulator at Boraphet Village	0629100	1736955
2	Klong Bon at Panomsaet Village	0644256	1738126
3	Klong Tatako at Wang Mahakorn Village	0635302	1733263
4	irrigation canal 1 at Lamkatum Village	0639815	1736342
5	irrigation canal 2 at Klong Kud Village	0643252	1735653

These irrigation canals were constructed by RID to divert water from Bung Boraphet for agricultural areas surrounding the lake. Water level recordings at these 5 gauging locations between December 2002 and May 2006 are shown in Figure 20 for further inflow and outflow estimation.

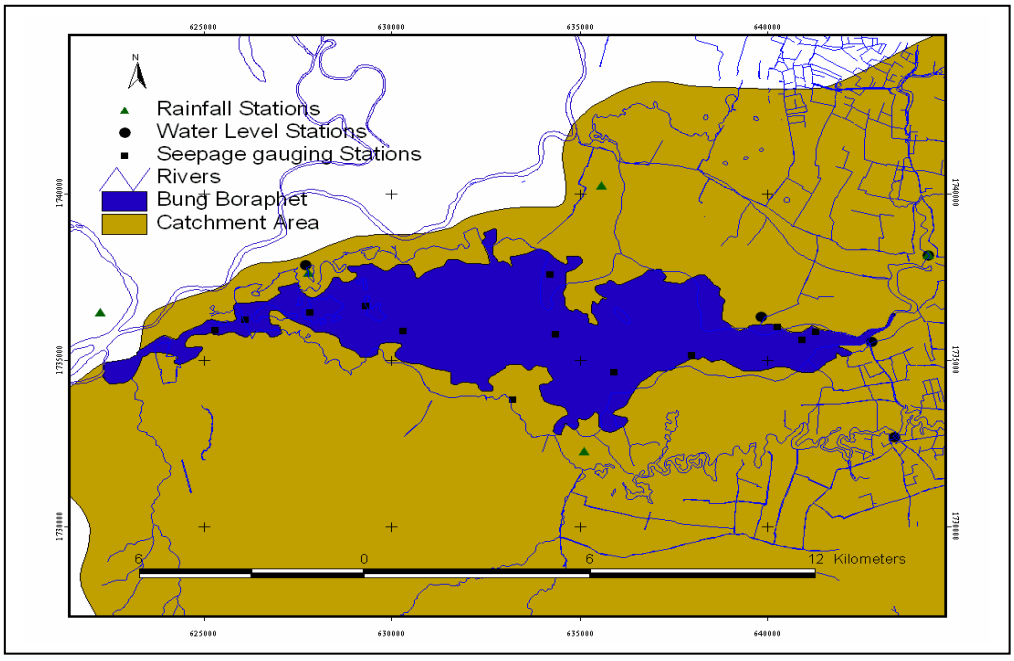

Figure 20 Locations of 5 gauging stations, 5 rainfall stations, and 12 PVC tubes surrounding Bung Boraphet

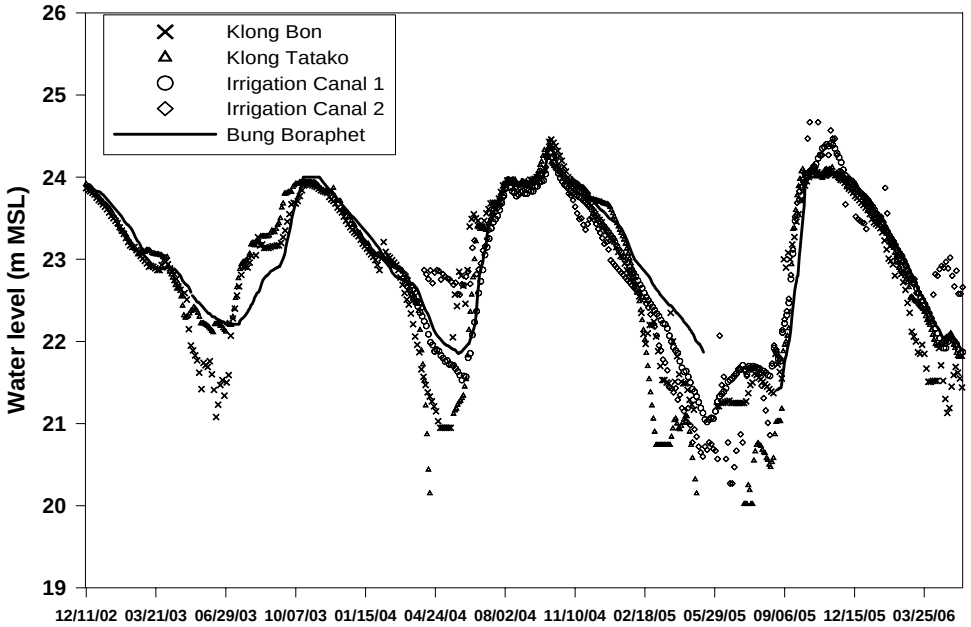

Figure 21 Water levels data at 5 gauging locations between December 2002 and June 2006

1.2.2 Inflow Rating Curves and Inflow Investigations

Total daily inflows are a summation of inflows from each tributary comprising Klong Bon, Klong Tatako and 2 irrigation canals. These inflows can be evaluated using daily water levels recording at the outlet locations of these tributaries as described above and their inflow rating curves preparing under this research using recording data between December 2002 and March 2006. According to most of inflows of Klong Bon tributary are in the channel, therefore there is only one rating curve at the outlet location as shown in Figure 22. It is not the case for Klong Tatako. For the water levels above approximately +24.30 m (MSL), flows at the outlet location of Klong tatako tributary are above the bankfull level that has the effect on the rating curve. Therefore, the rating curve at this location needs to be separated into two curves for the channel and overbank flow characteristics as shown in Figure 23 and 24, respectively. For other two irrigation canals, the canal capacities at the bankfull levels are more than inflows occurring at each canal. The rating curves for the irrigation canals 1 and 2 are shown in Figure 25 and 26, respectively. Daily

Inflows from two tributaries and two irrigation canals can be calculated using their rating curve reading for specific daily water levels at the particular location as summarized in block 2 of the water budget conceptual model in Figure 17.

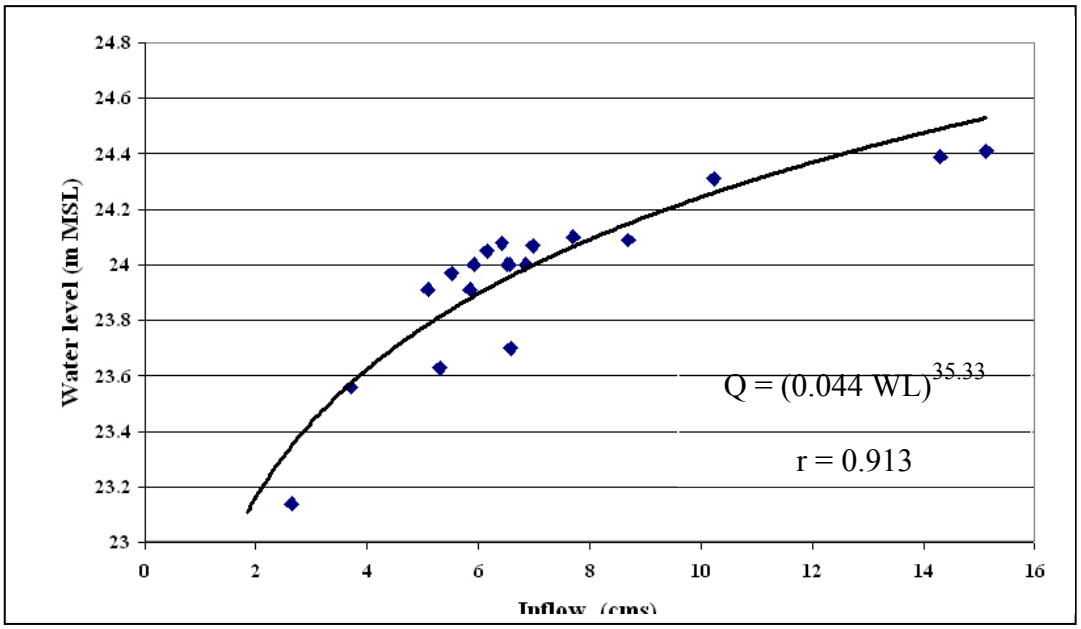

Figure 22 Inflow rating curve at the outlet of Klong Bon

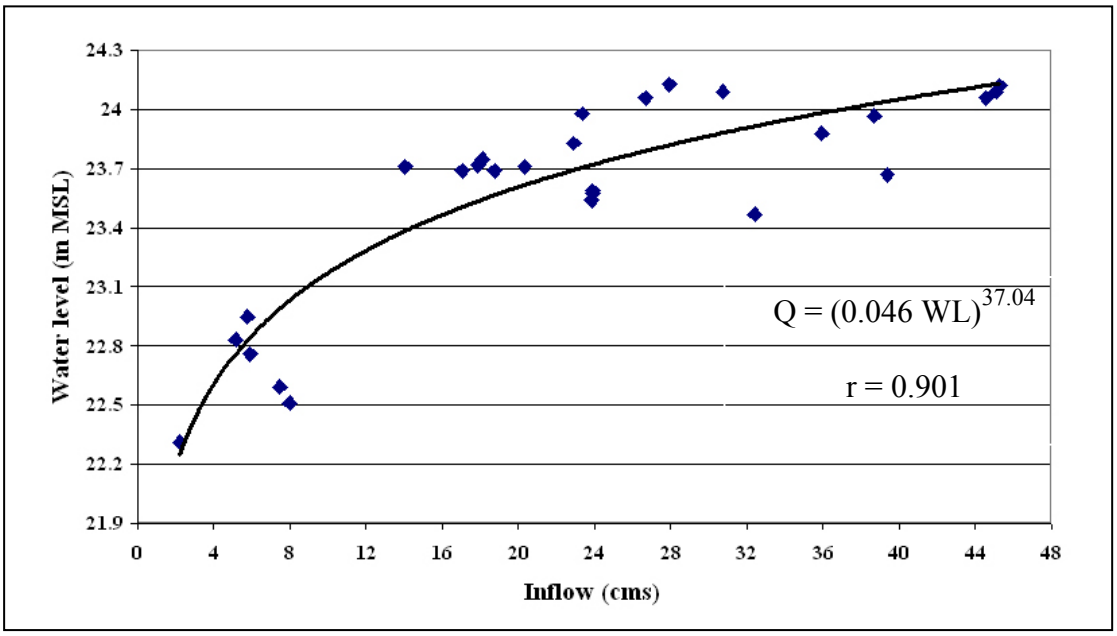

Figure 23 Channel Inflow rating curve at the outlet location of Klong Tatako

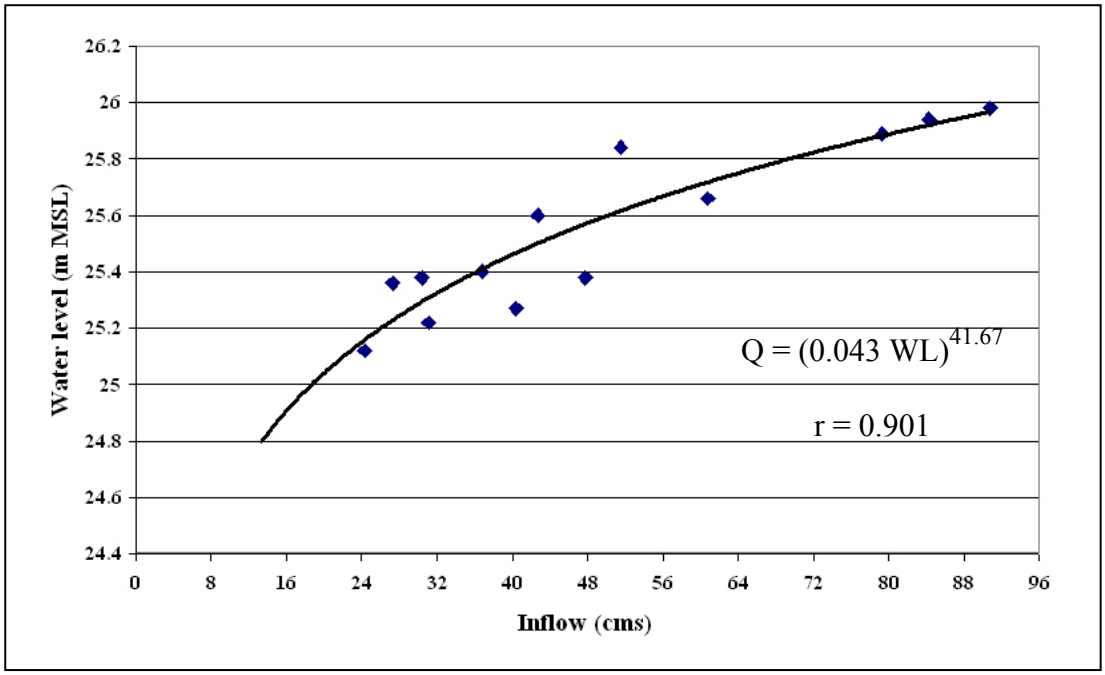

Figure 24 Overbank inflow rating curve at the outlet location of Klong Tatako

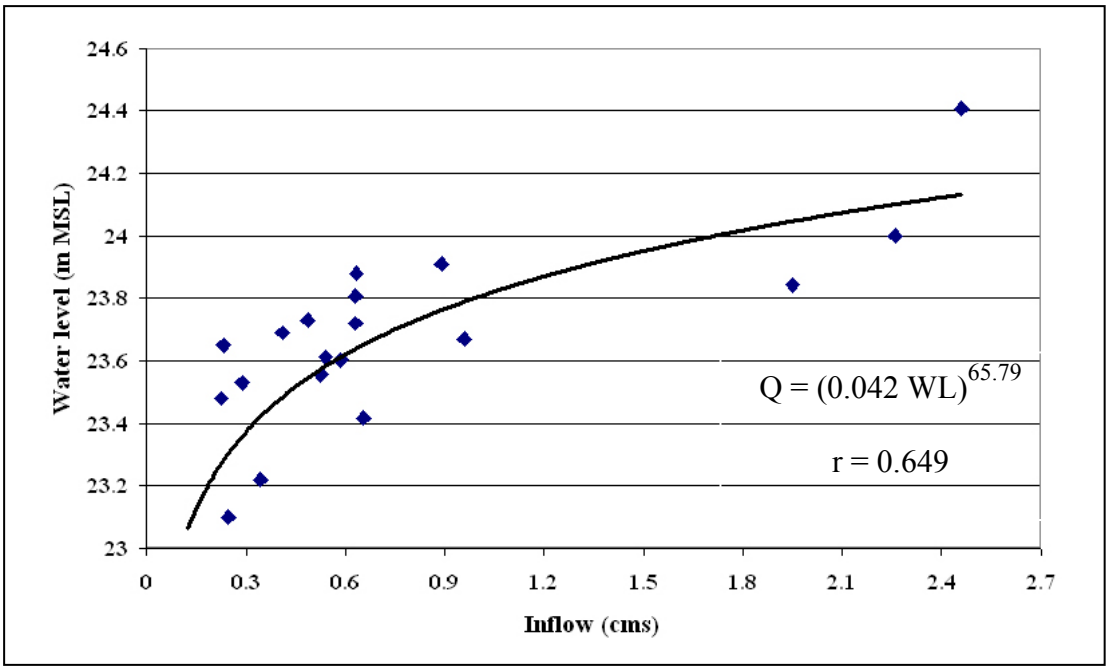

Figure 25 Inflow rating curve at the outlet location of irrigation canal 1

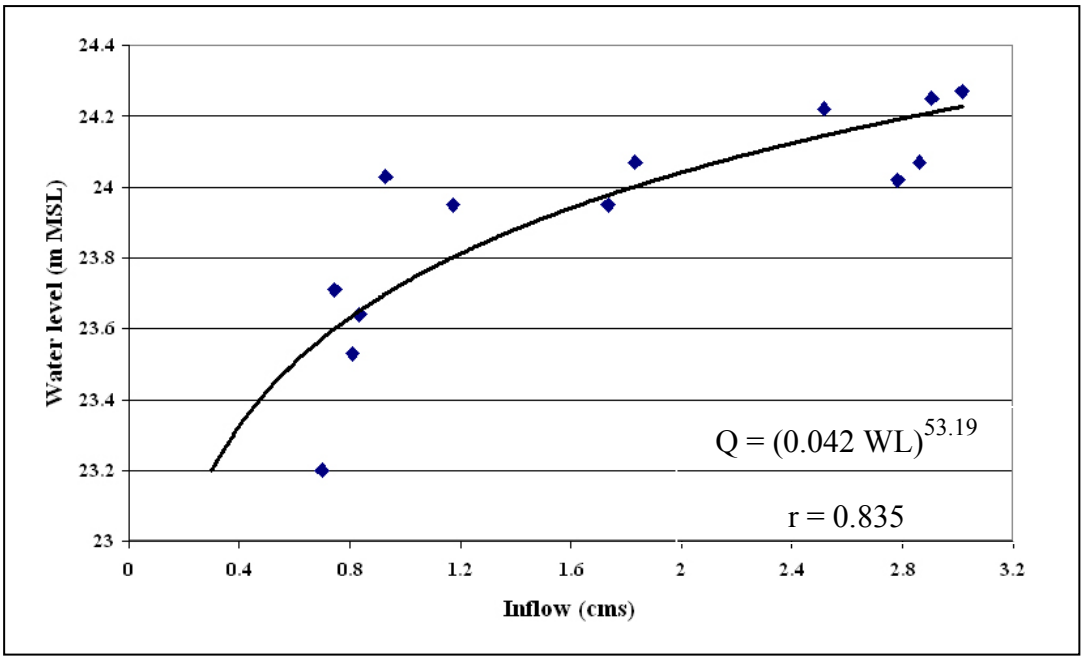

Figure 26 Inflow rating curve at the outlet location of irrigation canal 2

1.2.3 Outflow Rating Curves and Outflow Investigations

Daily total outflows are a summation of: 1) outflow from tributaries, 2) outflow for water supply and aquaculture and 3) outflow from weir and regulator. Description of each outflow component is included in the following:

1) Outflows from tributaries

Total daily outflows from tributaries are a summation of outflows from each tributary at Klong Bon, Klong Tatako, and 2 irrigation canals. These outflows can be analyzed using daily water level recorded at the outlet locations of these tributaries as explained earlier and their outflow rating curves. Most of the outflows from tributaries are delivered to the paddy farms in Bung Boraphet conservation zone and its surroundings during the dry season. Only 0.10 MCM between December and February is usually delivered as one source of the water supply for Tatako Distinct Waterworks Authority (Provincial Waterworks Authority (PWA), 2005). Between the beginning and the middle (around the end of

February) of the dry season, lake water levels are higher than water levels of tributaries and irrigation canals. Therefore, lake water flows to tributaries by gravity. Gravitational outflow rating curves at the outlet locations of Klong Bon, Klong Tatako, and two irrigation canals are shown in Figures 27, 28, 29 and 30, respectively. Gravitational outflows are continuing until the points that lake water levels intersect with tributaries water levels. From these points lake water cannot flow to tributaries by gravity but needs to be diverted by pumping to irrigation areas via tributaries and irrigation canals. Pumping discharges to each tributary and irrigation canal depend on lake water levels. Therefore, regulated outflow rating curves for Klong Bon, Klong Tatako, and two irrigation canals are the relationships between lake water levels and discharges at these locations as shown in Figure 31, 32, 33, and 34, respectively. Daily outflows from two tributaries and two irrigation canals can be calculated using their rating curve reading for specific daily water levels at the particular location as summarized in block 3 of the water budget conceptual model in Figure 17.

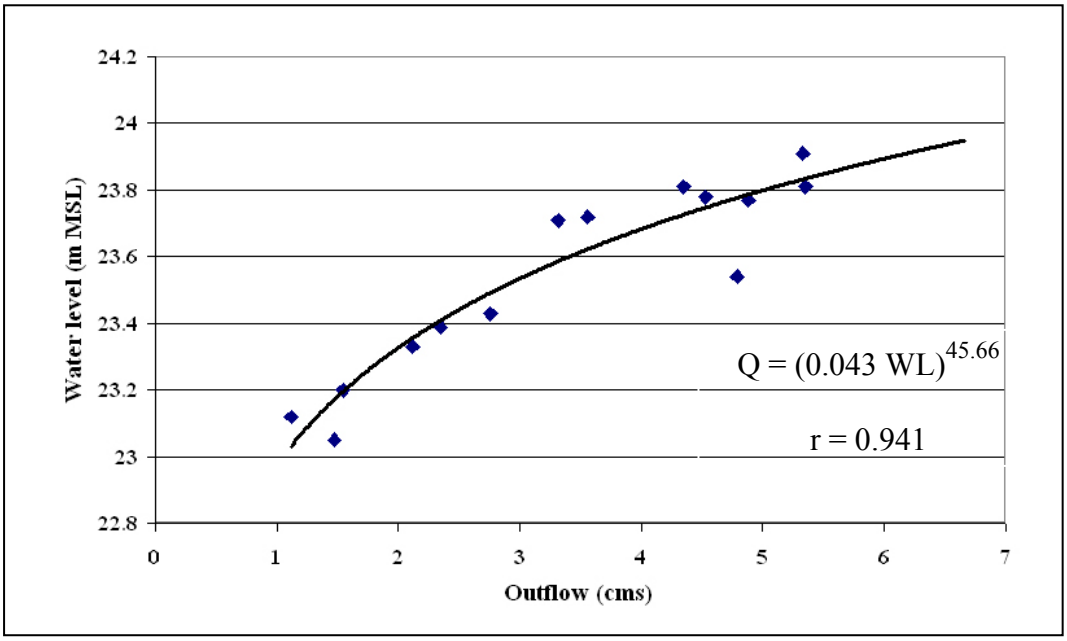

Figure 27 Gravitational outflow rating curve at the outlet location of Klong Bon

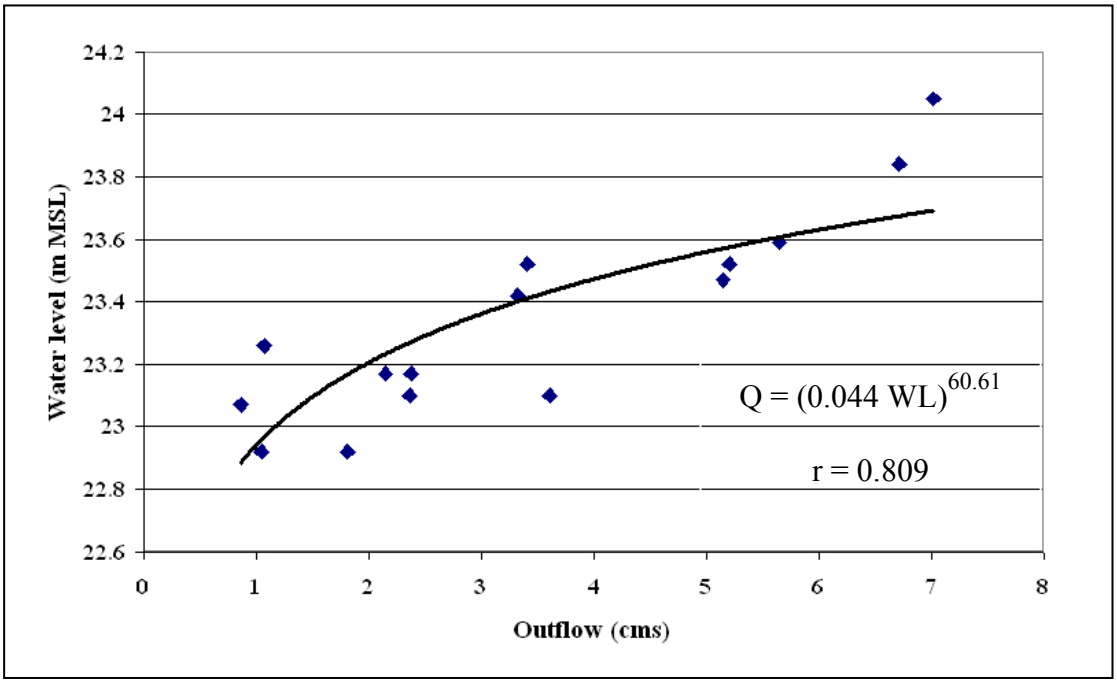

Figure 28 Gravitational outflow rating curve at the outlet location of Klong Tatako

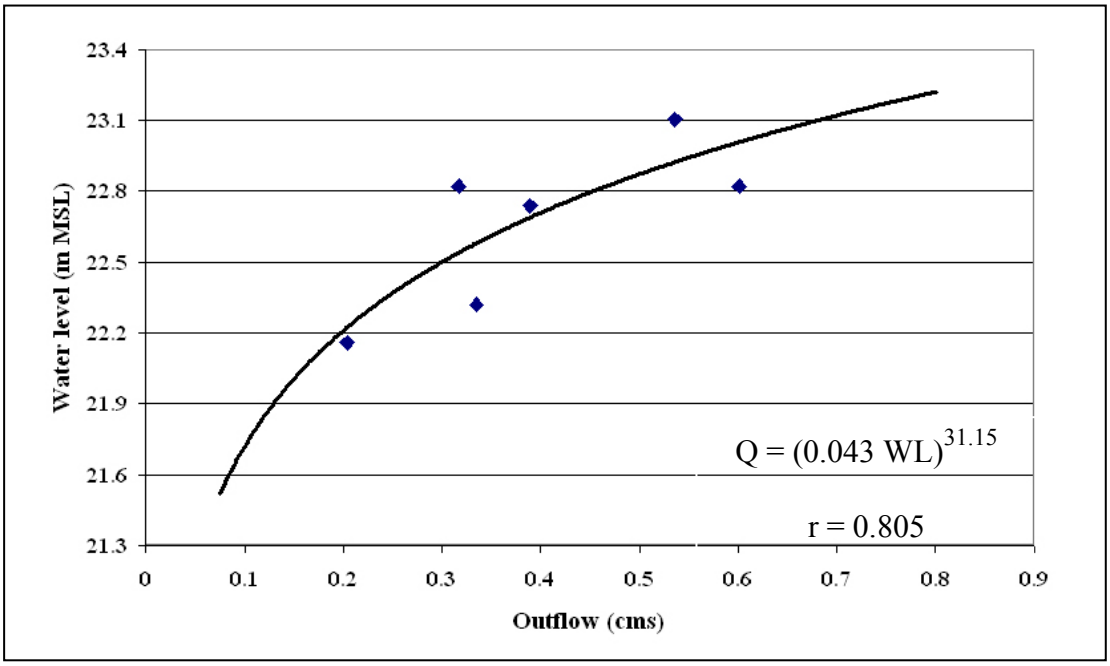

Figure 29 Gravitational outflow rating curve at the outlet location of irrigation canal 1

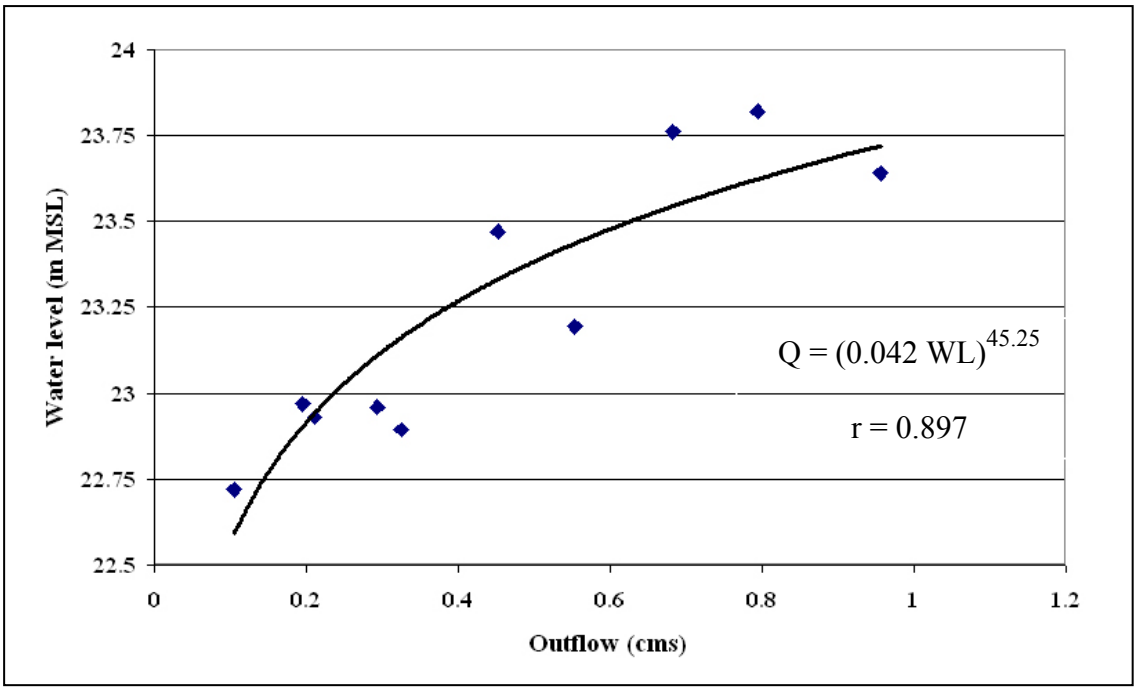

Figure 30 Gravitational outflow rating curve at the outlet location of irrigation canal 2

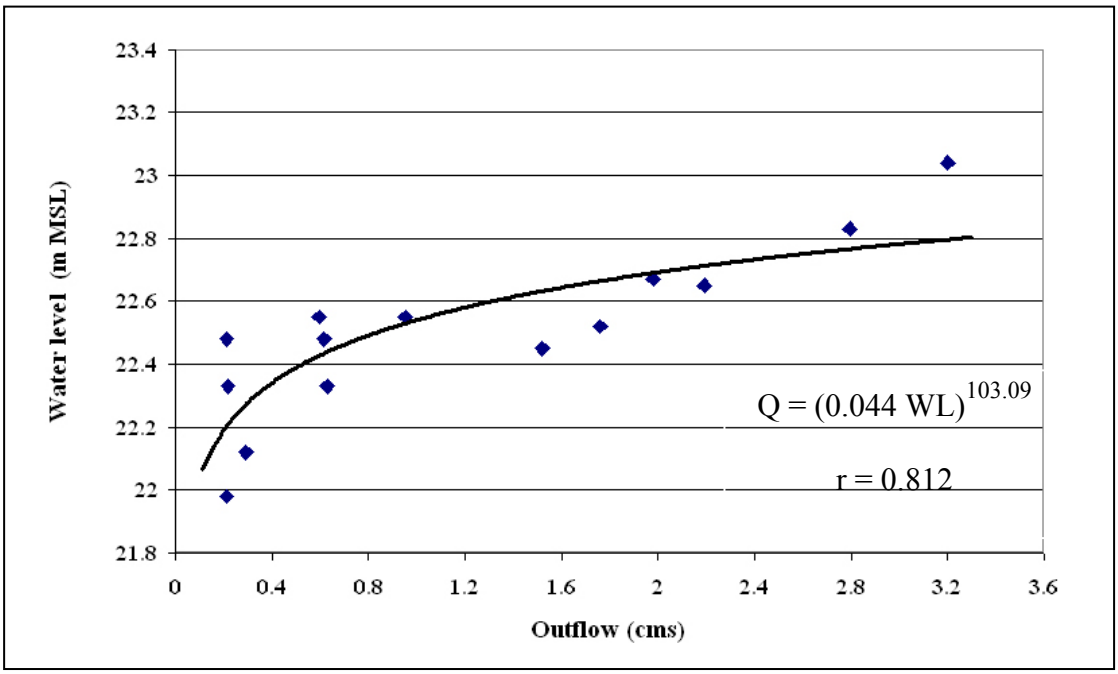

Figure 31 Regulated outflow rating curve at the outlet location of Klong Bon

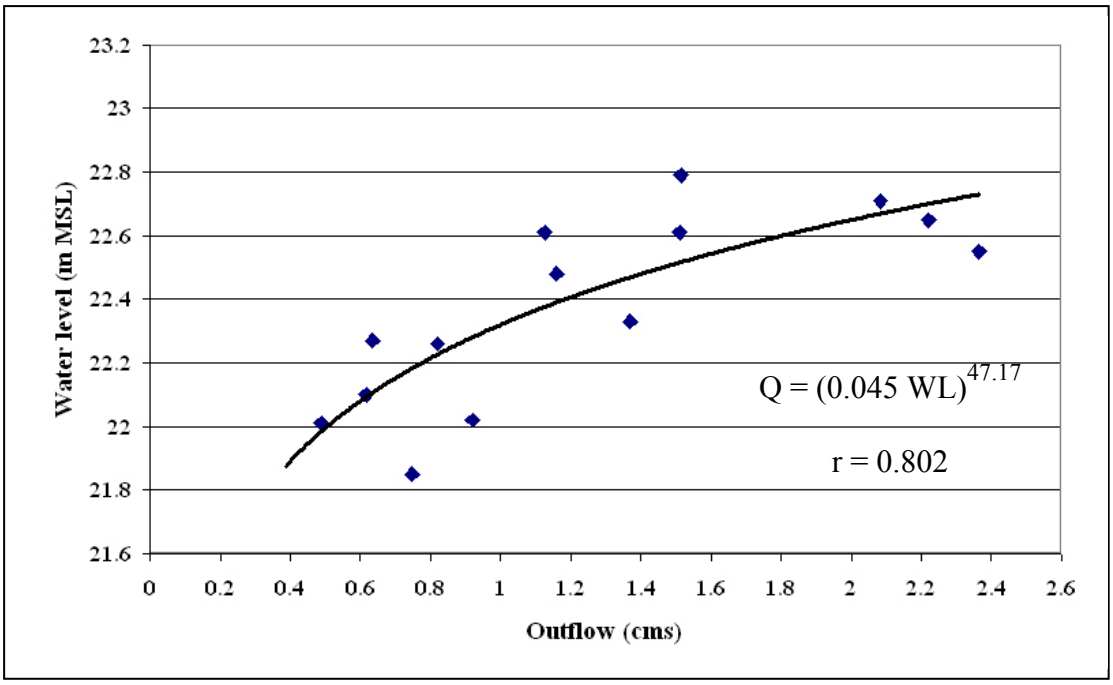

Figure 32 Regulated outflow rating curve at the outlet location of Klong Tatako

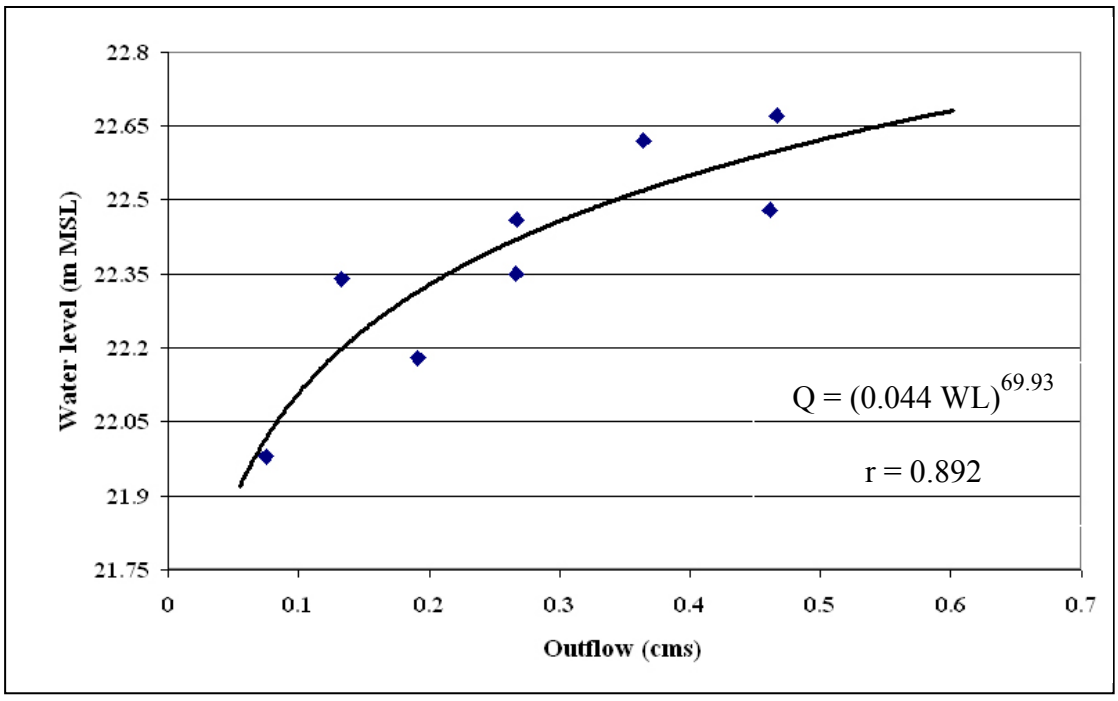

Figure 33 Regulated outflow rating curve at the outlet location of irrigation canal 1

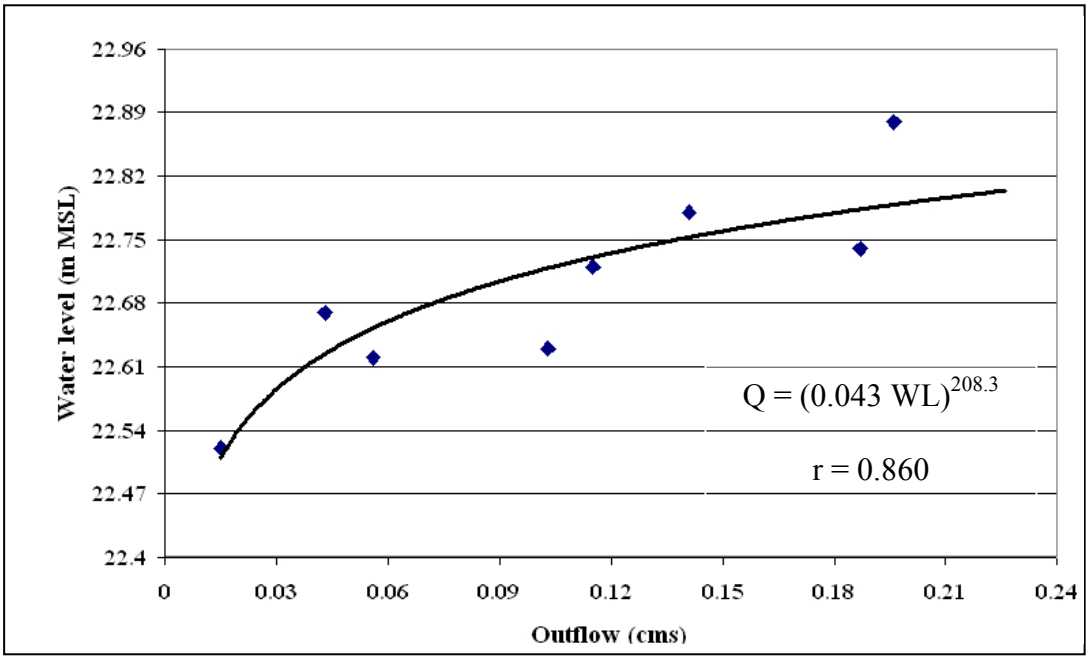

Figure 34 Regulated outflow rating curve at the outlet location of irrigation canal 2

2) Outflows for Aquaculture

Outflows for this purpose are not diverted via lake tributaries and irrigation canals. A total area for aquaculture is approximately 2 square kilometers, and is located between the regulator and the irrigation canal one (as shown in Figure 16). A daily water demand of approximately 0.01 MCM can be transferred directly to the aquaculture areas. Daily outflow for water supply and aquaculture - as mentioned in block 5 of the water budget conceptual model in Figure 17- is very small, therefore it was not used for the water budget calculation.

3) Outflows from Weir and Regulator

Outflows from the weir and regulator usually occur during the wet season when the lake water levels are above the weir and regulator crests, which are at the same level of +24.00 m (MSL). These outflows can be estimated using daily recordings of the water level at the weir and regulator and outflow rating curves of each location as summarized in block 6 of the water budget conceptual

model in Figure 17. The lake water levels and the rating curves for weir and regulator are shown in Figure 19, 35, and 36, respectively.

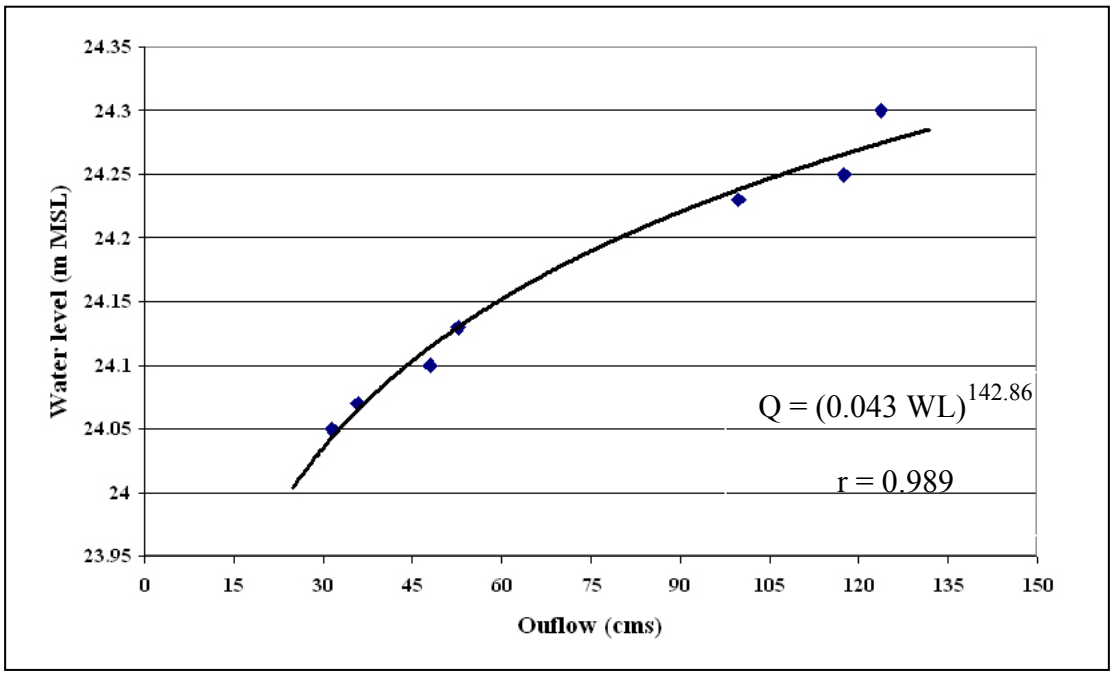

Figure 35 Outflow rating curve at the weir

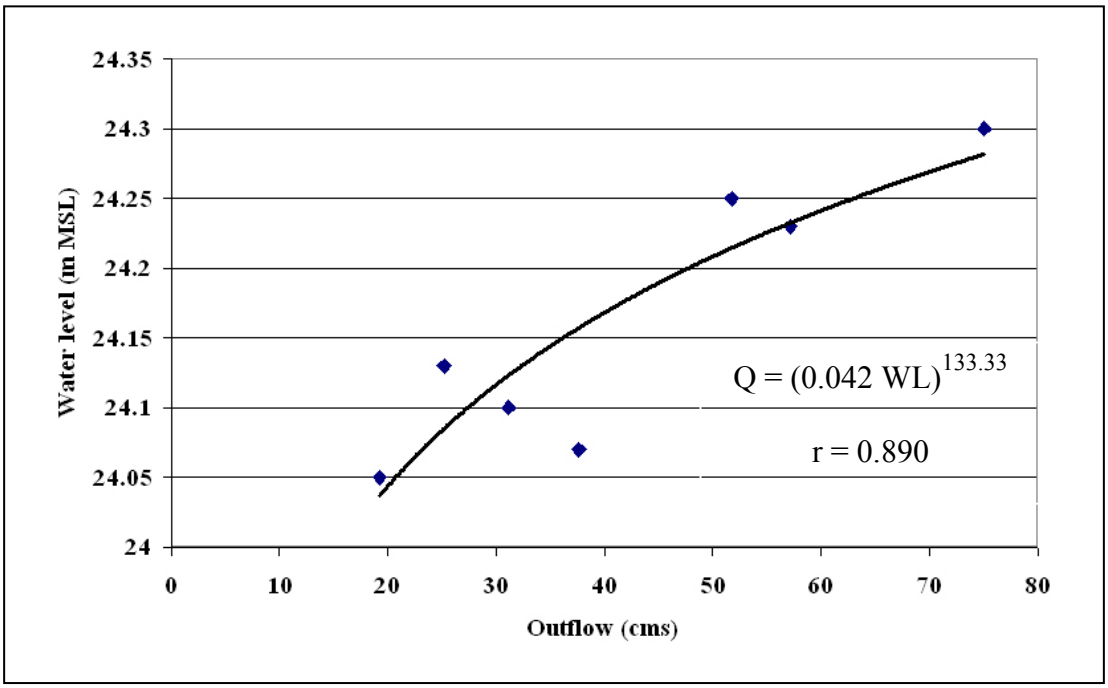

Figure 36 Outflow rating curve at the regulator

1.3 Lake direct rainfall

The daily direct rainfall onto the lake surface was estimated using rainfall data from the meteorological station at Muang Nakhon Sawan, which is approximately 10 km west of Bung Boraphet. Since the 1st of May 2005, non-recording rainfall gauges were installed at four other stations surrounding the lake to improve the direct rainfall estimate. Figure 37 shows the locations of five rainfall stations situated at Huadong Village, Local offiice of FD, Nong Khai Village, Panomsaet Village, and Muang Nakhon Sawan, respectively. The daily direct rainfall onto the lake surface was calculated by weighting the rainfall depths recorded at five rainfall stations using the Thiessen Polygon. The daily direct rainfall volume over the lake surface was calculated by a multiplication of the daily rainfall depth and the lake surface area at specific lake water levels, as summarized in block 7 of the water budget conceptual model in Figure 17.

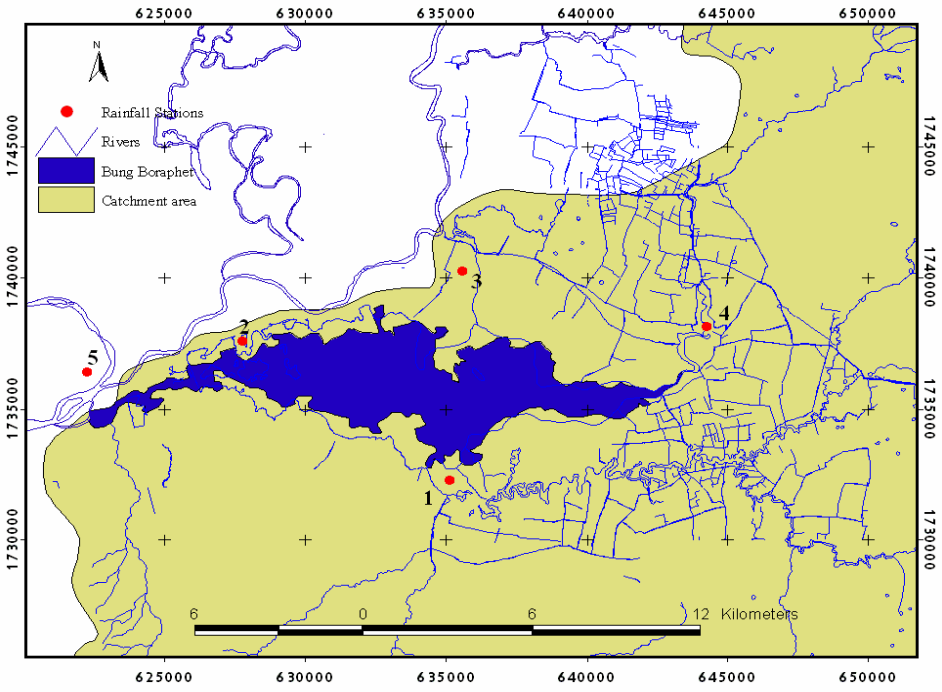

Figure 37 Locations of five rainfall stations used for direct rainfall estimation

1.4 Evaporation

The daily evaporation depth from the lake surface was estimated from the Class A pan evaporation data, recorded at the meteorological station located at Muang Nakorn Sawan meteorological office, using a pan-coefficient as suggested by Chow (1964). Pan-coefficient normally varies between 0.65 and 0.85 (Mutreja, 1986). Water budget calibration results have shown that the pan coefficient in the dry season is higher than that of the wet season. This is because the lake water levels in the dry season, especially between March and June, are lower than the lake levels in the wet season. Moreover, average relative humidity values in the dry and wet seasons are around 64 and 77 percent, respectively. Solar radiation and relative humidity are two main factors that have an effect on the pan coefficient value. In this study, a value of 0.8 was therefore applied during the wet season between July and November. In the dry season, the value of 0.85 was applied between December and February and the value of 0.9 was applied between March and June. These coefficient values were chosen to make the best fit between recorded and simulated lake water stages. The daily lake evaporation volume from the lake surface was calculated by a multiplication of the daily lake evaporation depth and the lake surface area at specific lake water levels, as summarized in block 8 of the water budget conceptual model in Figure 17.

.

1.5 Net seepage loss rate

Lance (1995) suggested that lake seepage can be considered as the net exchange of inflow and outflow with the groundwater system of the lake. In this study, the seepage loss rate from the lake bed was measured directly by the installation of 12 PVC tubes with a 4 inches diameter all over the lake as shown in Figure 38 to represent various soil properties. The gauges were installed vertically by driving the open ended PVC tubes approximately 50 cm into the lake bed and leaving 60 cm above the water surface. Then tops of the tubes were stoppered to prevent water exchange with the atmosphere. The change in water level within each tube measured at 2-3 month intervals was assumed to represent the net exchange between

the lake and the groundwater system at that location. A daily seepage level loss for the lake was calculated from the average of the daily seepage loss values recorded at all 12 locations. The daily volume of seepage from the lake bed was calculated by multiplying the daily lake seepage depth and the lake surface area, as summarized in block 9 of the water budget conceptual model in Figure 17.

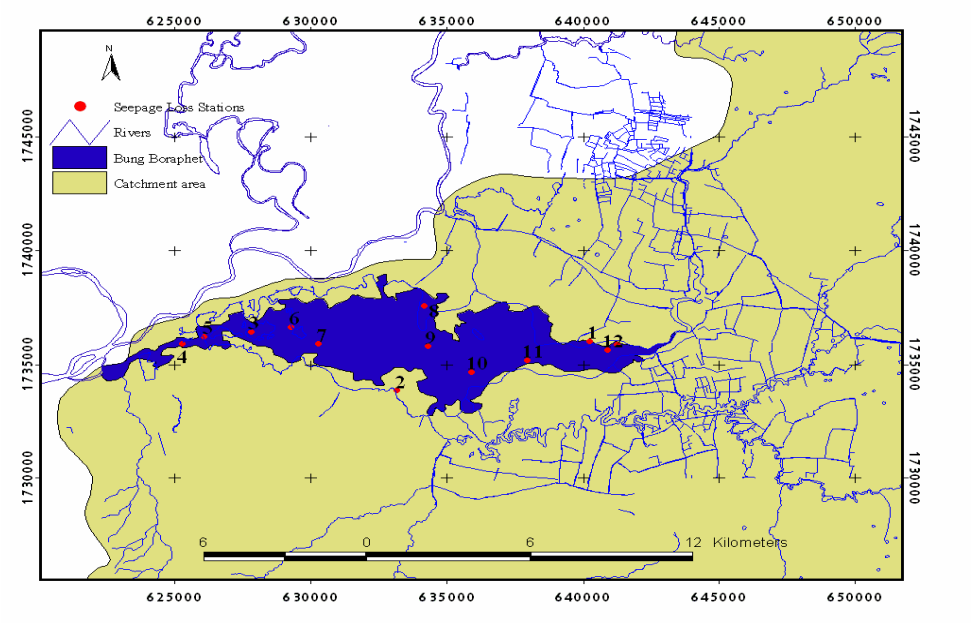

Figure 38 Locations of 12 PVC tubes installing for lake seepage investigation

2. An application of remote sensing to investigate changes in characteristic of Bung Boraphet and its surrounding area.

Temporal and spatial variations of the characteristics of Bung Boraphet and its surrounding areas were examined by the analysis of the Landsat5 images. For images interpretation, PCI Geomatica ™ V.9.1 software was used to identify the different land use and Bung Boraphet's physical characteristics. The processes for applying the remote sensing technique for this dissertation are described as in the followings.

2.1 To collect three Landsat5 images of the last decade (between 1993 and 2003) since the weir crest has been raised to the current level of +24.00 m (MSL). Since land use and physical characteristics of Bung Boraphet and its surroundings

would be affected by different low water levels, three satellite images were therefore collected at the same lake level of +23.00 m (MSL). Collecting dates of the Landsat5 images used in this study are shown in Table 7

Table 7 Collecting dates of the three Landsat5 images used in this study

Image Number	Collecting date
1	December 25, 1993
2	March 2, 2001
3	December 5, 2003

2.2 To assign the three primary colors of red (R), green (G), and blue (B) for the bands 4, 5 and 3, respectively, in the mixing colour process. The resulting product is called the colour composite image that shows the value of R:G:B ratio of each pixel. Different ratios, which depend on the reflectance of the spectral bands, can be used to classify land use patterns and other physical characteristics of the image.

2.3 To reduce the image geometric distortion by applying geometric correction technique. In this process, the ground control points (GCPs), which are well defined locations such as bends of the rivers and road intersections, were located both on the distortion image and on a reference digital map, as shown in Figure 39. To improve an accuracy of the image geometric correction, many GCPs should be defined over the entire image. The distortion images are then adjusted by statistical methods, eg. the least square method, to determine coefficients that can be used to interrelate the geometric correct coordinate and the distorted image coordinate.

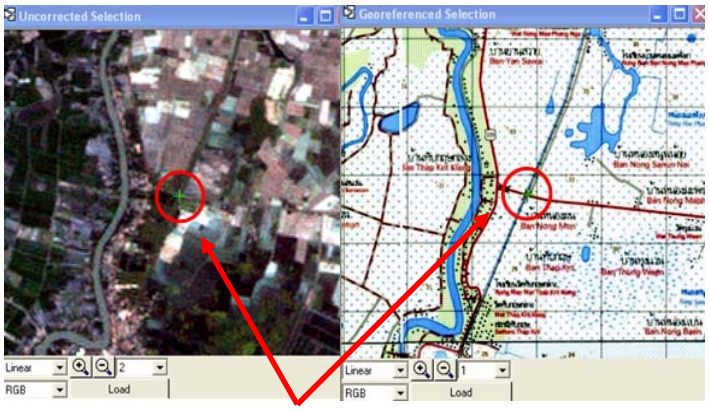

Road intersection used as a GCP

Figure 39 The ground control point used for geometric correction

2.4 To improve the visual interpretability of an image by the image enhancement process. In the utility tools of the PCI Geomatica software, there are many methods used for optional image enhancement. These methods include linear, root, equalization, adaptive, and infrequency. The most suitable method will bring the clearest image visualization. Examples of different image visualizations using different enhancement techniques are shown in Figure 40.

2.5 To prepare the boundary areas of the classified images for the analysis of the physical characteristics in Bung Boraphet and the land use patterns of the surrounding areas. The clipping technique was used to carry out this process by separating the interested area from the entire area. The result of this process is shown in Figure 41.

2.6 To assign the training areas for supervised classification of the physical characteristics in the lake and land use patterns of the lake's surroundings. Within this training process, the representative training areas of the spectral attributes of each land cover type will be specified in the scene.

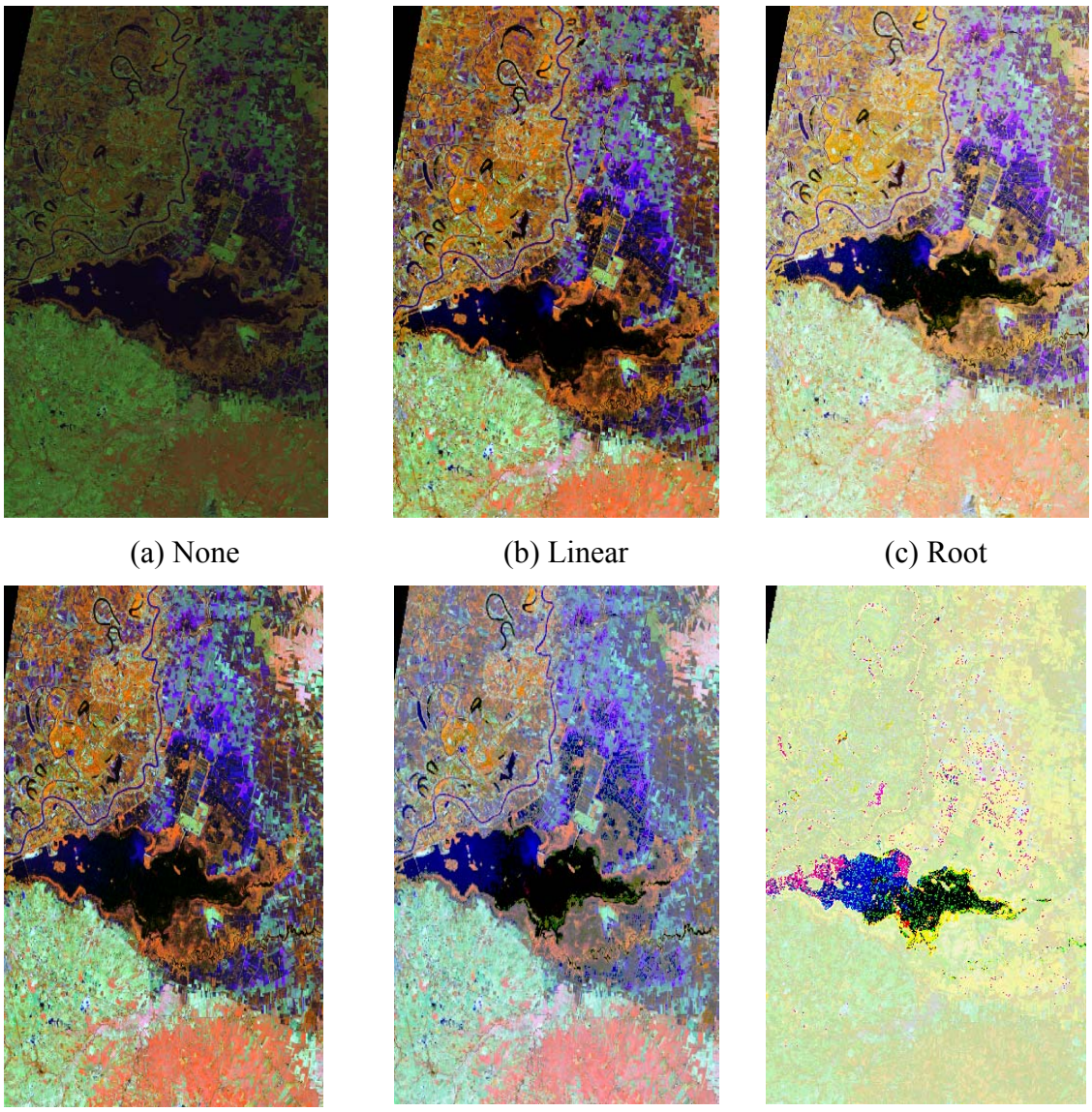

(a) None (b) Linear (c) Root

(d) Adaptive (e) Equalization (f) Infrequency

Figure 40 Different image visualizations using different enhancement techniques

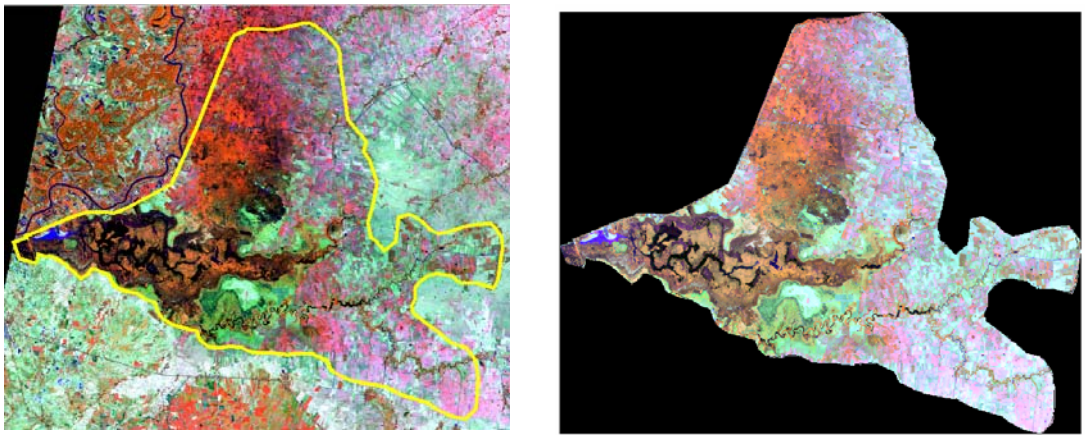

(a) An entire area before applying the clipping technique

(b) An interested area after applying the clipping technique

Figure 41 Areas before and after applying the clipping technique

The training area used in this study and an example of assigning training area process in PCI Geomatica software are shown in table 8 and Figure 42, respectively. It should be reminded that before conducting the process, a well understanding in physical characteristics and land use patterns of the study area is required.

Table 8 Training area for supervised classification in Bung Boraphet and its surrounding area.

Bung Boraphet	The surrounding area of Bung Boraphet
1. Clear Water	1. Paddy field
2. Turbid Water	2. Land prepared for paddy field
3. Floating Plant	3.Dry or open area
4. Submerged Plant	4. Swamp forest

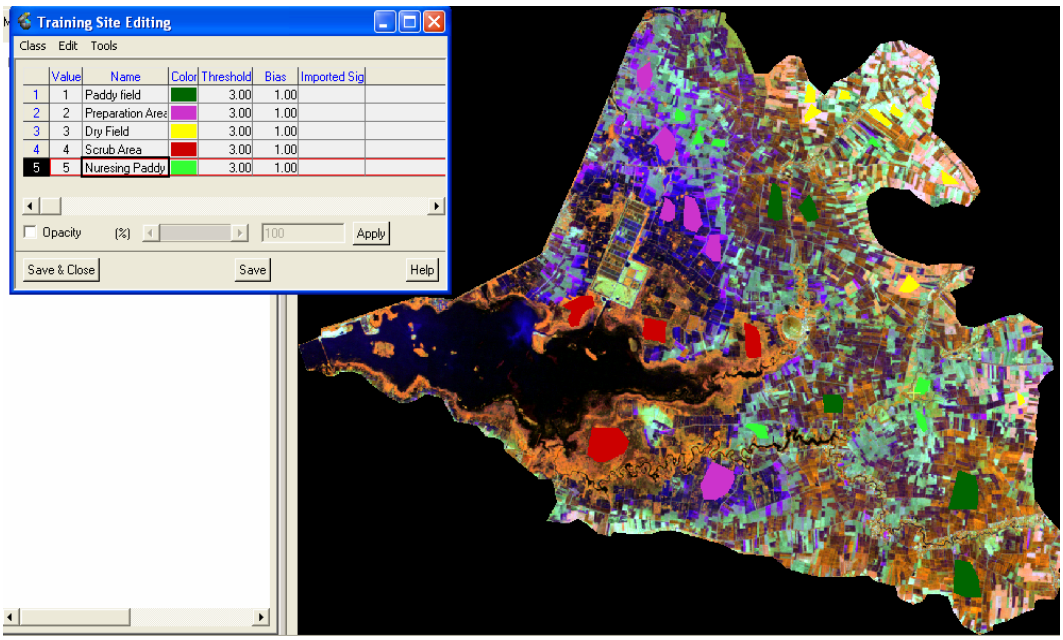

Figure 42 An example assigning training area for PCI Geomatica software

After the training process using a supervised classification method, different ranges of numerical values for each land cover will be used to classify different physical characteristics in the lake and land use patterns of the lake's surroundings. If the numerical values of any pixel cannot be categorized within any land cover, it will be distinguished as "unknown area". The percentage of an unknown area should be less than 2 percent of the overall area. More training areas can be used to reduce the percentage an unknown area. After this classification process, the number of pixels and the percentage for each land cover will be printed as shown in Figure 43.

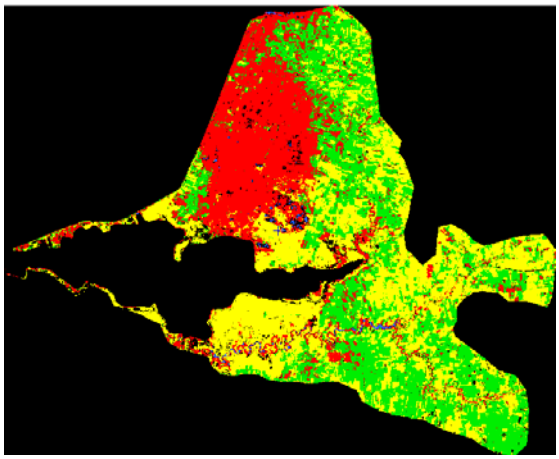

(a) Classified image

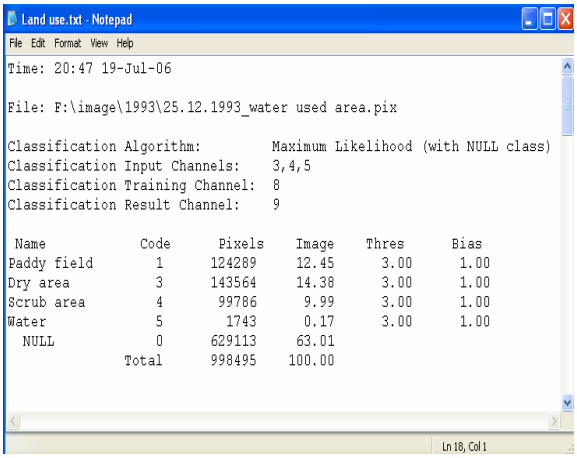

(b) Report of an image classification

Figure 43 The number of pixels and the percentage for each land cover

3. The Study of Bung Boraphet's water quality

To understand the present situation of water quality in Bung Boraphet, spatial and temporal variation of water quality parameters were therefore investigated. In this dissertation, the considered water quality parameters including - DO, BOD, suspended sediment (SS), secchi depth, turbidity, water temperature, chlorophyll-A, total phosphorus, phosphate phosphorus, total nitrogen, ammonia nitrogen, nitrate nitrogen, TKN, and pH – were then collected. After analyze these parameters, critical water quality parameter affecting the sustainability of the lake will be identified and will be studied using the hydrodynamic model (RMA2) and the water quality model (RMA11) for finding the suitable control measures.

3.1 Water quality data collection

The data collection was carried out for 12 times between December 2002 and October 2004 at several locations in Bung Boraphet and its tributaries as shown in Figure 44 and Table 9. The details of data collection for each time can be described in Table 10. Observed water quality parameters obtained from the filed data collections are shown in Table 11.

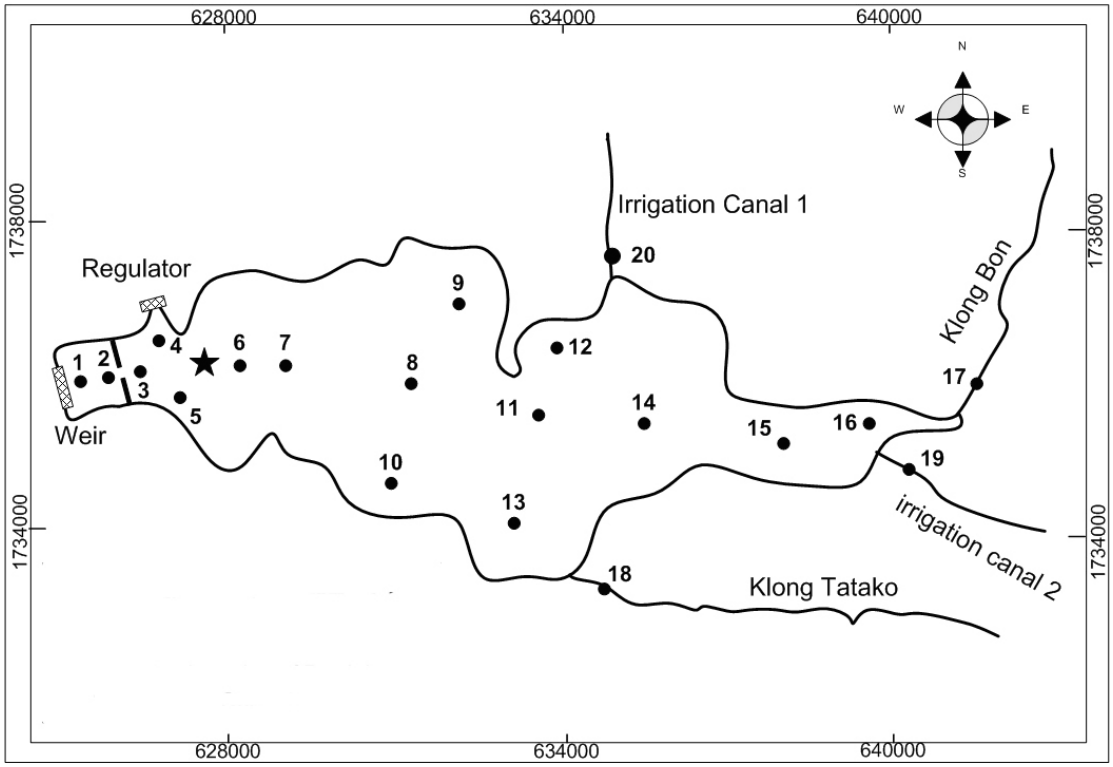

Figure 44 The water quality observation locations

Table 9 The coordinate and description of water quality observation locations

No.	Station name	Coordinate		Note
		E	N	
1	Weir	0625038	1736338	In the Lake
2	Bet. old and new weir	0625825	1736395	In the Lake
3	Old weir	0626533	1736380	In the Lake
4	Front of pier	0629100	1736955	In the Lake
5	Pai Kwang	0627606	1736217	In the Lake
6	Behind sediment mout.	0629315	1736610	In the Lake
7	Kao Wat	0630276	1736362	In the Lake
8	Clear Water	0633184	1736349	In the Lake
9	Kung Takok	0633498	1737324	In the Lake
10	Front of bird park	0631818	134882	In the Lake
11	Ta-Ruang Island	0635738	1735675	In the Lake
12	Pak-Nongkrai Village	0635626	1736332	In the Lake
13	Black Water	0634890	1734426	In the Lake
14	Lam Thong	0637853	1735257	In the Lake
15	Lotus area	0640527	1735578	In the Lake
16	Turbid Area	0642336	1736024	In the Lake
17	Klong Bon	0644256	1738126	Inflow and outflow point
18	Klong Tatako	0635302	1733263	Inflow and outflow point
19	Irrigation Canal 1	0639815	1736342	Inflow and outflow point
20	Irrigation Canal 2	0643252	1735653	Inflow and outflow point

Table 10

Table 10 (Continued)

Table 10 (Continued)

Table 11

Table 11 (Continued)

Table 11 (Continued)

Table 11 (Continued)

Table 11 (Continued)

Table 11 (Continued)

3.2 Data Collections and Model Setup for the RMA2 Model Calibration

In the calibration process of the RMA2, which is the hydrodynamic model, flow velocities at different locations in the lake are the observed data to be compared with the velocities resulting from the model at the same locations. Since velocities in the lake are normally very low until they cannot be measured most of the time, the calibration period therefore need to be carried out during high velocity periods in flooding seasons that usually occur only once or twice a year. Data collections for the calibration process were finally carried out between 9th and 13th October 2004, when the lake water levels were above the weir crest. In the model calibration process, the schematic was also needed to clarify input data. The schematic - which shows the upstream and downstream boundary conditions, and the observed velocity locations within Bung Boraphet - is shown in Figure 45. Data needed for model calibration are explained in the followings.

3.2.1 The Upstream Boundary Condition

The upstream boundary conditions are the observed daily discharges collected at Klong Bon, Klong Tatako, and 2 irrigation canals as their locations shown in Figure 45. The observed daily discharges at these 4 locations during the calibration period are shown in Table 12.

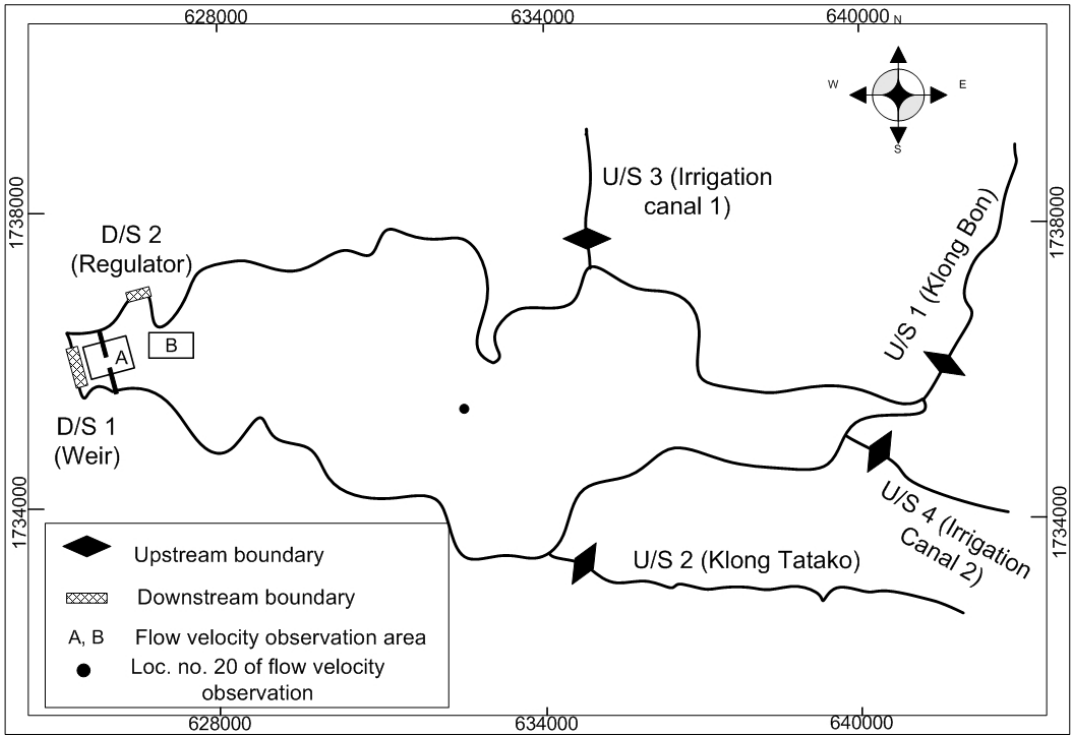

(a) Schematic of RMA2 Model

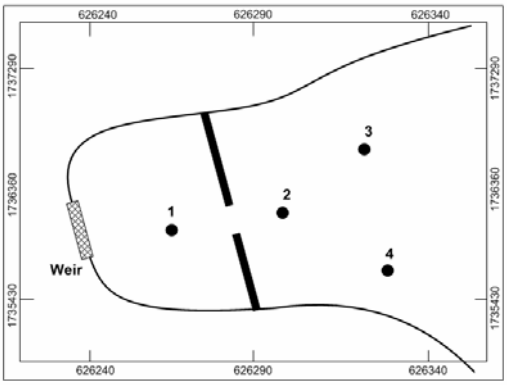

(b) Observation locations in area A

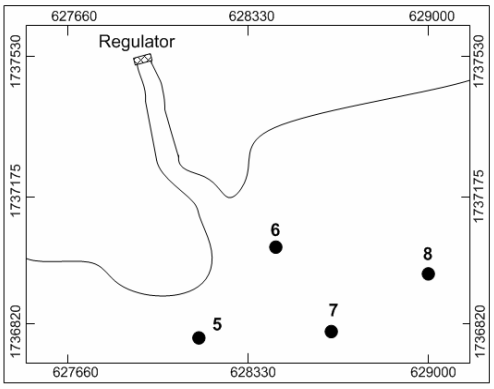

(b) Observation locations in area B

Figure 45 The schematic for the RMA2 Model and observed flow velocity locations

Table 12 The observed daily discharges at 4 locations during the calibration period in October 2004

Upstream Number	Location	Discharge (m^3/s)				
		9^{th}	10^{th}	11^{th}	12^{th}	13^{th}
U/S 1	Klong Bon	17.79	16.53	15.13	14.3	10.23
U/S 2	Klong Tatako	47.84	47.08	46.34	45.61	44.89
U/S 3	Irrigation Canal 1	5.67	5.23	4.65	4.51	4.44
U/S 4	Irrigation Canal2	3.71	3.34	2.75	2.65	1.98

3.2.2 The Downstream Boundary Condition

The downstrem boundary conditions are the observed daily water levels of the lake collected at the weir and the regulator as their locations shown in Figure 45. As these two locations have the same water levels, the data was therefore observed only one location at the regulator by the FD. The observed daily water levels at these two locations during the calibration period are shown in Table 13.

Table 13 The observed daily water levels at the regulator during the calibration period in October 2004

Date	Water level (m, MSL)
9^{th}	24.10
10^{th}	24.08
11^{th}	24.05
12^{th}	24.05
13^{th}	24.04

3.2.3 The Meteorological data

The meteorological parameters needed for the model calibration consist of the wind speeds, wind directions, evaporations, and rainfall depths. These data were observed at the nearest meteorological station located at Muang Nakorn Sawan, about 10 km northwestern of the lake. The observed meteorological data during the calibration period are shown in Table 14.

Table 14 The observed meteorological data during the calibration period in October 2004

Date	Meteorological data			
	Wind speed (knots)	Wind direction (degree)	Evaporation (mm)	Rainfall (mm)
9 th	6	130	4.13	0
10th	12	70	4.28	0
11th	8	40	3.85	0
12th	6	60	4.13	0
13th	6	30	4.05	0

3.2.4 The Bathymetry and the mesh generation of Bung Boraphet

For the model uses, the bathymetry of Bung Boraphet has to be prepared using the volume-area-elevation curve and the spot data surveyed by the RID in 2002. The lake area within the elevation below the weir crest (+24.00 m, MSL) was delineated and used as the boundary for the RMA2 model usage. The finite element mesh within this boundary area was then generated using the meshing technique provided in the model utilities (see Figure 46). The contour lines between the lowest elevation (+17.00 m, MSL.) and the highest elevation (+25.00 m, MSL.) were later created by the model utilities (see Figure 47).

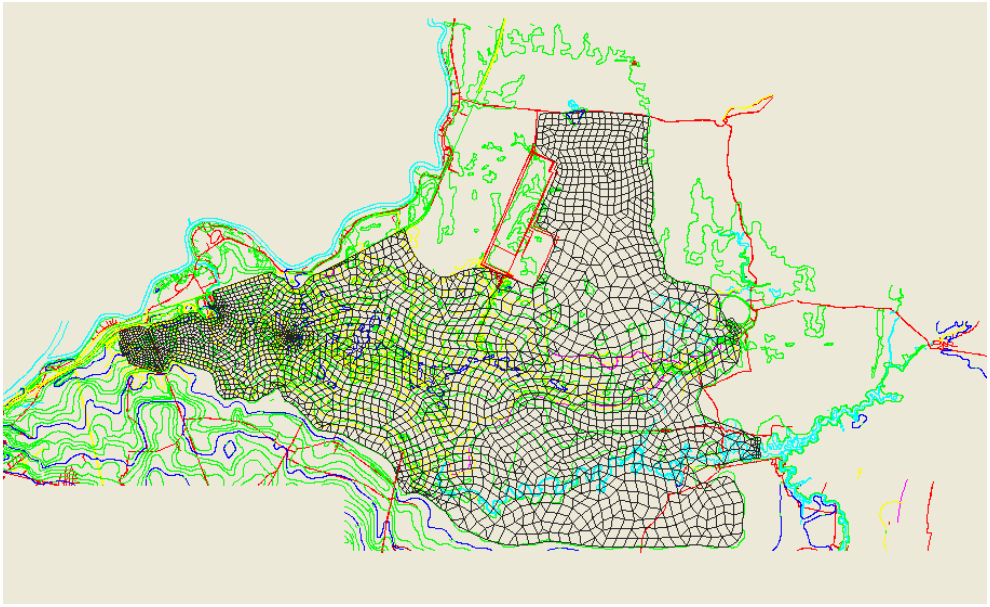

Figure 46 The finite element mesh within this boundary area

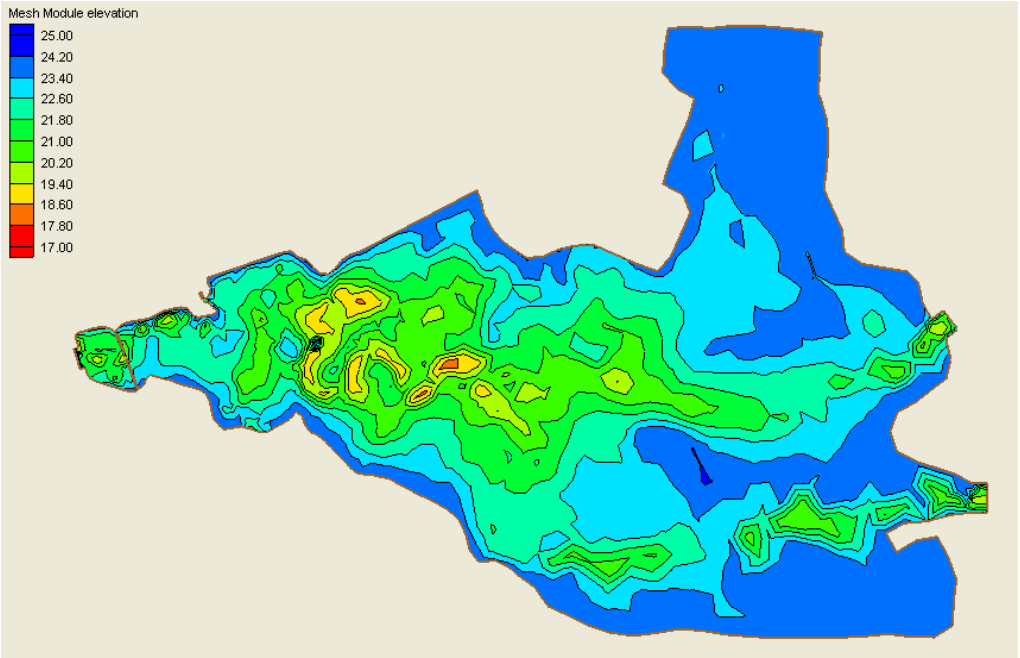

Figure 47 The contour lines between the lowest and the highest elevations

3.2.5 Model control parameters

Beside the data input for the RMA2 Model as explained between items 3.2.1 and 3.2.4, the model control parameters are also needed as the input data. The control parameters consist of the roughness coefficients (Manning's n) along the lake bottom and the turbulence exchange coefficient in x and y direction (E). The suitable values of the roughness coefficients and the turbulence exchange coefficient at nine observed points can be adjusted until the calculated velocity close to the observed velocity. However the control parameters have to be identified at every mesh, therefore any meshes located close to any observed points were used the similar values. Moreover, any physical characteristics that would affect the control parameter values - such as the open water, lotus zone, and submerge plant zone - were also used to consider the most suitable control parameters.

3.2.6 The flow velocity data

The flow velocity data was observed at several stations, as their locations shown in Figure 45. Even the flow velocities at these locations closed to the overflow point at the regulator were significantly higher than other regions in the lake. However the velocities were still too low to be measured accurately by the current meter, the floating cylinder rods with 1.5 inches in diameter were therefore used to measure the water velocities. During the calibration procedure, the observed water velocities will be compared to the water velocities calculated using the RMA2 Model. The measured velocities at these locations during the calibration period are shown in Table 15.

Table 15 Observed water velocities at 9 locations during the calibration period in October 2004

Date	Time	Flow Velocity (m/s)								
		Loc.1	Loc.2	Loc.3	Loc.4	Loc.5	Loc.6	Loc.7	Loc.8	Loc.9
9 th	14.00	0.0320	-	-	-	-	-	-	-	-
9 th	16.00	-	0.0602	0.0310	0.0290	0.0302	0.0152	-	-	-
9 th	17.00	-	-	-	-	-	-	-	0.0089	0.0059
10th	11.00	0.0410	0.0662	-	-	0.0329	0.0154	0.0203	0.0105	-
10th	12.00	-	-	0.0310	0.0366	-	-	-	-	-
10th	15.00	0.0430	-	-	-	0.0313	-	0.0198	-	-
10th	16.00	-	0.0668	0.0320	0.0370	-	-	-	0.0102	0.0061
11th	11.00	0.0402	0.0669	0.0320	0.0362	0.0312	0.0159	0.0188	0.0117	-
11th	14.00	-	0.0648	-	-	-	-	-	-	-
11th	15.00	-	-	-	-	0.0310	0.0157	-	-	-
11th	16.00	-	-	-	-	-	-	0.0199	0.0118	-
12th	11.00	0.0371	0.0610	-	-	-	-	-	-	-
12th	12.00			0.0311	0.0351	0.0285	0.0145	0.0162	0.0103	0.0054
12th	14.00	-	-	-	-	-	0.0146	0.0164	-	-
12th	17.00	-	-	-	-	-	-	-	-	0.0053
13th	10.00	-	-	-	0.0301	-	-	-	-	-
13th	11.00	-	-	-	-	0.0260	0.0130	0.0159	0.0108	0.0052
13th	12.00	0.0312	0.0587	0.0288	-	-	-	-	-	-

3.3 Data collections and model setup for the RMA2 Model application

After the RMA2 Model was calibrated by adjusting the control parameters, it will be applied to evaluate the flow velocities and water depth for using as the in put data of the RMA11 Model. This application was carried out during the calibration period of RMA11 between 11th February and 11th July 2003. During this period, the lake water level was drawn down from +23.39 to 22.21 m (MSL) because

of abstraction water from the tributaries and irrigation canals upstream of the lake for rice irrigation in the surrounding area. Therefore, there may be times when portions of the area in Bung Boraphet may become devoid of water. To imitate this condition, the wet/dry checking algorithm provided in RMA2 was therefore applied. Once an element dries in RMA2, newly formed area boundary is re-created by eliminating dry element. However this wet/dry checking algorithm can limit the stability of the model (Stoscheck and Matheja, 2000). To reduce this unstable, the boundary area was then re-generated by delineating along the contour line at +23.00 m (MSL). However the model control parameters of each mesh location are also as same as the results of RMA2 calibration. The new finite element mesh and the contour lines within the elevation below +23.00 m (MSL) are shown in Figure 48 and Fig 49, respectively

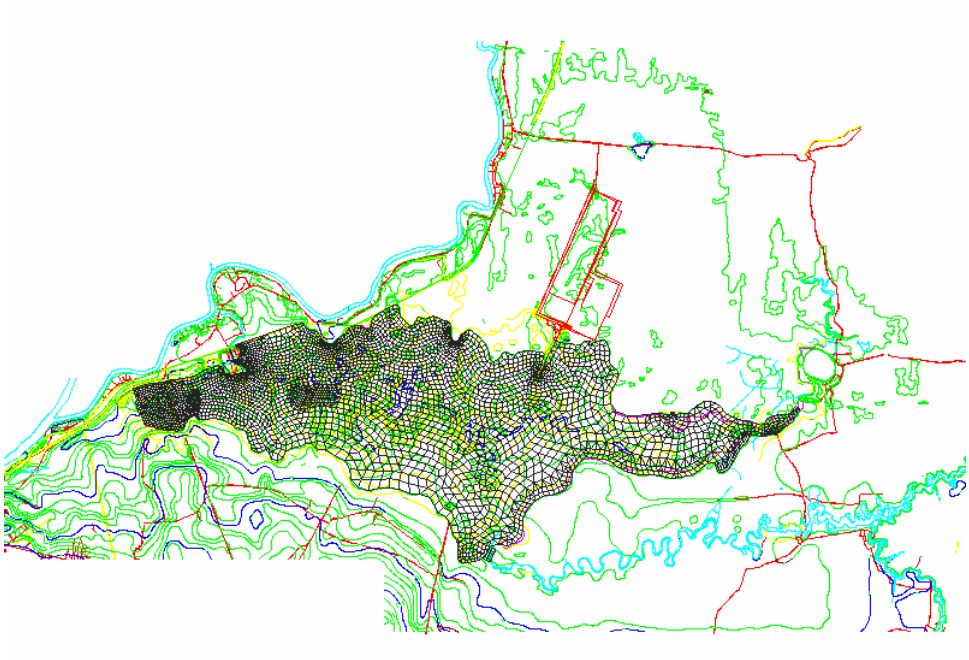

Figure 48 The new finite element mesh of the RMA2 Model using for the RMA11 calibration

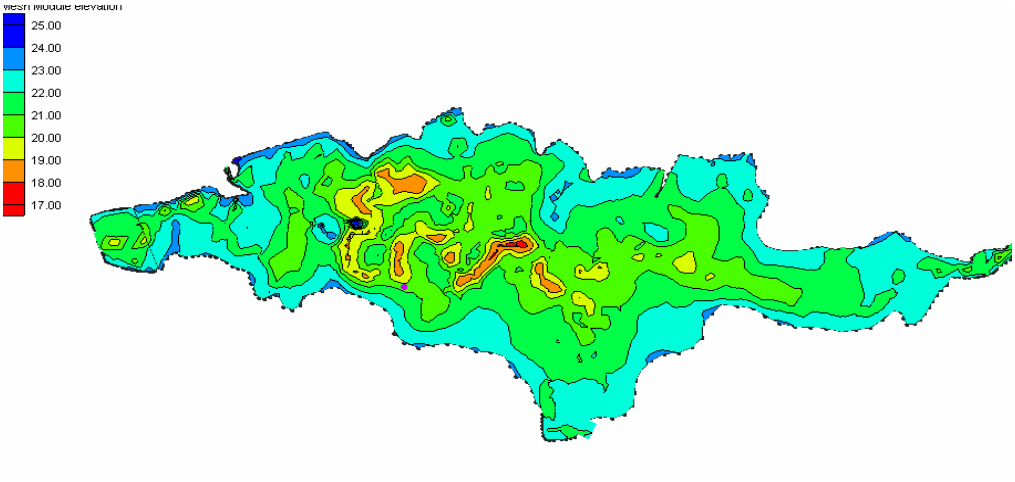

Figure 49 The contour lines within the elevation below +23.00 m (MSL)

The upstream boundary conditions of the RMA2 model used for this period area are the calculated daily discharge at Klong Bon, Klong Tatako and the 2 irrigation canals, which were evaluated from the daily water budget study of Bung Boraphet provided by Sriwongsitanon et.al. (2007). Daily calculated discharges of these locations during this period are shown in Figure 50.

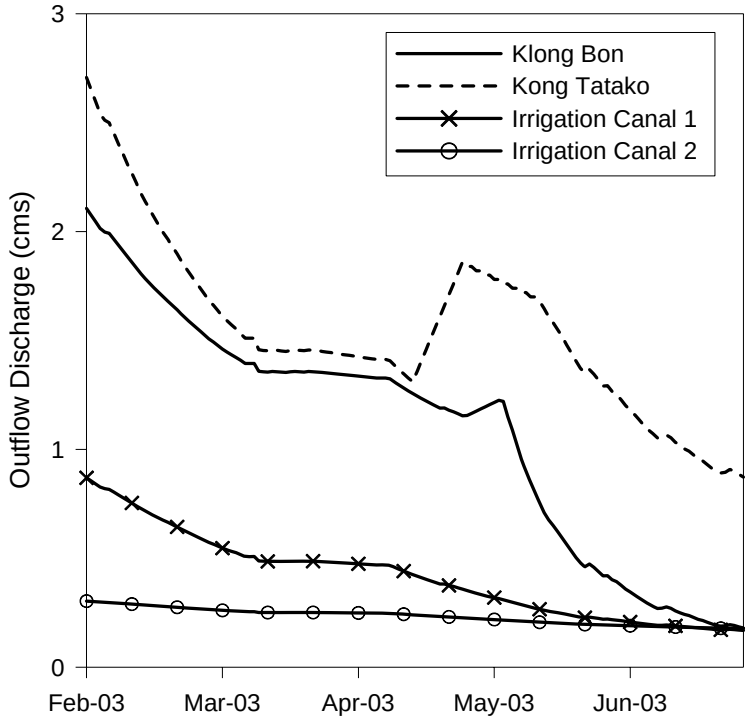

Figure 50 Upstream boundary condition of RMA2 model application

The downstream boundary conditions of the RMA2 Model used for this application are also the observed daily water levels of the lake at the weir and the regulator. The observed daily water levels at these two locations during the application period can be shown in Figure 51. While the meteorological parameters needed for the model application consisting of the wind speeds, wind directions, evaporations, and rainfall depths were also the observed data at Muang Nakorn Sawan meteorological station.

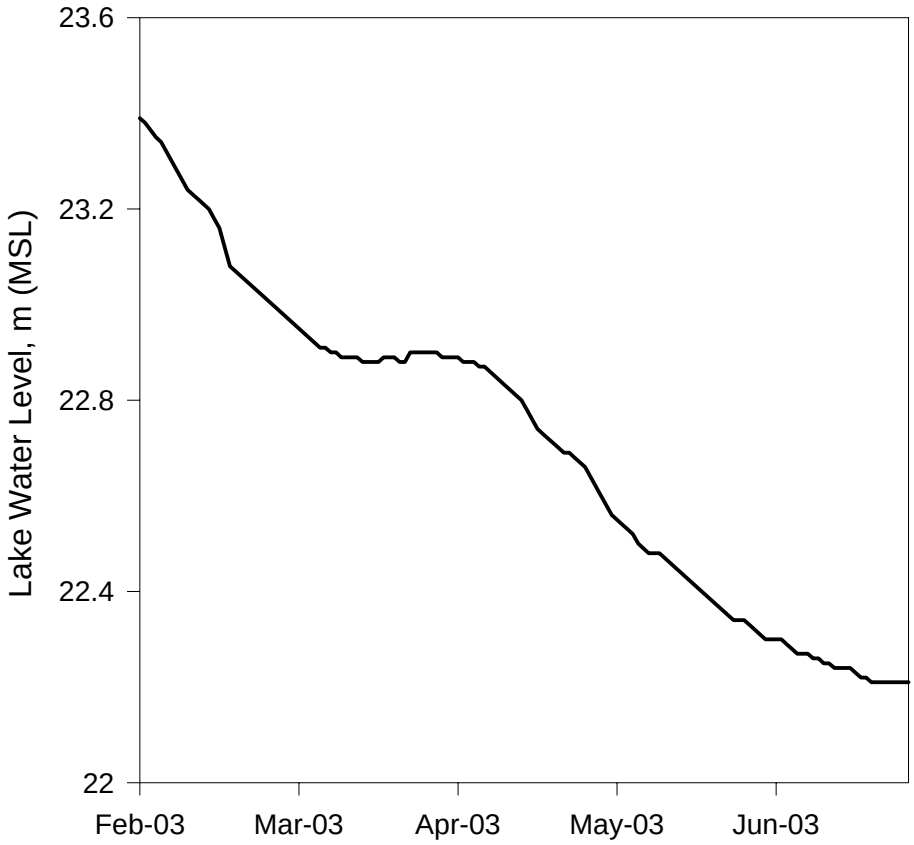

Figure 51 The observed daily water levels at the regulator between 11 February 2003 and 11 July 2003

3.4 Data Collections and Model Setup for the RMA11 Model Calibration

In the calibration process of the RMA11, which is the water quality model, suspended sediment concentrations (SS) at different locations in the lake are the observed data to be compared with the SS resulting from the model at the same locations. Data collections for the calibration process were carried out between 10th February and 11th July 2003, when the outflow period occurred. In the model calibration process, the schematic was also needed to clarify input data. The schematic - which shows the boundary conditions, and the SS calibrated locations within Bung Boraphet - is shown in Figure 52. Data needed for model calibration is explained in the followings.

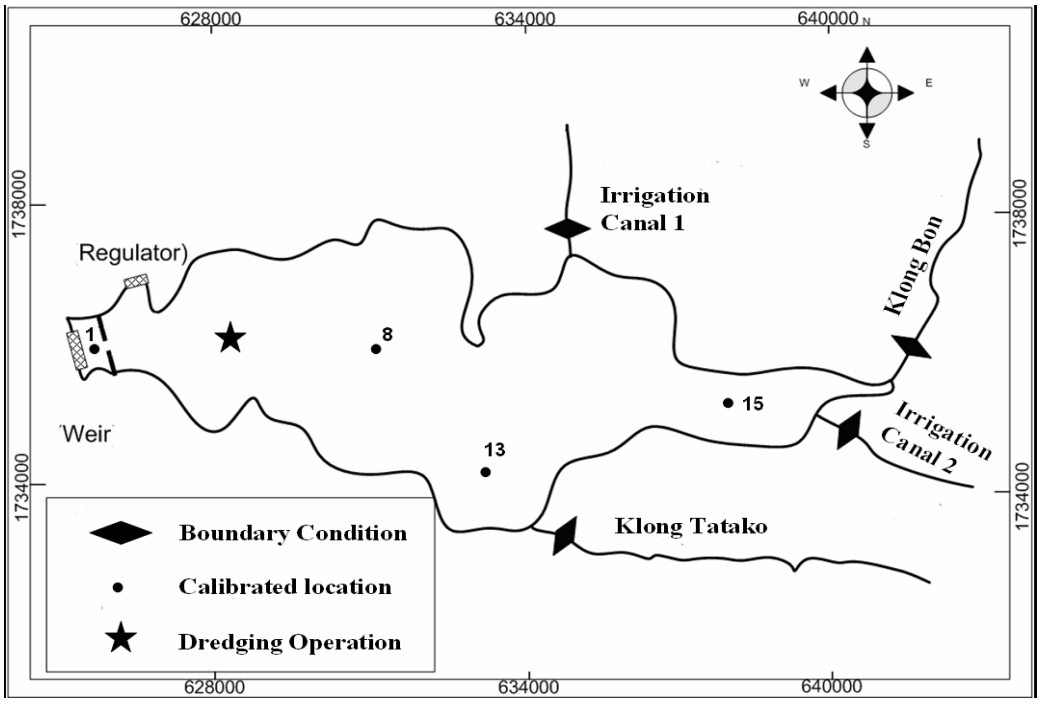

Figure 52 A schematic for the RMA11 Model and SS calibrated locations

3.4.1 Suspended sediment loading

Since the calibration period of the RMA11 Model is in the outflow period, there was no external SS loading occurring in that period. However,

there was an internal SS loading resulting from dredging operation that was carried out by the FD.

Since the data of SS loading from dredging operation is not available. It needs to be estimated (by trial and error) using the RMA11 Model to get the best fit between the observed and calculated SS concentrations at the same locations.

3.4.2 Boundary Condition

The boundary conditions are the daily SS concentration at the outlet of Klong Bon, Klong Tatako, and 2 irrigation canals as their locations shown in Figure 52. However, SS concentrations at these 4 locations were collected only two times on the 10th February and 11th July 2003. Daily SS concentrations at these locations needed to be interpolated during these two days to be used as the boundary condition. Interpolated results are shown in Figure 53.

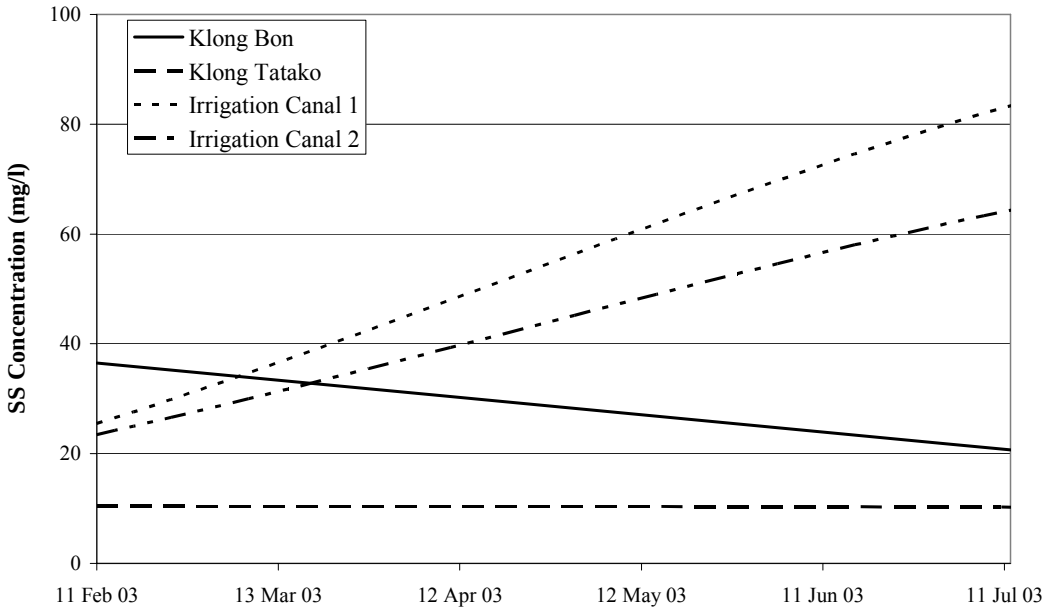

Figure 53 Daily SS concentrations at the outlet of four tributaries

3.4.3 Model control parameters

Model control parameters of the RMA11 Model are needed as the input data for model calibration. The control parameters consist of 8 parameters as in the followings.

1) diffusion coefficient in x and y direction for each element type which varies between 100 and 500 m^2/s

2) Von Karmans constant which has the optimum value varied between 0.4 and 0.6

3) erosion rate constant for the bottom layer which has the optimum value varied between 8.0E-7 and 5.0E-4

4) critical shear stress for top layer which has the optimum value varied between 0.026 and 0.1 N/m^2

5) critical shear stress for bottom layer which has the optimum value varied between 0.026 and 0.1 N/m^2

6) critical shear stress for deposition of new layer which has the optimum value varied between 0.026 and 0.1 N/m^2

7) bed roughness height which has the optimum value varied between 0.5 mm and 5 mm

8) settling velocity which has the optimum value varied between 5.0E-6 and 9.0E-5 m/s)

The value for these parameters has to be adjusted until the calculated SS concentration at four locations (at numbers 1, 8, 13, and 15 as shown in Figure 52) close to the observed SS concentration.

3.4.4 The observation of SS for RMA11 calibration

As roughly explained above about the observed SS concentration that had been collected at four locations within the lake, details of the observation time and SS concentration value at these locations are shown in Table 16.

Table 16 Observation time and SS concentration value at 4 locations to be used for model calibration

Date	Time	SS Concentration			
		no.1	no.8	no.13	No.15
10 Feb 03	13.20	16.00	11.00	-	13.00
10 Feb 03	19.35	-	12.00	9.00	14.00
11 Feb 03	10.05	-	12.00	-	9.00
11 Feb 03	13.25	-		-	31.00
27 Apr 03	11.15	-	13.00	8.00	17.00
22 May 03	10.30	34.00	10.00	-	38.00
11 July 03	12.00	15.30	10.05	-	-

RESULTS AND DICUSSION

Based on the objectives of this study, results and discussion can be separated into four parts. The major problems facing the sustainability of Bung Boraphet is described in the first part. The results and discussion of water quantity analysis of Bung Boraphet, remote sensing investigation of Bung Boraphet and its surrounding areas, and the water quality analysis of Bung Boraphet are explained in the second, third, and fourth parts, respectively. Details of each part are described as in the followings.

1. The major problems facing the sustainability of Bung Boraphet

Learning from the field surveying, primary data collection and interviewing with the all stakeholders, the major problems facing the sustainability of Bung Boraphet can be declared as in the following.

1.1 Illegal settlements in BB conservation zone

Some of the area in the conservation zone has been invaded by more than 30,000 people. Residential neighborhoods and government institutional areas are settled in this zone. There are only 66 square kilometres out of 212 square kilometres - the original conservation area - left without invaders. Causes and effects of illegal settlements are described below.

1.1.1 Causes of illegal settlements

There are two main causes of illegal settlements in BB conservation zone occurring since this zone was initially announced in 1937. These are according to unclear boundary of BB conservation zone and no punishment applied to invaders. Detail of each item is described below.

1) Unclear boundary of BB conservation zone

The Finance Ministry announced the BB conservation zone for the area of around 212 square kilometres and installed bench marks to locate its boundary. However, most of the bench marks were continuously removed or dislocated by invaders. As the result, invaders can easily settle in this zone and this problem is already very complicate to solve because they has claimed their right for their long time settlements.

2) No punishment applied to invaders

There is no punishment applied to invaders. Therefore the number of invaders continuously increases with time until there are more than 30,000 people in 2006. Invaders not only occupy the area in the conservation zone but also claim their right to use water storage in BB according to their farming practices. They normally demonstrate at the provincial office or ask for local politician support for their needs. In the wet season, they usually request to the Fisheries Department (FD) to open the regulator to reduce flooding in their paddy farms even FD needs to store more water for the dry season. In the dry season, they always request to the Royal Irrigation Department (RID) to divert more water by pumping from BB into tributaries and irrigation canals that can be easily taken to serve their paddy farms even the water level is lower than +23.00 m (MSL), which is the minimum recommended level suggested by FD for sustainable flora and fauna biodiversity and ecosystem integrity in the wetlands.

1.1.2 Effects of illegal settlement

Many problems occurred according to the illegal settlements as described below.

1) At present, water storage of the lake is around 100 million cubic metres (between the level +23.00 and +24.00 m MSL – weir crest level) that can be

used during the dry season. The study of daily water balance carried out in this research has shown that nearly half of the stored water evaporates. Another half is mainly used for paddy farm in BB conservation area and surroundings. However, the water level recording by FD between 1993 and 2005 has shown that the water levels for 9 years out of 13 years are lower than the level of +23.00 m MSL. The situation was more severe in the last 4 years, when the average minimum water level was around +22.06 metres (MSL). This phenomenon would severely interfere the well being of fish and other flora and fauna biodiversity.

2) The illegal settlements in BB conservation zone caused an environmental degradation. This is according to the following issues.

a. Agricultural practice using chemical pesticide, insecticide, and fertilizer, and then discharging into BB to affect water quality of the lake and increase algae bloom problem,

b. Waste water from residential neighbourhoods and government institutional areas,

c. Harvesting pressure on fish and bird population by using unsuitable and especially illegal fishery instruments such as an electrical appliance, over fishing, bird hunting, and damaging their habitats,

d. Lack of serious punishment for illegal actions,

e. Lack of water quality and biodiversity data described environmental degradation for public understanding,

f. Lack of public awareness and public participation involving an environmental protection of their lake.

3) BB has been known among Thai people as the symbol of Nakhon Sawan Province according to its large water surface with beautiful scenery of its wetland and flora and fauna biodiversity. BB is therefore one of the province tourist attractions which generates income for the local people. Overuse of water for paddy farms and environmental degradation generated by invaders will have tremendous effects on BB integrity and BB will no longer be known as a symbol of Nakhon Sawan Province. This would affect people well being and their satisfaction. BB can be later promoted as an ecotourism destination that would bring more income to local people once the situations of BB recovers to a certain level.

1.2 Decreasing water capacity in BB by sedimentation

Like most of the lakes, BB is facing sedimentation problem lead to water storage decreasing from time to time. Causes and effects of sedimentation are described below.

1.2.1 Causes of sedimentation can be distinguished into three categories as concluded in the followings.

1) According to the number of population continuously increase with time but land resource is limited. Forest areas are changing into agricultural, residential, and industrial areas. Sedimentation is potentially increased especially during large flood events because of these changes. This is also the case happening in the BB catchment area. Most of sedimentation comes from two main tributaries, Klong Bon and Klong Tatako. Some sediment also comes from Nan River via the regulator at Klong Boraphet occurring once FD opens the regulator to divert flows from the Nan River into BB and when the water levels in the Nan River are higher than the regulator crest.

2) There are more than 65 percent of agricultural areas in the BB catchment area of around 4,288 square kilometers. For agricultural practices, farmers

usually apply fertilizer for their farms. The residual of their uses is then discharged into natural canals and some of the water will finally flow into BB in the wet season. As a result, algae bloom has been occurred in BB particularly in the dry season between December and July. Died off algae will be submerged and accumulated as sediment on BB bed. However, some algae will be washed away from BB during flooding period when water levels are higher than the weir crest. It can be concluded that nutrient resulting from fertilizer applied for agricultural areas is one of the main causes of BB sedimentation.

3) FD has realized sedimentation problem of the lake, therefore daily dredging operation has been continuously carried out for more than 20 years with a capacity of around 1 million cubic metres per year since 1993. However, dredged sediments have not been managed properly by leaving them in the lake creating the sediment's mountains. During dredging operation, re-suspension process occurs and some of dredged sediments flow back into BB. Field investigation carried out in this study has shown an evidence of higher turbidity compared with surrounding areas happening at dredging operation locations.

1.2.2 Effects of sedimentation can be summarized into three categories as concluded in the followings.

1) Water capacity in BB is decreasing by sedimentation. The Royal Irrigation Department (2004) reported that sedimentation in BB from its catchment area is around 2.0 million cubic metres per year calculated using sediment data recorded at runoff stations in the Nan River. However, the physical characteristics in the Nan River are quite different from that of in the BB. Land slope and channel slope of the Nan River and its tributaries are a lot steeper than that of the BB's tributaries. Therefore, sedimentation in BB should not be as much as in the Nan River. As mentioned earlier, FD has been carried out dredging operation since 1993 with a capacity of around 1 million cubic metres per year. However, sediment in BB tends to increase with time. Therefore, sedimentation occurring in the lake should be between 1 and 2 million cubic metres per year. If sedimentation occurring in the lake

around 1.5 million cubic metres per year, the storage capacity of the lake (177 million cubic metres) without dredging operation will be reduced for 50 percent in around 60 years.

2) Water shortage situation will be worsened with time as sedimentation increasingly affecting water storage capacity in the lake. At present, water storage of the lake between the level +23.00 (m MSL) (minimum recommended level for biodiversity) and +24.00 m MSL (weir crest) is around 100 million cubic metres. Nearly half of the stored water evaporates. Only 50 million cubic metres in dry season is not sufficient for irrigation in most of the years. With increasing sedimentation of the lake, water shortage in dry season tends to be more critical. Thai government has been trying to solve this problem, and in 2000 RID was requested to carry out a study on the topic "Bung Boraphet Development Strategies". However, the consulting companies carried this study suggested many strategies to relieve the water shortage problem. One of the strategies that have been highlight is a construction of dikes around BB using existing local roads around BB together with a construction more dikes. They recommended that dike constructions will be a concrete boundary for BB conservation zone to stop more illegal settlement, and will be used to store more water that can be functioned with weir crest heightening to the level +25.00 m (MSL). With these suggested structural measures to relieve water shortage problem would bring BB to be a flat reservoir and would damage BB wetland environment. Therefore, sustainable strategies to solve water shortage problem are really needed with highly concerning environmental integrity.

3) As mentioned earlier that algae bloom is one of the main causes of BB sedimentation, it also brings other problems to the lake. Once the algae peak and then collapse, aquatic animal life will be threatened by dissolved oxygen concentrations reduction and decay products from algae (Jones 1987 and Paerl 1988). A large fraction of nutrient can be stored in the lake sediments (James, *et al.* 1995b). This nutrient can be mobilized into the overlying water column because of various processes, such as diffusion (Moore *et al.* 1998), wind suspension (Hanlon, 1999), and bioturbation (Van Rees *et al.* 1996). This internal loading makes the lake

ecosystem very resilient to changes in its nutrient concentration when external inputs vary, a situation that is common in shallow eutrophic lakes (Sas 1989, Moss *et al.* 1996).

1.3 Lack of Plan of Management (POM) for BB

There are many stakeholders have responsibility or take some actions on BB and its surroundings. They have their own policies and ideas to carry out their interests independently. However, their acting on BB would affect other stakeholders in one way or another. Therefore the integrated plan of management accepted by all stakeholders is highly recommended for BB sustainability.

2. The results and discussion of water quantity analysis of Bung Boraphet

2.1 Daily water budget calibration

The lake water budget calculation was carried out based on Eq. (1) that explains the lake water volume variation depending on changes of hydrologic-budget components in the lake system as expressed in the conceptual model (Figure 17). A daily water budget simulation of the lake was carried out between December 2002 and May 2006 by the comparison of recorded and calculated lake water levels. An initial lake water level and water volume on the 11th of December 2002 was used to start the simulation process. The initial condition was also updated every time at the beginning of the changing point between inflow and outflow characteristics referred to as the numbers 1 to 7 shown in Figure 54 and at the end of the cropping seasons where there was no irrigation water demand referred to as the numbers 8 to 10. Lake water level and water volume will then be changed daily according to changes in the hydrologic-budget components that can be estimated using the methodologies as explained in the section of the investigation of hydrologic-budget components. The calculation was carried out daily until the middle of May 2006. The comparisons between observed and calculated daily lake water levels between the 11th of December 2002 and the 19th of May 2006 are shown in Figure 54.

The goodness of fit between the observed and calculated lake water levels were evaluated using three statistical measures which are the correlation coefficient (Chapra and Canale, 2002), root mean square error (Madsen, 2000), and the efficiency index or Nash-Sutcliffe criterion (Nash and Sutcliffe, 1970; Krause et al, 2005). Equations used to calculate these parameters are expressed in Table 17.

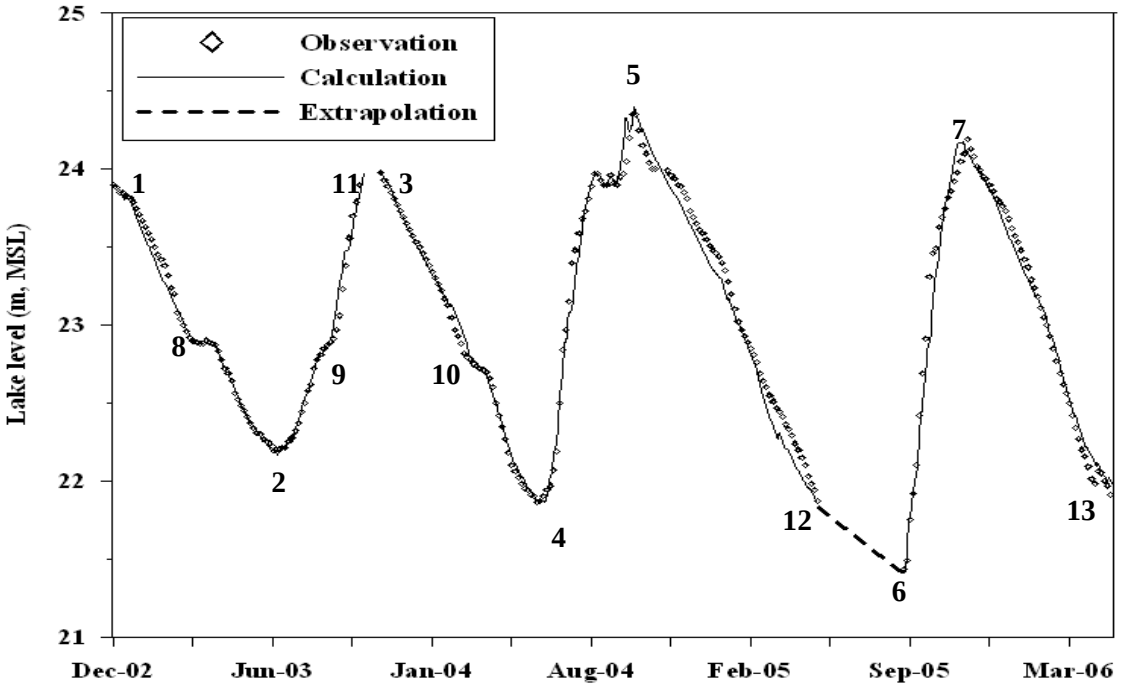

Figure 54 Comparisons between observed and calculated daily lake water levels between December 2003 and May 2006

Table 17 Statistical parameters used to identify the goodness of fit of the lake water levels

Statistical variables	Equations
Correlation Coefficient (r)	$r = \frac{\sum_{i=1}^{N}(H_{mi} - \overline{H}_m)\times(H_{ci} - \overline{H}_c)}{\sqrt{\left[\sum_{i=1}^{N}(H_{mi} - \overline{H}_m)^2 \times \sum_{i=1}^{N}(H_{ci} - \overline{H}_c)^2\right]}}$
Root Mean Square Error (RMSE)	$RMSE = \left(\frac{\sum_{i=1}^{N}(H_{mi} - H_{ci})^2}{N}\right)^{0.5}$
Efficiency Index (EI)	$EI = \frac{\sum_{i=1}^{N}(H_{mi} - \overline{H}_m)^2 - \sum_{i=1}^{N}(H_{mi} - H_{ci})^2}{\sum_{i=1}^{N}(H_{mi} - \overline{H}_m)^2} \times 100\ \%$

where, H_{mi} is the observed water level on day i, $\overline{H}_m$ is an average value of observed water level, H_{ci} is the calculated water level on day i, $\overline{H}_c$ is an average value of calculated water level, N is the number of data point. The best fit between the calculated and observed water levels using these parameters occur while the correlation coefficient (r) equals 1, the root mean square error (RMSE) equals 0, and the efficiency index (EI) is 100 percent.

Besides the comparison between observed and calculated daily lake water levels, a comparison between observed and calculated daily lake water storages was also investigated. Differences of observed and calculated daily lake water storages during inflow and outflow periods are shown in Figure 55 and Figure 56, respectively. Statistical values calculated from the comparison between observed and calculated lake water storage for inflow and outflow periods are shown in Table 18. It can be concluded that the calculation results of the daily lake water levels and water storages are acceptable. Therefore, the methodologies used to calculate the hydrologic-budget

components are also suitable to be applied for a future water budget prediction that is necessary for the wise use of water resources of the lake.

Table 18 Statistical values calculated from the comparisons between observed and calculated lake water levels and water storages

Comparison Parameter	Periods of Comparison	r	RMSE	EI (%)
lake water level	inflow and outflow	0.994	0.076 (m)	98.70
lake water storage	inflow	0.956	12.36 (MCM)	91.16
lake water storage	outflow	0.993	6.14 MCM	98.40

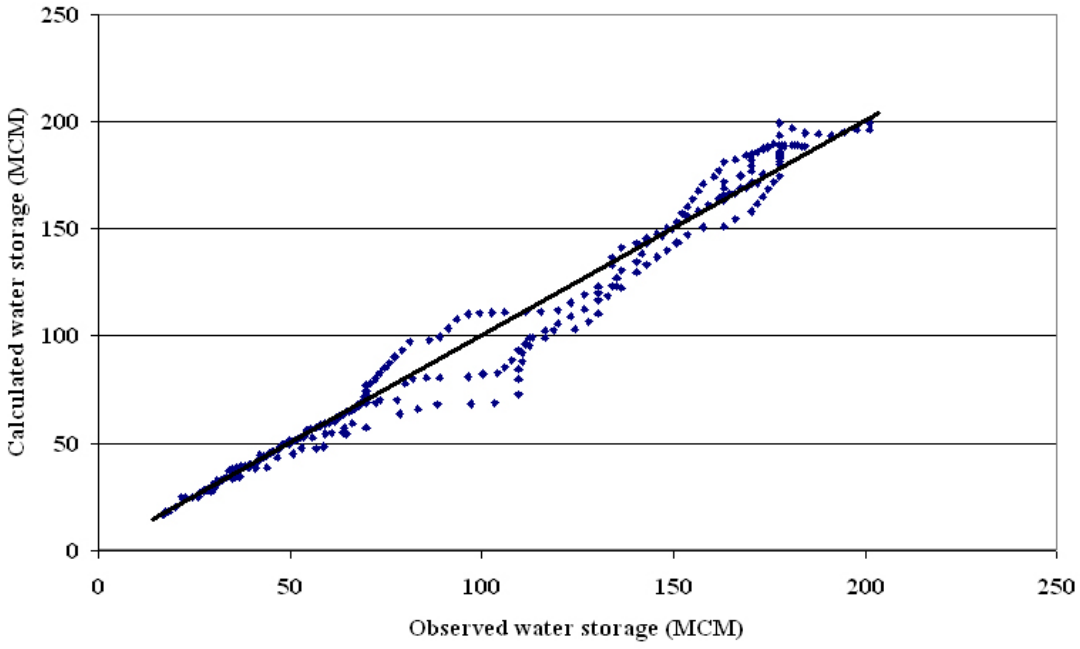

Figure 55 Differences of observed and calculated daily lake water storages during inflow periods

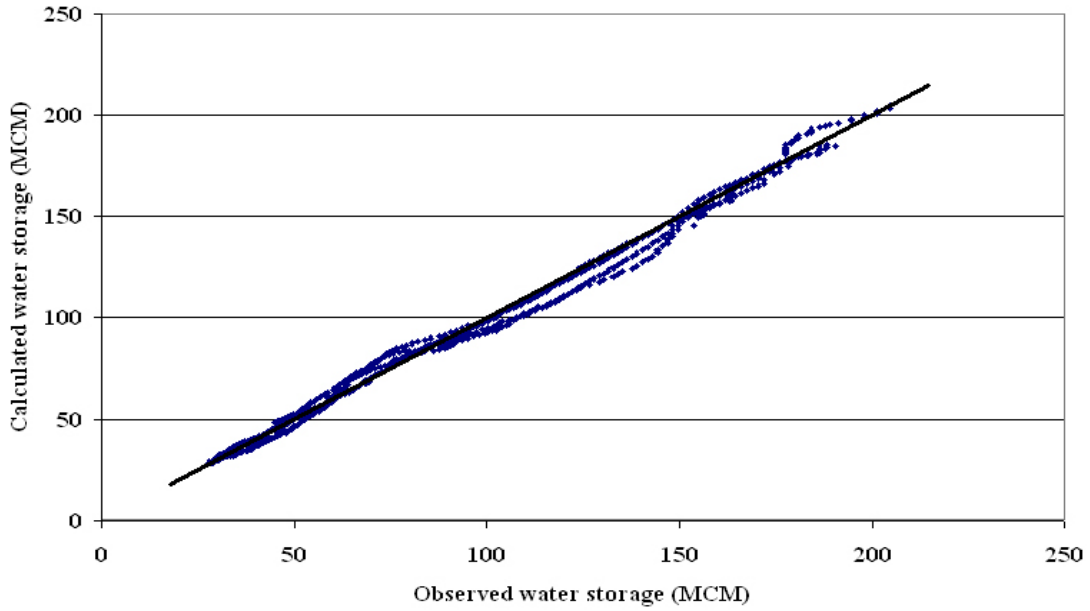

Figure 56 Differences of observed and calculated daily lake water storages during outflow periods

2.2 Daily hydrologic budget component

Results gained from the water budget calculation can be used to distinguished hydrologic-budget components for the daily basis. All hydrologic-components related to daily water budget calculations during inflow and outflow periods between December 2002 and May 2006 are shown in Table 19. During the inflow periods when water flows from tributaries to the lake, average overall inflows of 215.3 MCM originate from direct rainfall over the lake water surface and lake tributaries with the average inflows of 59.72 and 152.72 MCM, respectively, which are around 27.70 and 70.96 percent, respectively. Average inflows via lake tributaries including Klong Tatago, Klong Bon, and irrigation canals 1 and 2 are approximately 106.15, 42.09, 3.13, and 1.40 MCM, respectively, which are 49.33, 19.53, 1.45, and 0.65 percent, respectively. Evaporation and seepage loss are the main losses occurring during the inflow periods. However, there were large flood events occurring in 2004 and 2005 resulting in water flowing out of the lake via the weir and regulator. During the inflow periods, average overall losses of 38.54 MCM through

evaporation, seepage, weir, and regulator are approximately 35.17, 0.06, 2.69, 0.62 MCM, respectively, which are 92.43, 0.16, 5.94, and 1.47 percent, respectively. Therefore the difference between average overall inflows and losses during the inflow periods is around 176.76 MCM.

During the outflow periods when water flows from the lake to tributaries, most of losses occur by evaporation and water diversion via tributaries. Small amount of losses occurred through seepage loss and the overflows from the weir and regulator after large flood events are other two sources of losses. Average overall losses of 150.68 MCM according to these four categories are approximately 63.34, 83.05, 0.11, 4.18 MCM, respectively, which are 42.04, 55.11, 0.07, and 2.78 percent, respectively. Outflows through Klong Tatako, Klong Bon, and irrigation canals 1 and 2 are approximately 43.57, 26.87, 9.99, and 2.62 MCM, respectively, which are 52.46, 32.35, 12.03, and 3.16 percent, respectively. During the outflow periods, direct rainfall over the lake surface is the only source of inflow with an average value of 9.69 MCM. Therefore the difference between average overall losses and inflows during the outflow periods is around 140.99 MCM. The water level record has shown that the average minimum water level of the lake is around 21.99 m (MSL) which has water storage of approximately 32.02 MCM. This level is a lot lower than the minimum level of 23.00 metre (MSL) with water storage of approximately 75.15 MCM, recommended by FD for flora and fauna biodiversity. The only way to increase the water level to the recommended level is to reduce water diversion to the irrigation canal via tributaries from 83.05 MCM to 38.35 MCM. Therefore, only half of the irrigation areas can be irrigated that would be very difficult to negotiate with farmers. On the other hand, the recommended level of 23.00 meter (MSL) may need to be reduced to the level that is really not affecting biodiversity. If the lake level reduces to 22.50 m (MSL), there will be an extra 25 MCM of water storage that can be used for irrigation areas. All of these alternatives need to be further investigated using a daily water budget calculation that is proved to be a very useful tool for the wise use of water resource management of the lake

2.3 Water budget scenario

The water budget was used to analyze the changes in the lake's water level for six scenarios (Table 20 and Figure 57) in which stored or abstracted water volume was changed (Case 1- Case 5), and the minimum water level was maintained by Nan River diversion (Case 6).

One proposal - suggested by the Royal Irrigation Department (RID, 2004) - is to raise the weir crest by 0.5 m to +24.5 m (MSL), to increase the stored water volume for dry season irrigation. In three scenarios (Cases 3, 4 and 5), we also varied the water volume abstracted each day for irrigation as a fixed percentage of the volume abstracted between 2002 and 2006, which was set to 100%. Another proposal - suggested by the Department of Water Resources (DWR, 2006) – is to maintain the minimum water level at +23 m (MSL) by flow diversion from the Nan River (Case 6).

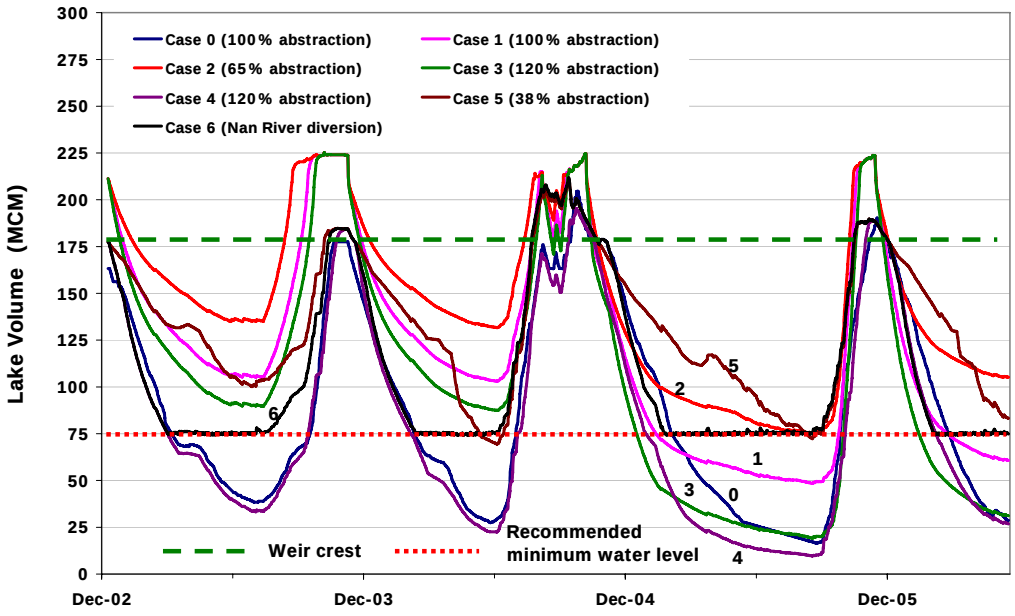

Figure 57 Water budget scenarios in Bung Boraphet for different management responses

Table 19

Table 19 (Continued)

Table 20 Minimum water volumes and levels for different scenarios

Scenario case	Weir crest		Percentage of water usage compared with current situation	Minimum water	
	Level (m, MSL)	Volume (MCM)		Level (m, MSL)	Volume (MCM)
Case 0 (Current situation)	24	178	100	21.41	17
Case 1	24.5	211	100	22.46	48
Case 2	24.5	211	65	23.00	75
Case 3	24.5	211	120	21.55	20
Case 4	24	178	120	20.96	10
Case 5	24	178	38	23.00	75
Case 6	24	178	100	23.00	75

The current situation (Figure 57, Case 0) has the weir crest at +24 m (MSL) (178 MCM), and abstraction is 100%. The recomended minimum water level for sustainable biodiversity is +23 m (MSL) (75 MCM). However, water has been abstracted until the minimum water level in 2005 became as low as +21.41 m (MSL) (17 MCM), that is a lot lower than the recommended low level.

In Case 1 the weir crest is raised to +24.5 m (MSL) and water usage remains at 100%. The water budget scenario predicts the minimum water level would then fall to +22.46 m (MSL), which is about 0.5 m below the level recommended for sustainable fisheries. On the other hand (Case 2), water budget scenario predicts that if the weir height is raised to +24.5 m (MSL), water abstraction has to be reduced by 35%, to achieve the recommended minimum water level (+23 m (MSL)).

A likely scenario (Case 3) is that if the weir crest is increased to +24.5 m (MSL), and farmers will also increase their abstraction. Assuming water abstraction increased to 120% of Case 0, water budget scenario predicts a minimum lake level of +21.55 m (MSL) – similar to the current condition.

Case 4, assumes no change to the weir crest, but an increase in abstraction by 20%. That would draw the water level down to +20.96 m (MSL), which is below the current minimum and more than 2 m below the recommended level for maintaining biodiversity. This scenario shows the minimum lake level is very sensitive to any increase in abstraction for dry season irrigation.

Case 5 shows that if the weir height is not raised, water abstraction from the lake has to be reduced by 62% to achieve the recommended minimum level of +23 m (MSL).

Case 6 shows that if the recommended level has to be maintained without raising the weir crest and changing water abstraction, extra flows have to be diverted from the Nan River during the dry season. The water budget scenario predicts maximum water diversion occurring in 2005 would be 132 MCM with the total pumping operation of 102 days, operating duration of 8 hours per day, and a pumping flow rate of 45 cms.

3. Results and discussion of Remote Sensing Investigation

The Landsat 5 image collected between 1993 and 2003 was used to conducting the temporal and spatial analysis of land use change in Bung Boraphet and its surrounding area. After manipulation and interpretation processes by using PCI Geomatica software, the physical characteristic and land use classification of both in Bung Boraphet and its surrounding area are shown in Figure 58. In Figure 58 (a), green and yellow areas denote emergent and submerged plant cover, blue denotes clear water, and red is turbid water, while green, pink, red and yellow areas in Figure

58 (b) denote paddy field, prepared land for paddy field, swamp forest, and dry area, respectively.

The analysis shows that the irrigated land that use stored water of Bung Boraphet rose around 100% (from 37 to 75.8 km^2) between 1993 and 2003, meanwhile the swamp forest had the obvious decreasing trend. At the same period, the plant cover areas in Bung Boraphet, both submerged and emergent aquatic vegetation, diminished around 50% (from 16.1 to 7.9 km^2). In the other hand, turbid water area that contains a plume of sediment has been increased around 20 times, compared between 1993 and 2003.

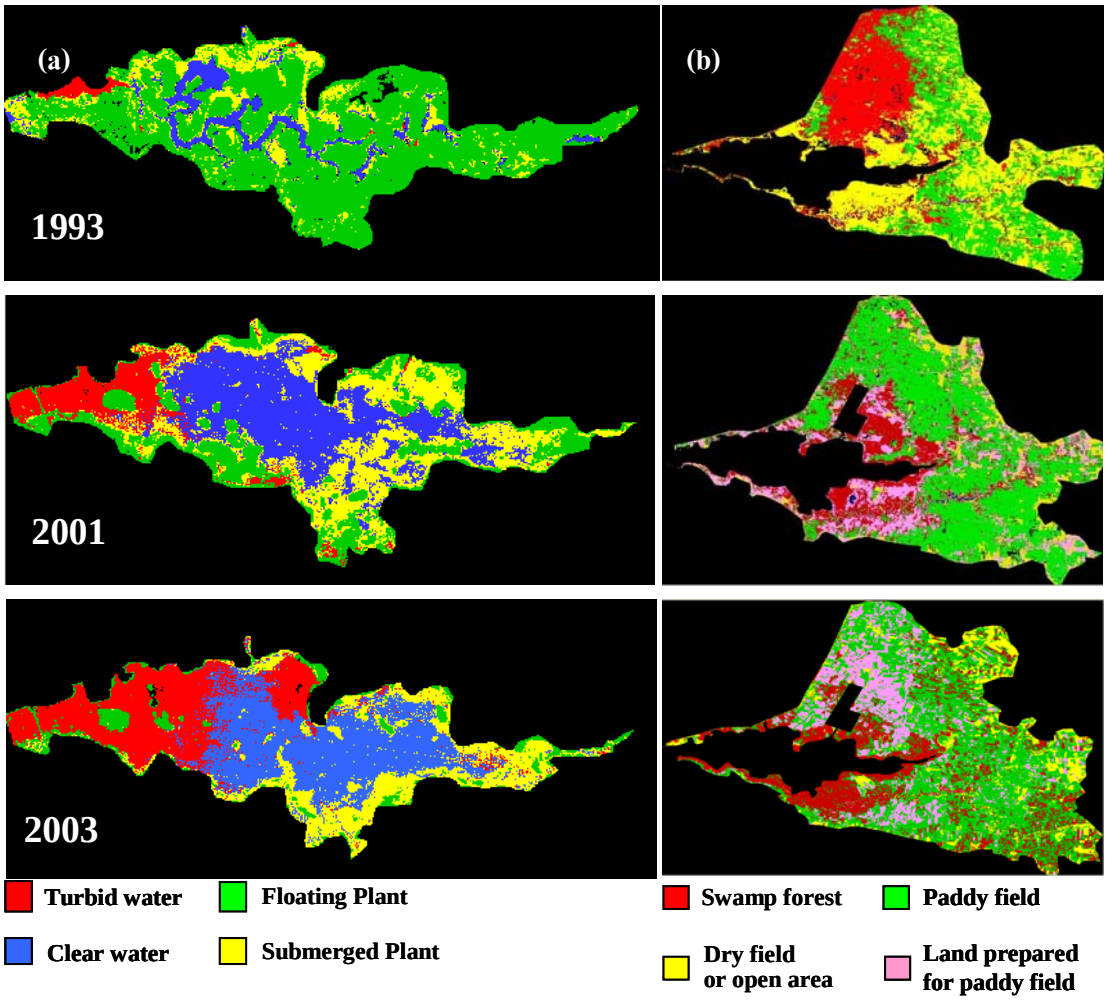

Figure 58 Landsat imagery showing changes in the (a) Bung Boraphet, and (b) the surrounding area

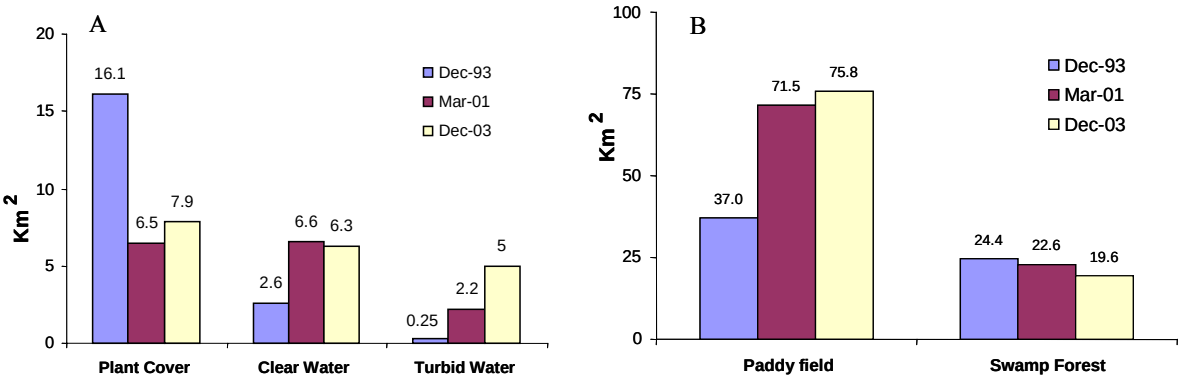

Figure 59 Changes in land use and composition of (A) Bung Boraphet and (B) the surrounding area between 1993 and 2003, from analysis of Landsat images.

4. Results and discussion of water quality analysis of Bung Boraphet

4.1 The present situation of water quality situation in Bung Boraphet

Eight Observed water quality parameters (DO, BOD, TN, TKN, Nitrate, TP, Phosphate, and SS) obtained from the filed data collections at 16 locations in Bung Boraphet, and at the outlet of four tributaries (Klong Bon, Klong Thatako, Irrigation Canal 1, and Irrigation Canal 2) for 12 events as shown in Table 11, can be used to analyze the situation of water quality in Bung Boraphet and its tributaries. Changes of the values of each water quality parameter with space and time can be summarized as in the followings.

4.1.1 Dissolved Oxygen (DO)

Spatial variation of DO concentration in Bung Boraphet and its tributaries is shown in Figure 60. In the figure, the average, the maximum, and the minimum DO concentration calculated for all events at each location are shown. It can be seen that the average DO concentration in the lake are higher than that of at the outlet of those four tributaries nearly one time with the average values of around 6.85 and 3.71 mg/l, respectively. Ranges of the average DO concentration in the lake are

between 5.35 and 8.33 mg/l, and in the tributaries are between 2.30 and 4.20 mg/l. The minimum DO concentrations in the lake are also higher in the lake than that of in the tributaries around four times with the average values of around 3.97 and 0.92 mg/l, respectively. Ranges of the minimum DO concentration in the lake are between 1.68 and 5.59 mg/l, and in the tributaries are between 0.21 and 1.56 mg/l. The minimum DO concentration that lower than 2 mg/l within the lake obviously occurring close to the outlet of those four tributaries around the location numbers 11, 12, and 15 with the minimum values of 1.83, 1.97, and 1.68 mg/l, respectively. Since these lowest values of DO concentration at these locations were persisted only for a short period of time and limited within small regions, then aquatic animals can be adjusted themselves or stay away from these regions until the situation is getting better. It can be therefore concluded that DO concentration in the lake is not in the critical situation.

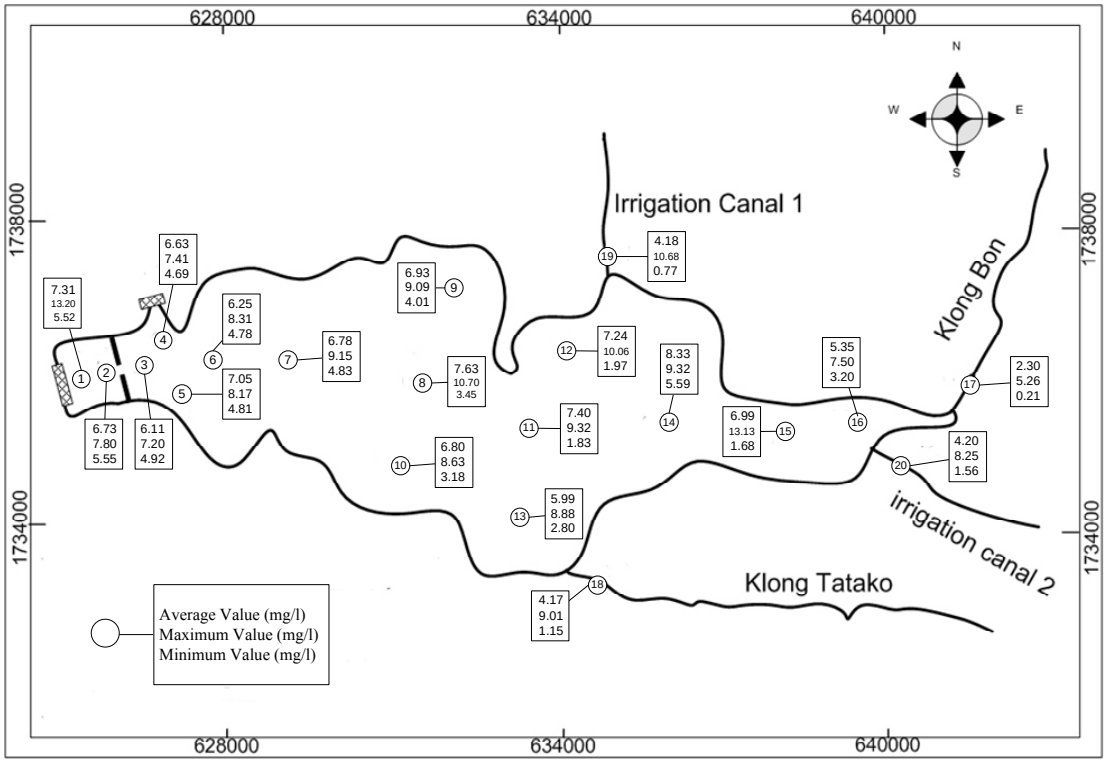

Figure 60 Spatial variation of DO concentration in Bung Boraphet and its tributaries

Temporal variation of DO concentration in Bung Boraphet and its tributaries can also be plotted as shown in Figure 61. In the figure, the average, the maximum, and the minimum DO concentration calculated for all locations at each event are identified. The data points show that most of the average DO concentrations in the lake are normally higher than that of at the outlet of those four tributaries for a particular event. It also can be seen that during the water levels in the lake are rising, DO concentrations at the outlet of four tributaries tend to increase. On the other hand, the water levels in the lake are falling, DO concentrations at the tributaries tend to decrease. These evidences confirm the fact that water quality in the lake has higher DO concentration than the DO concentration outside the lake or the lake can be used to improve the water quality.

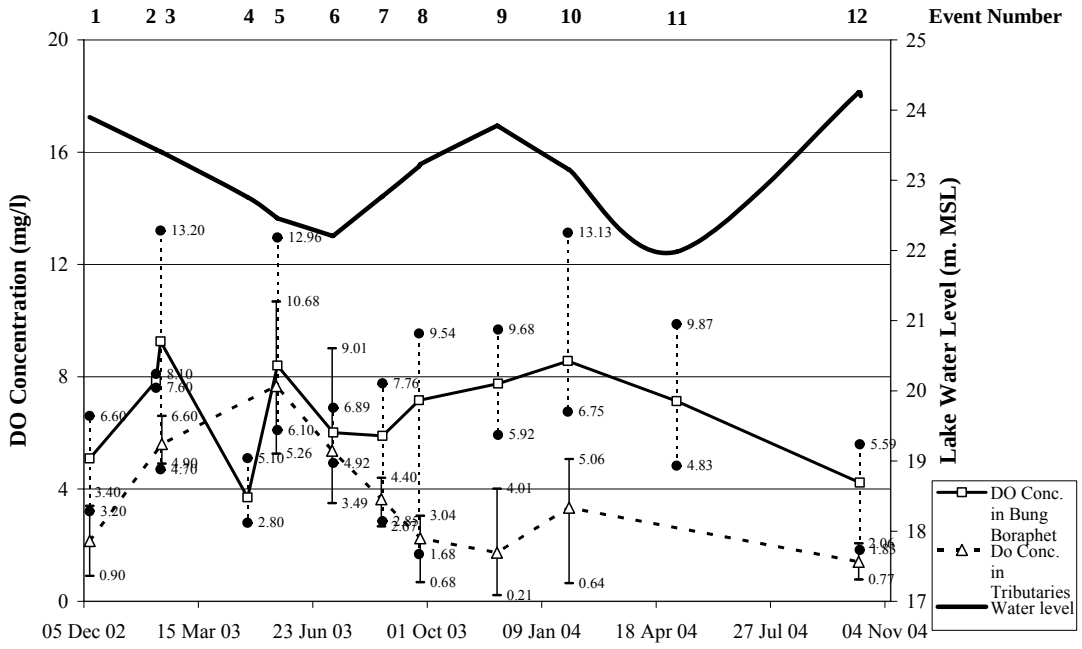

Figure 61 Temporal variation of DO concentration in Bung Boraphet and its tributaries

4.1.2 Biochemical oxygen demand (BOD)

Spatial variation of BOD concentration in Bung Boraphet and its tributaries is shown in Figure 62. In the figure, the average, the maximum, and the minimum BOD concentration calculated for all events at each location are shown. It can be seen that the average BOD concentration in the lake are a bit lower than that of at the outlet of those four tributaries with the average values of around 2.68 and 3.19 mg/l, respectively. Ranges of the average BOD concentration in the lake are between 1.37 and 3.89 mg/l, and in the tributaries are between 1.20 and 6.40 mg/l. The maximum BOD concentrations in the lake are also lower in the lake than that of in the tributaries with the average values of around 4.19 and 5.57 mg/l, respectively. Ranges of the maximum BOD concentration in the lake are between 2.40 and 6.89 mg/l, and in the tributaries are between 4.90 and 6.40 mg/l. All of the maximum BOD concentrations at the outlet of four tributaries are above 4 mg/l, which is the highest BOD concentration value to be considered as deemed clean water. Half of the observed locations (8 out of 16 locations) in the lake also have the maximum BOD concentration more than 4 mg/l. However, there are only 2 locations out of 16 locations that have the maximum BOD concentrations more than 5 mg/l, which is the highest value to be suitable for fisheries. Even these highest BOD concentration values are not frequently occur in the lake, water quality control still needs awareness.

Temporal variation of BOD concentration in Bung Boraphet and its tributaries can also be plotted as shown in Figure 63. In the figure, the average, the maximum, and the minimum BOD concentration calculated for all locations at each event are identified. The data points for each event within the lake and in the tributaries are not going in the same patterns. In some events, the BOD concentrations in the lake are higher than that of in the tributaries, but in some other events the opposite occur. However, BOD concentrations within the lake and in the tributaries tend to increase and to decrease at the same time, but they are not corresponded to the pattern of the rising and falling water levels of the lake. These evidences can be pointed out that the lake does not have significant ability to reduce

BOD concentration that come from external loading, furthermore there are also BOD loading occur within the lake itself.

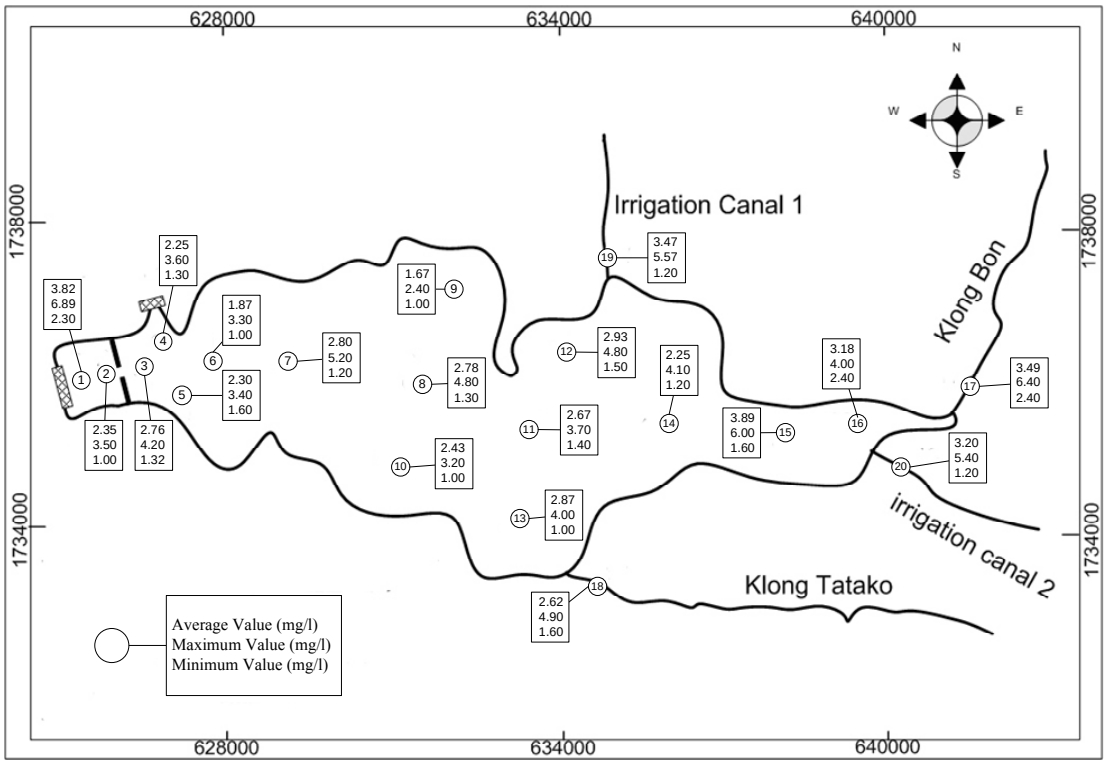

Figure 62 Spatial variation of BOD concentration in Bung Boraphet and its tributaries

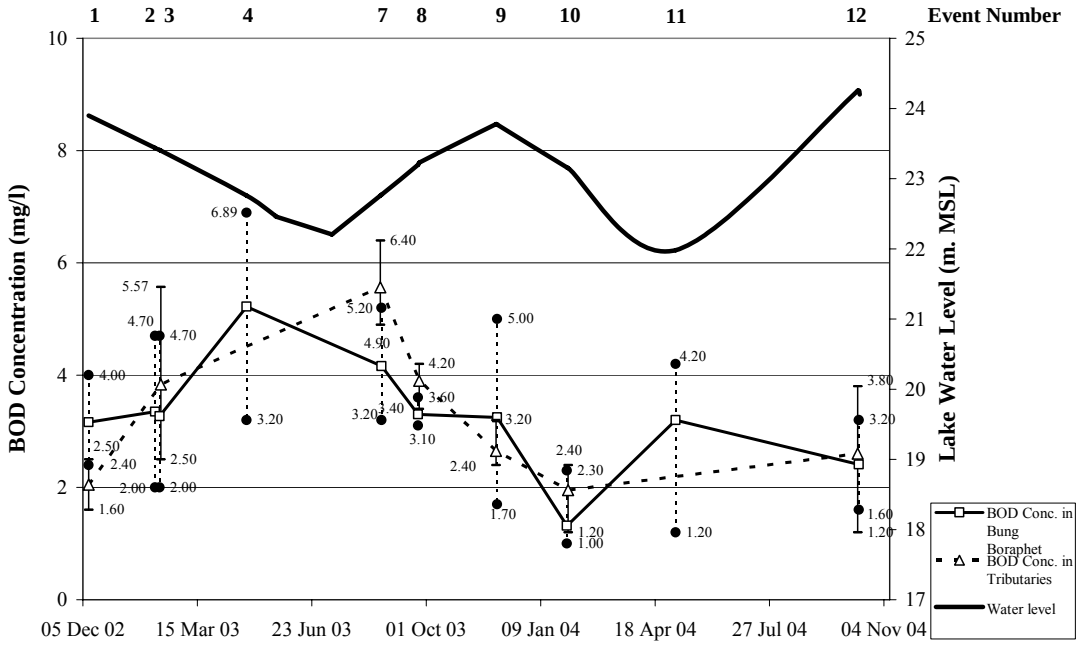

Figure 63 Temporal variation of BOD concentration in Bung Boraphet and its tributaries

4.1.3 Nutrients

Nutrient pollution, especially from nitrogen and phosphorus, has consistently ranked as one of the top causes of degradation in some waters. Excess nitrogen and phosphorus lead to significant water quality problems including harmful algal blooms, hypoxia and declines in wildlife and wildlife habitat. Nitrogen and phosphorus can be found in different forms. In this study, usual forms of nitrogen and phosphorus were therefore collected to be used as the indicators to identify the water quality of the lake and its tributaries.

Total nitrogen (TN) in a natural water body can be found in organic nitrogen and inorganic nitrogen. Inorganic nitrogen consists of ammonia (NH_3), nitrate-nitrogen (NO_3-N) and nitrite (NO_2). TKN is the summation between organic nitrogen and ammonia (NH_3). These different forms of nitrogen can be explained as in the following relationship; TN = TKN + (NO_3 –N) + NO_2.

Total Phosphorus (TP) in aquatic systems involves three major fractions which are particulate organic phosphorus (POP) found in dead organic matter and phytoplankton, dissolved organic phosphorus (DOP) excreted by organisms, especially zooplankton and dissolved inorganic phosphorus (DIP), mostly as phosphate (PO_4^{3-}). Even there are several forms of phosphorus in natural environment, phosphorus in water body is usually found in the form of phosphates (PO_4^{3-}). TP and PO_4^{3-} were therefore collected to be used as the indicators to identify the phosphorus situation of the lake and its tributaries.

Table 11 shows the observation values of different forms of nitrogen (total nitrogen (TN), total Kjeldahl nitrogen (TKN), and nitrate-nitrogen (NO_3-N)), and different forms of phosphorus (total phosphorus (TP), phosphate (PO_4^{3-})) collected at 16 locations in the lake and its tributaries for 12 events. Values of different forms of nitrogen and phosphorus changing with space and time can be summarized as in the followings.

1) Nitrogen

There are three forms of nitrogen (TN, TKN, and NO_3-N) collected in this study. Spatial and temporal variations of these nitrogen components are summarized as in the followings.

1.1) Total Nitrogen

Spatial variation of TN concentration in Bung Boraphet and its tributaries is shown in Figure 64. In the figure, the average, the maximum, and the minimum TN concentration calculated for all events at each location are shown. From the data points of the average TN concentration in the lake and in the tributaries, it can be summarized that the average values of TN concentration in the lake is lower than in the tributaries with the values of around 0.55 and 0.85 mg/l, respectively. Ranges of the average TN concentration in the lake are

between 0.29 and 1.03 mg/l, and in the tributaries are between 0.77 and 0.98 mg/l. The maximum TN concentrations in the lake are also lower than that of in the tributaries more than one time with the average values of around 0.84 and 2.02 mg/l, respectively. Ranges of the maximum TN concentration in the lake are between 0.33 and 1.85 mg/l, and in the tributaries are between 1.43 and 2.69 mg/l. All of the maximum TN concentrations at the outlet of four tributaries are above 1 mg/l, which is the highest TN concentration value that still suitable for fishery and conservation of environment. In the lake, there are also 5 locations (location numbers 1, 8, 13, 15 and 16) that have the maximum TN concentration more than 1 mg/l. These high values occurred close to lake's tributaries.

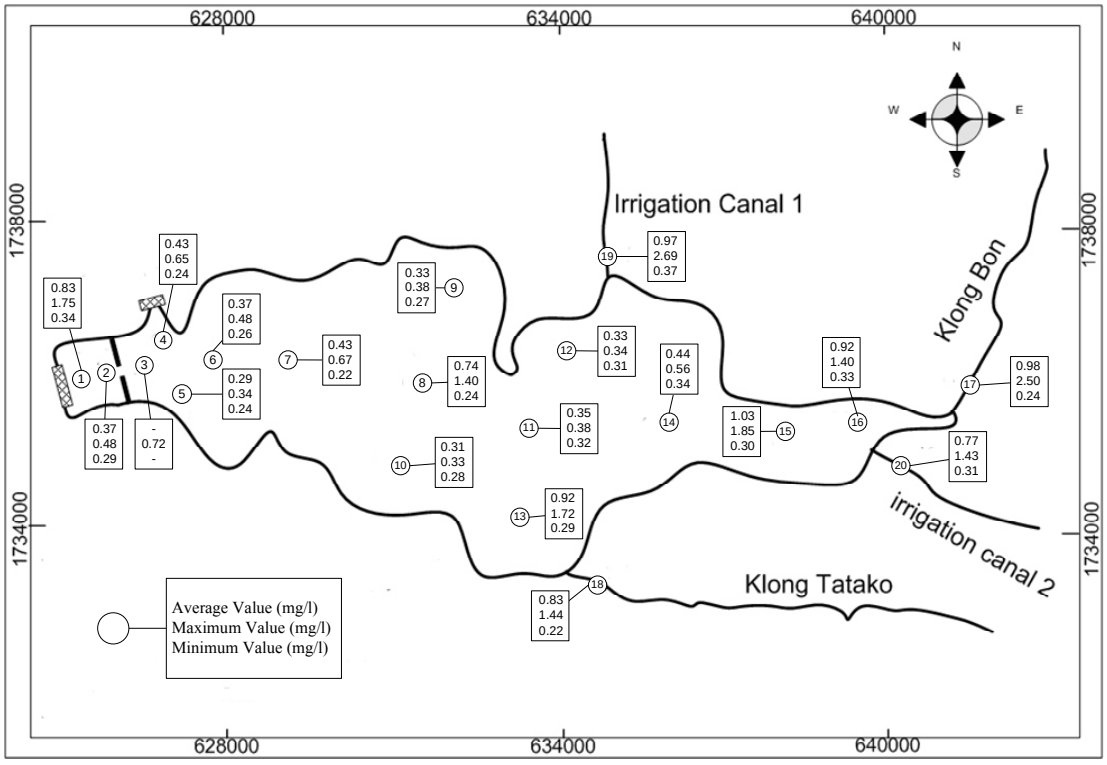

Figure 64 Spatial Variation of TN concentration in Bung Boraphet and its tributaries

Temporal variation of TN concentration in Bung Boraphet and its tributaries can also be plotted as shown in Figure 65. In the figure, the average, the maximum, and the minimum TN concentration calculated for all locations at each event are identified. It can be pointed that TN concentrations in the

lake and tributaries between December 2002 and August 2003 varied in the higher range than TN concentration of the events collected after August 2003 (between October 2003 and April 2004). Most of TN concentrations in the first half are also higher than 1 mg/l but TN concentrations in the second half are lower than 1 mg/l. It was suspected that the reason for this change could be related to the large floods occurring in October and November 2002. These floods would bring a lot of nutrients from the paddy field to the tributaries and the lake. Once these nutrients accumulating in the lake, it would take a long time to reduce these high values. Once there was no large flood in 2003, the situation of TN concentrations was therefore getting better as we can see the lower TN concentrations in 2004.

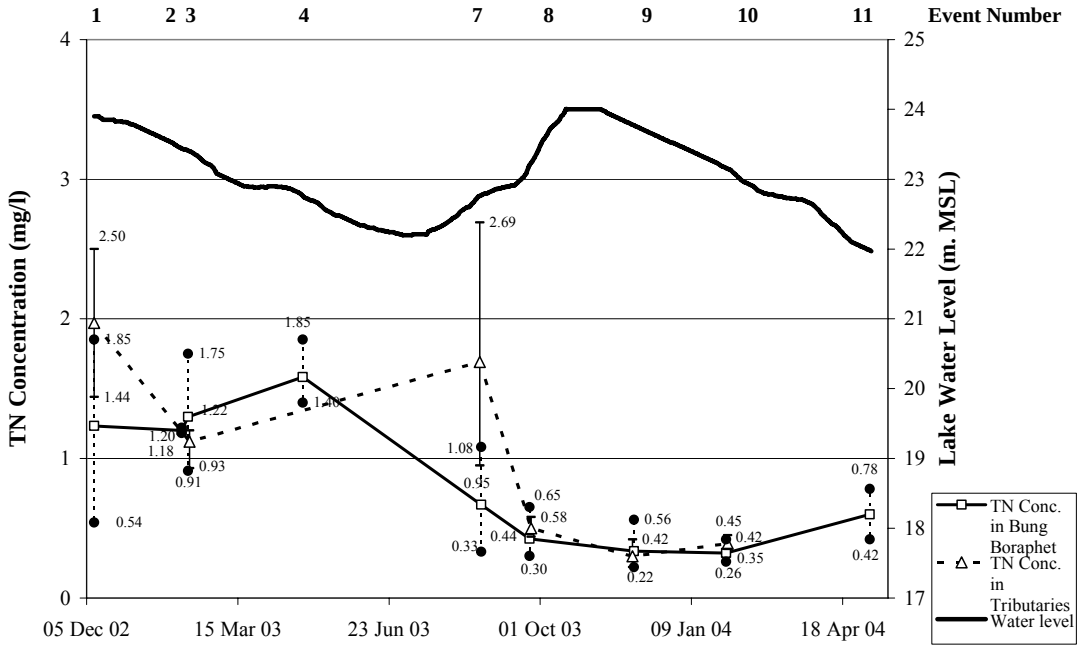

Figure 65 Temporal variation of TN concentration in Bung Boraphet and its tributaries

1.2) Total Kjeldahl Nitrogen (TKN)

Since total nitrogen is a combination of TKN, nitrate (NO_3) and nitrite (NO_2), observed TKN concentrations at different locations

and events are also described. Spatial variation of TKN concentration in Bung Boraphet and its tributaries as shown in Figure 66 show similar pattern as TN concentration (Figure 64). From the data points of the average TKN concentration in the lake and in the tributaries, it can be summarized that the average values of TKN concentration in the lake is lower than in the tributaries with the values of around 0.43 and 0.59 mg/l, respectively. Ranges of the average TKN concentration in the lake are between 0.22 and 0.88 mg/l, and in the tributaries are between 0.31 and 0.77 mg/l. The maximum TKN concentrations in the lake are also lower than that of in the tributaries more than one time with the average values of around 0.70 and 1.75 mg/l, respectively. Ranges of the maximum TKN concentration in the lake are between 0.24 and 1.70 mg/l, and in the tributaries are between 1.39 and 1.80 mg/l. However these TKN concentration values are still below 5 mg/l, which is the highest TKN concentration value that is recommended to prevent the algae bloom and lake eutrophication. It can be therefore concluded that Bung Boraphet and its tributaries are safe of algae bloom and eutrophication.

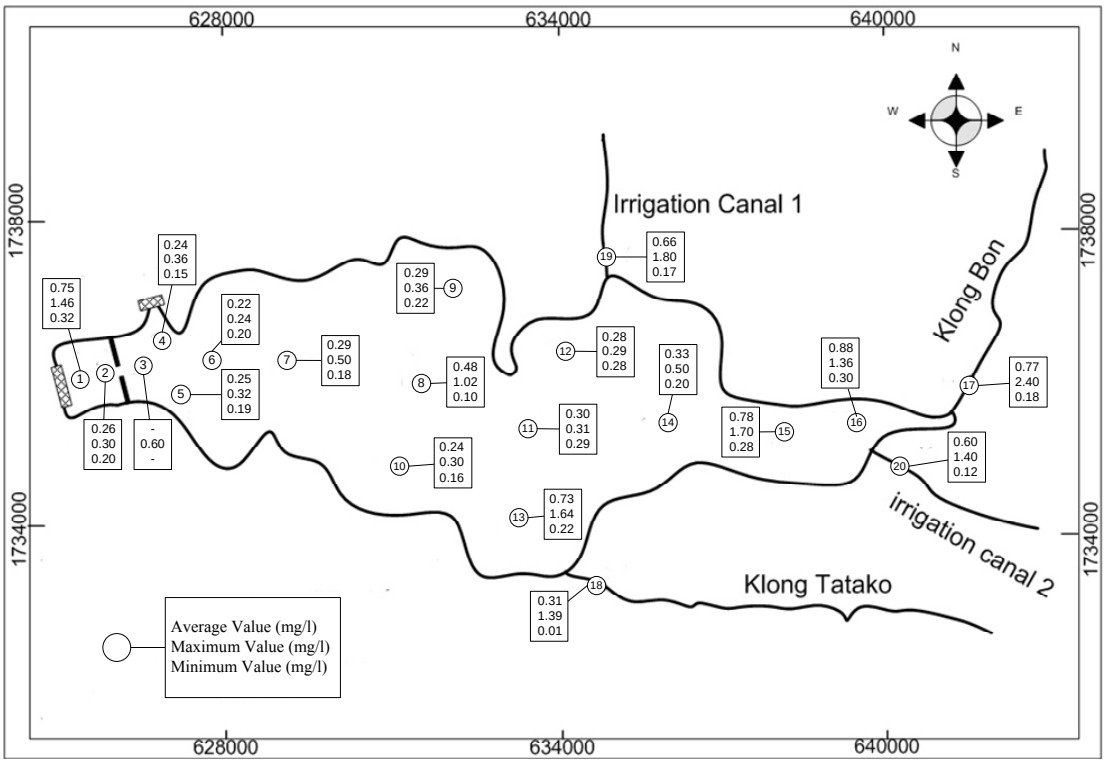

Figure 66 Spatial Variation of TKN concentration in Bung Boraphet and its tributaries

Temporal variation of TKN concentration in Bung Boraphet and its tributaries can also be plotted as shown in Figure 67. TKN concentrations in the lake and tributaries between December 2002 and August 2003 varied in the higher range than TKN concentration of the events collected after August 2003 (between October 2003 and November 2004). Most of TKN concentrations in the first half are also higher than in the second half. The patterns of TKN concentration are similar to the patterns of TN concentration.

Since the data points of TN and TKN concentrations as shown above are highly related and have similar patterns, every data point of TN and TKN concentrations at the same event and location are compared. The results show that TKN concentrations for 47 events at the same location have the average value of around 84% of the average value of TN concentrations with the range between 67.5% and 96.6 %.

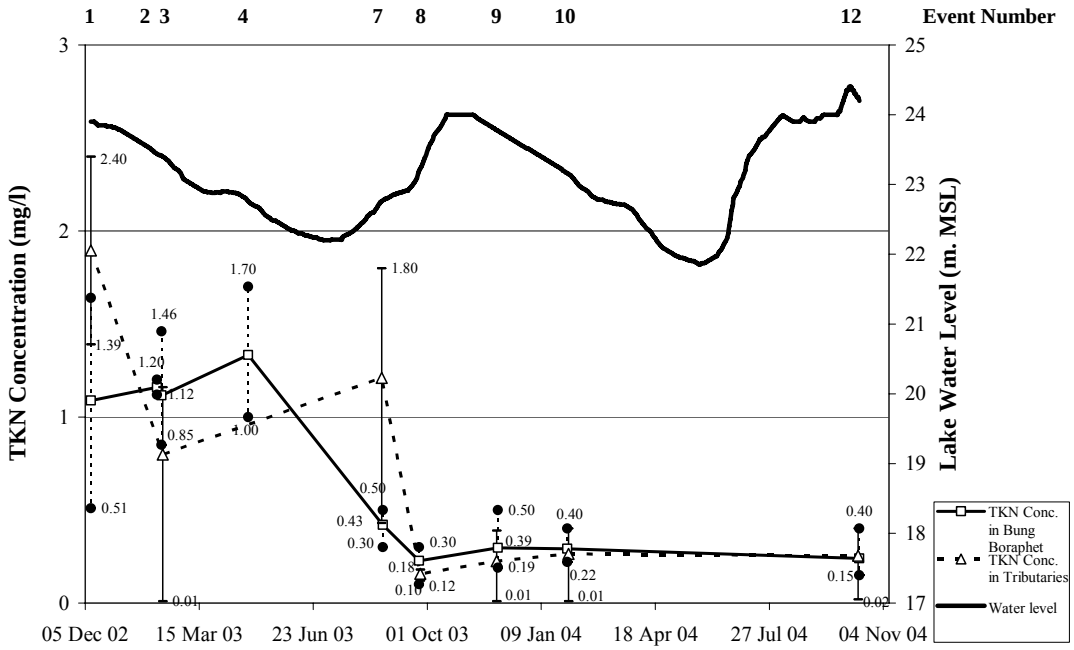

Figure 67 Temporal variation of TKN concentration in Bung Boraphet and its tributaries

1.3) Nitrate-Nitrogen (NO_3-N)

Spatial variation of NO_3-N concentration in Bung Boraphet and its tributaries is shown in Figure 68. In the figure, the average, the maximum, and the minimum NO_3-N concentration calculated for all events at each location are shown. From the data points of the average NO_3-N concentration in the lake and in the tributaries, it can be summarized that the average values of NO_3-N concentration in the lake is lower than in the tributaries with the values of around 0.04 and 0.14 mg/l mg/l, respectively. Ranges of the average NO_3-N concentration in the lake are between 0.02 and 0.10 mg/l, and in the tributaries are between 0.08 and 0.20 mg/l. The maximum NO_3-N concentrations in the lake are around 5 times less than that of in the tributaries with the average values of around 0.11 and 0.61 mg/l for the lake and tributaries, respectively. Ranges of the maximum NO_3-N concentration in the lake are between 0.02 and 0.55 mg/l, and in the tributaries are between 0.39 and 0.87 mg/l. These maximum NO_3-N concentrations are under 1 mg/l that is classified as unpolluted water. NO_3-N concentrations in the lake and tributaries are therefore not in the critical situation to worry about.

As explained above about the relationship between TN and TKN concentrations that TKN concentrations for 47 events at the same location have the average value of around 84% of the average value of TKN concentrations, NO_3-N concentration can be calculated in the same manner. The results show that NO_3-N concentrations have the average value of around 7.6% of the average value of TN concentrations with the range between 2.7% and 22.6 %. This range is quite large, temporal variation of NO_3-N concentration in Bung Boraphet and its tributaries would help to explain the variations as shown in Figure 69. In the figure, it can be seen that most of NO_3-N concentration in the lake and tributaries are very low (lower than 0.02 mg/l). However, there are only 3 events in February, April, and August 2003 that have higher values of NO_3-N concentration. This is especially in August 2003 that has the average value in the lake and in tributaries of around 0.21 and 0.65 mg/l, respectively. These higher values of NO_3-N concentration cause the

percentage of NO_3-N concentration to the TN concentration increase to 22.6% as explained above.

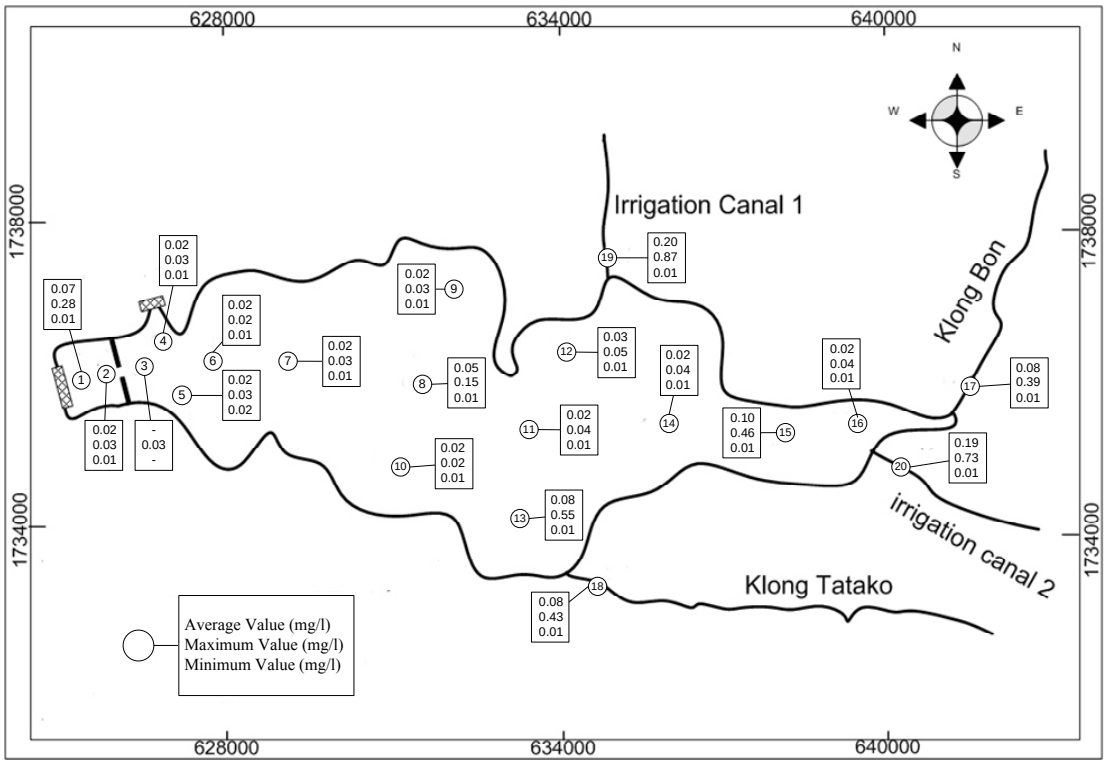

Figure 68 Spatial Variation of NO_3-N concentration in Bung Boraphet and its tributaries

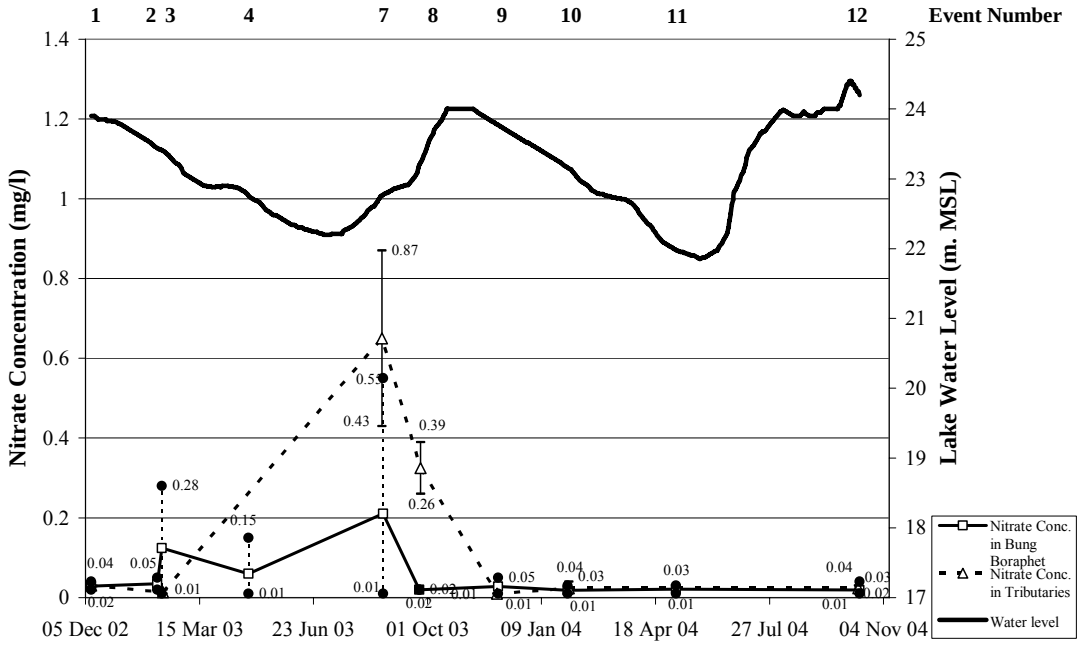

Figure 69 Temporal variation of NO_3-N concentration in Bung Boraphet and its tributaries

2) Phosphorus

There are two forms of phosphorus (TP and PO_4^{3-}) collected in this study. Spatial and temporal variations of these phosphorus components are summarized as in the followings.

2.1) Total phosphorus (TP)

Spatial variation of TP concentration in Bung Boraphet and its tributaries is shown in Figure 70. In the figure, the average, the maximum, and the minimum TP concentration calculated for all events at each location are shown. From the data points of the average TP concentration in the lake and in the tributaries, it can be concluded that the average TP concentrations in the lake are very close to that of in the tributaries with the average values of around 0.03, and 0.04 mg/l, respectively. Ranges of the average TP concentration in the lake are

between 0.02 and 0.05 mg/l, and in the tributaries are between 0.03 and 0.05 mg/l. The maximum TP concentrations in the lake are also a bit lower in the lake than that of in the tributaries with the average values of around 0.05 and 0.07 mg/l, respectively. Ranges of the maximum TP concentration in the lake are between 0.03 and 0.07 mg/l, and in the tributaries are between 0.05 and 0.09 mg/l. These maximum TP concentrations are a lot lower than 1.0 mg/l that is recommended as the highest value for fishery and conservation of environment. It can be therefore concluded that TP concentrations in the lake and its tributaries are in the safe range for the well being of flora, fauna, and its environment.

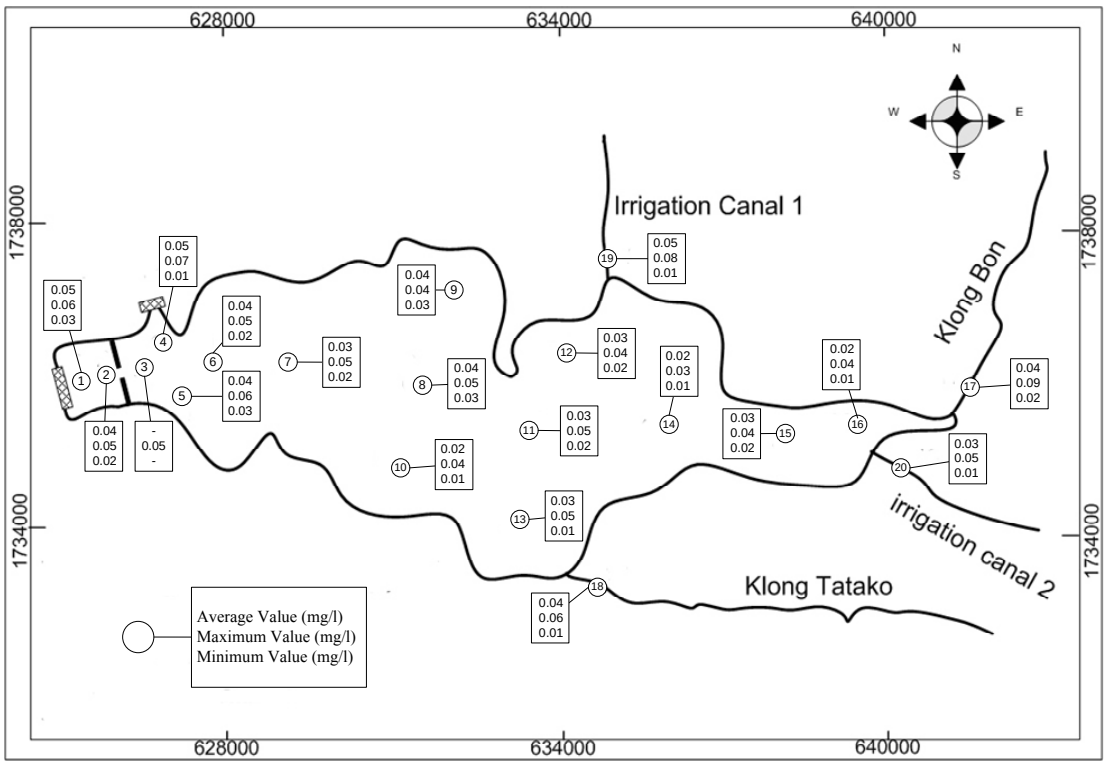

Figure 70 Spatial Variation of TP concentration in Bung Boraphet and its tributaries

Temporal variation of TP concentration in Bung Boraphet and its tributaries can also be plotted as shown in Figure 71. In the figure, the average, the maximum, and the minimum TP concentration calculated for all locations at each event are identified. It also can be seen that TP concentrations within the lake and in the tributaries tend to increase and to decrease at the same time.

Moreover TP concentrations in the lake and tributaries roughly increase and decrease with the rising and falling water levels of the lake, respectively. These corresponding patterns between lake water levels and TP concentrations are according to flood waters tend to carry a large number of TP from the paddy fields to the lake. TP concentrations were then consumed by plants during the outflow period (especially for dissolved inorganic phosphorus) and settled to the lake bottom (especially for particulate organic phosphorus POP).

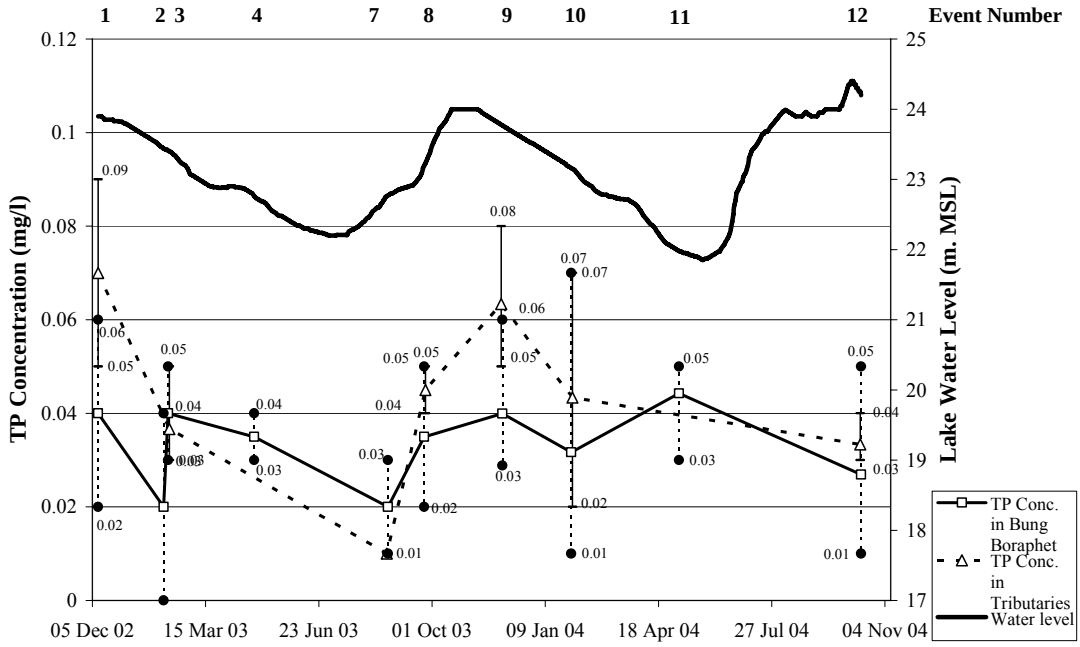

Figure 71 Temporal variation of TP concentration in Bung Boraphet and its tributaries

2.2) Phosphate-Phosphorus (PO_4^{3-})

As explained earlier that in the water body phosphorus mostly found in the form of TP and PO_4^{3-}. PO_4^{3-} concentrations in the lake and tributaries are observed and concluded in this section. Spatial variation of PO_4^{3-} concentration in Bung Boraphet and its tributaries as shown in Figure 72 show similar pattern as TP concentration (Figure 70). From the data points of the average

PO_4^{3-} concentration in the lake and in the tributaries, it can be summarized that the average values of PO_4^{3-} concentration in the lake is lower than in the tributaries with the values of around 0.02, and 0.03 mg/l, respectively. Ranges of the average PO_4^{3-} concentration in the lake are between 0.01 and 0.04 mg/l, and in the tributaries are between 0.02 and 0.03 mg/l. The maximum PO_4^{3-} concentrations in the lake are also a bit lower in the lake than that of in the tributaries with the average values of around 0.03 and 0.05 mg/l, respectively. Ranges of the maximum PO_4^{3-} concentration in the lake are between 0.02 and 0.06 mg/l, and in the tributaries are between 0.04 and 0.06 mg/l. These maximum PO_4^{3-} concentration values are still below than 0.1 mg/l, which is the highest PO_4^{3-} concentration value that is recommended to prevent the algae bloom and lake eutrophication. It can be therefore concluded that Bung Boraphet and its tributaries are safe of algae bloom and eutrophication.

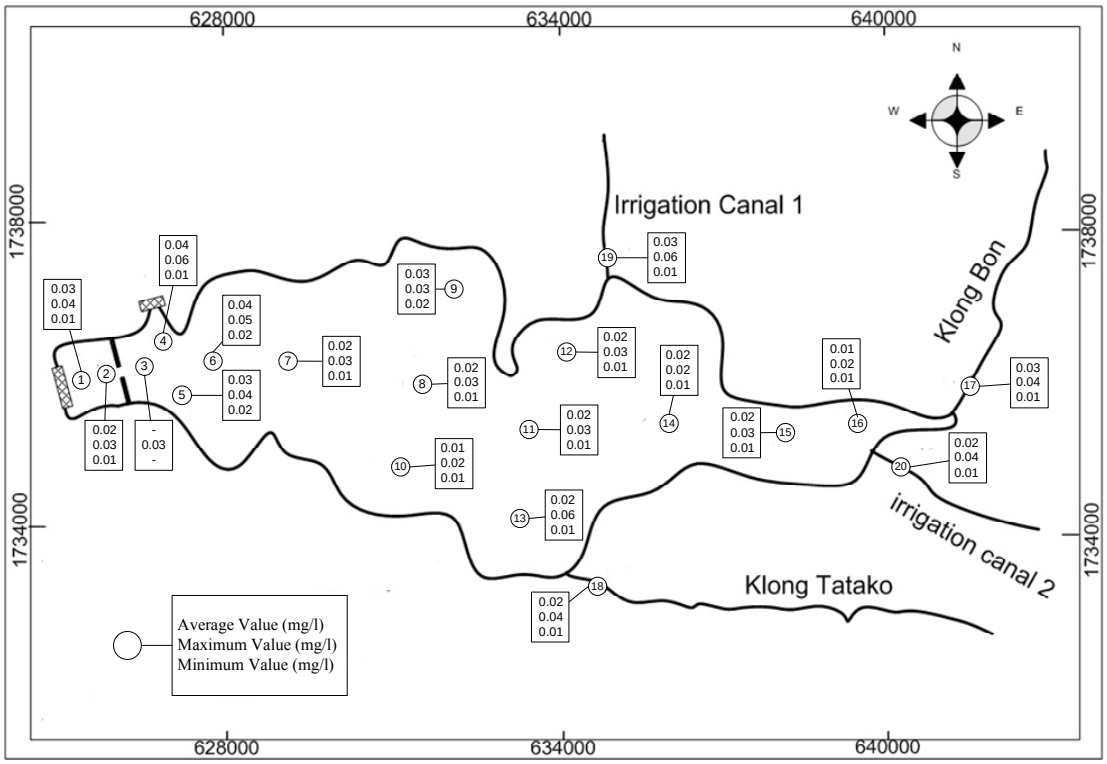

Figure 72 Spatial Variation of PO_4^{3-} concentration in Bung Boraphet and its tributaries

Temporal variation of PO_4^{3-} concentration in Bung Boraphet and its tributaries can also be plotted as shown in Figure 73. The patterns of PO_4^{3-} concentration are mostly similar to the patterns of TP concentration. Since the data points of TP and PO_4^{3-} concentrations as shown above are highly related and have similar patterns, every data point of TP and PO_4^{3-} concentrations at the same event and location are compared. The results show that PO_4^{3-} concentrations for 43 events at the same location have the average value of around 58.4% of the average value of TP concentrations with the range between 37.5% and 85.0 %.

Both nitrogen and phosphorus in different forms are considered as nutrients and both of them are related. The optimal TN/TP ratio for plants growth, known as the Redfield Ratio, is 16:1. Large differences from 16 at low TN/TP ratios can be an indication for potential nitrogen limitation and at high TN/TP ratios, potential phosphorus limitation of the primary production of plants. The observed TN and TP collected in the lake and tributaries at the same time and locations in this study for 40 data points show the average ratio of 41:1, which indicates potential phosphorus limitation of the primary production of plants. It can be concluded that Bung Boraphet and its tributaries potentially short of TP that is necessary for plant production. The situation of nutrients concentration in the lake and tributaries is still in the safe range for the well being of living organism and its environment.

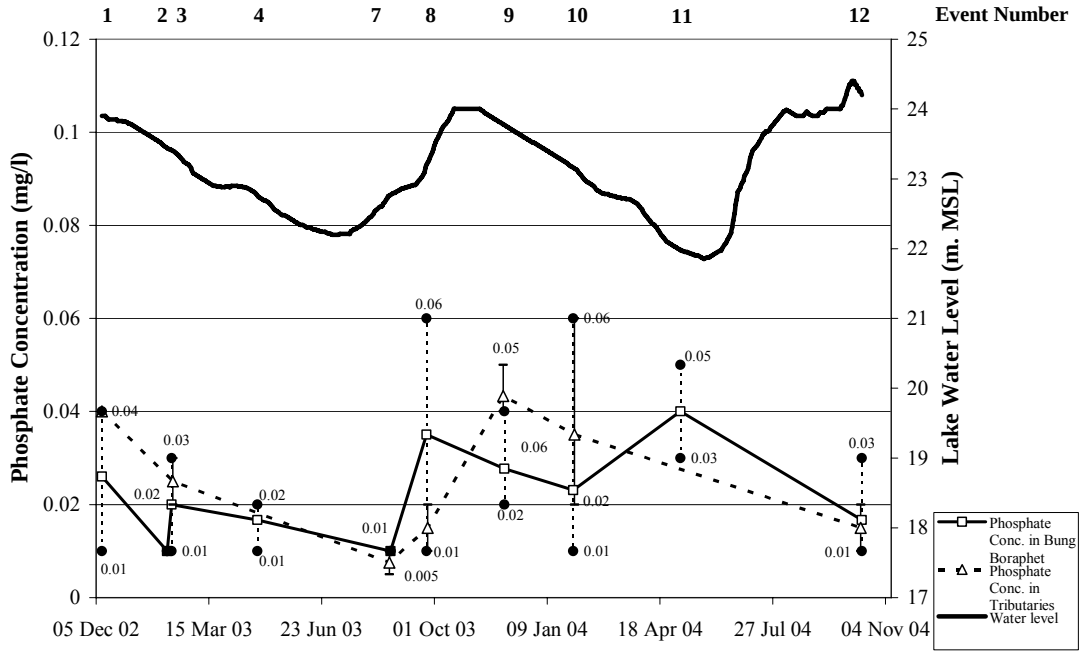

Figure 73 Temporal variation of PO_4^{3-} concentration in Bung Boraphet and its tributaries

4.1.4 Suspended Sediment (SS)

Spatial variation of SS concentration in Bung Boraphet and its tributaries is shown in Figure 74. In the figure, the average, the maximum, and the minimum SS concentration calculated for all events at each location are shown. It can be concluded that the average SS concentration in the lake are around 2.5 times of average SS concentration in its tributaries with the average values of around 18.40 and 44.79 mg/l, respectively. Ranges of the average SS concentration in the lake are between 10.06 and 50.38 mg/l, and in the tributaries are between 10.17 and 84.35 mg/l. The maximum SS concentrations in the lake are also lower in the lake than that of in the tributaries with the average values of around 42.28 and 168.95 mg/l, respectively. Ranges of the maximum SS concentration in the lake are between 5.20 and 134.50 mg/l, and in the tributaries are between 24.40 and 434.0 mg/l. Most of the maximum SS concentrations at the outlet of four tributaries are above 25 mg/l, which is the highest SS concentration value to be considered to be suitable for aquatic life

protection. More than half of the observed locations (9 out of 16 locations) in the lake also have the maximum SS concentration more than 25 mg/l. The maximum SS concentration that higher than 25 mg/l within the lake occurred close to location of the dredging operation carried out by the FD. Observed locations, that have the maximum SS concentrations higher than 25 mg/l, consist of the location numbers 1, 2, 3, 4, 5, 6, 7 and 9 with the maximum values of around 34, 91, 134, 117, 25, 91, 39, and 32 mg/l, respectively. The Figure 74 shows that these higher values of SS concentration mainly occurred around the areas between the weir and the middle part of the lake. It was suspected that dredging operation would have an effect on these higher SS concentrations.

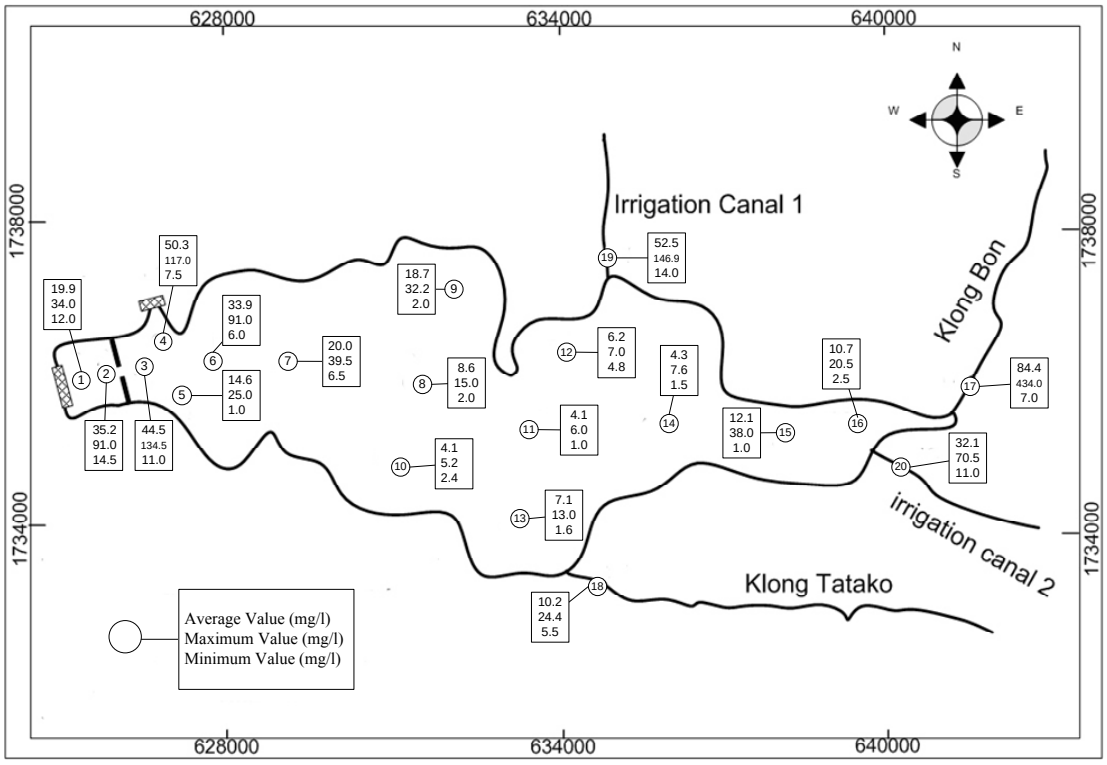

Figure 74 Spatial Variation of SS concentration in Bung Boraphet and its tributaries

Temporal variation of SS concentration in Bung Boraphet and its tributaries can also be plotted as shown in Figure 75. In the figure, the average, the maximum, and the minimum SS concentrations calculated for all locations at each event are identified. In the lake, there are 8 data points out of 12 data points that have

higher SS concentrations than that of in the tributaries. The reason that the average value of SS concentrations in the tributaries is higher than that of in the lake because the first event in December 2002 (after a large flood event) has very high SS concentration occurred in the tributaries with the maximum value of around 434 mg/l. This high value has a significant influence on the average SS concentration in the tributaries to be higher than the average SS concentration in the lake. This evidence shows that internal loads of SS concentration would have a significant affect on the overall SS concentration in the lake, especially the high values of SS concentration between the weir and the middle of the lake as mentioned earlier. This also confirms an assumption that a dredging operation would have a large affect on higher SS concentration in the lake. Special plot of temporal variation along the profile between the weir and another end of the lake was therefore plotted in Figure 76 to clearly see the changes. It obviously shows that at the location numbers 1, 2, 3, 6, and 7 have significant higher SS concentration for the average and the maximum values (average values of 31 and 78 mg/l, respectively) compared with the average and the maximum values (average values of 8 and 17 mg/l, respectively) at the location numbers 8, 11, 14, 15, and 16. With these data points show a high influence of dredging operation on SS concentrations in the lake to be a lot higher than that of in the tributaries, SS concentration happens to be one of the most influenced water quality parameters that have large affect on the lake sustainability.

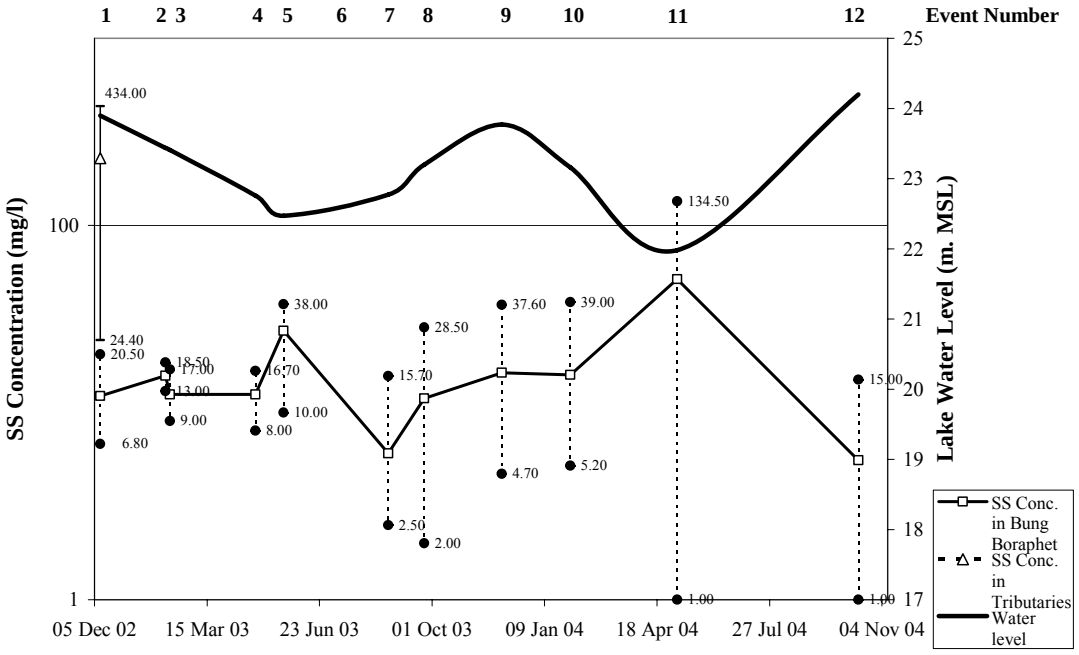

Figure 75 Temporal variation of SS concentration in Bung Boraphet and its tributaries

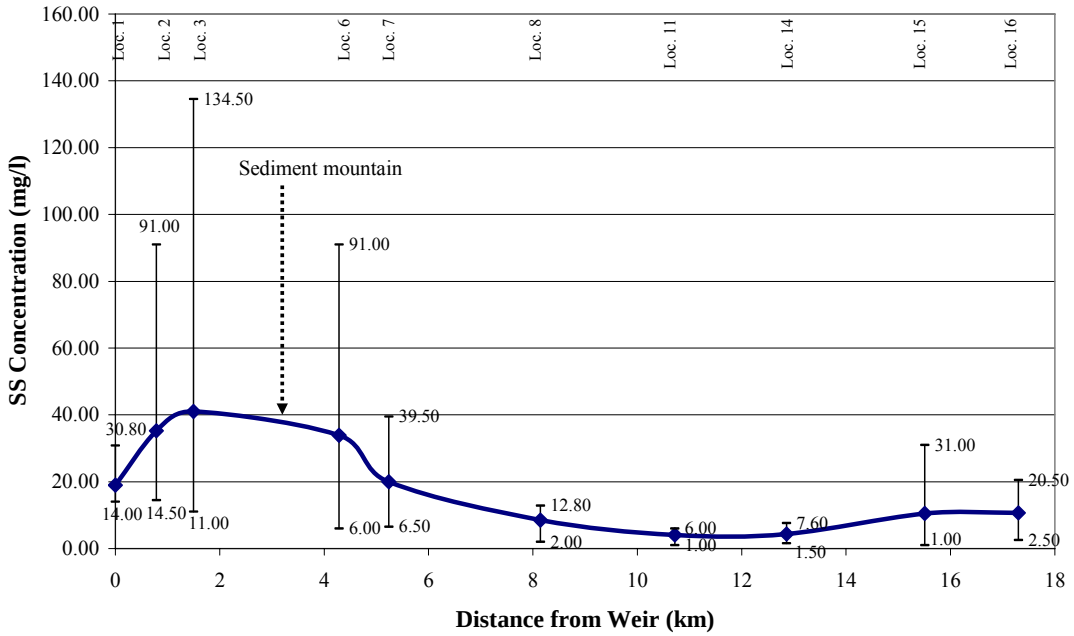

Figure 76 Temporal variation of SS concentration along the profile of the lake

In this study, turbidity and Secchi depth were also observed beside SS concentration. Relationships between these parameters are plotted. The Figure 77 shows the relationships between SS concentration and turbidity as the equation shown below.

$$y = 0.6066 \quad x^{1.21} \tag{42}$$

where

x = ss concentration (mg/l)

y = turbidity of water (NTU)

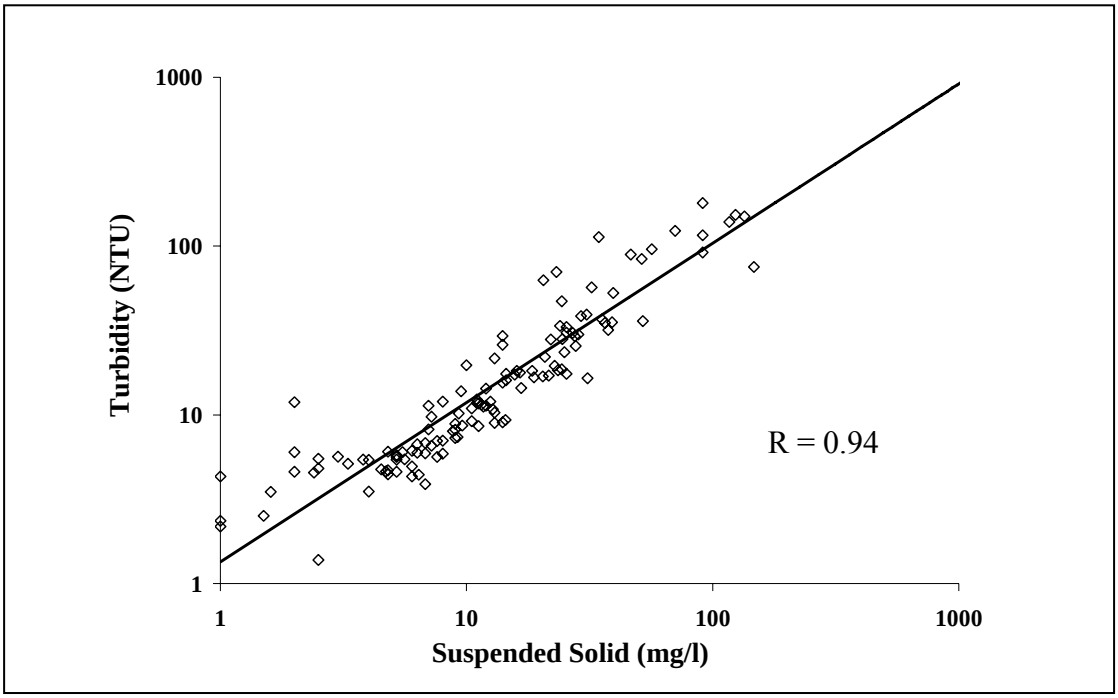

Figure 77 Relationships between SS concentration and turbidity

The Figure 78 shows the relationships between 1/Secchi depth and SS concentration as the equation shown below.

$$y = 34.285 \ln(x) + 5.1049 \quad (43)$$

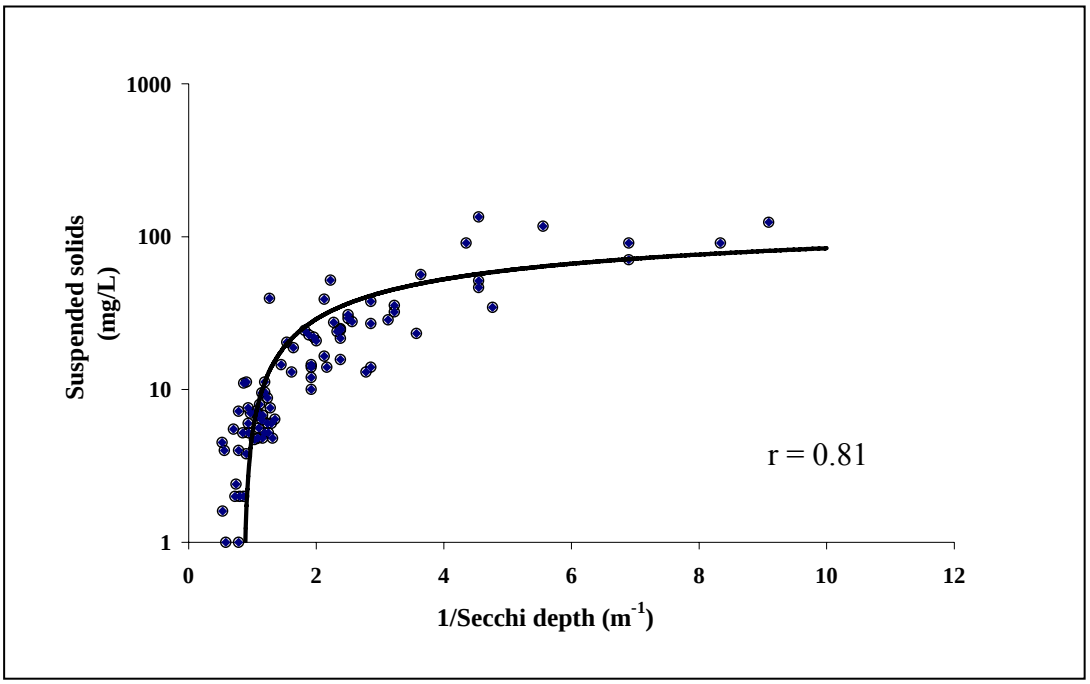

Figure 78 Relationships between 1/Secchi depth and SS concentration

The Figure 79 shows the relationships between 1/Secchi depth and turbidity as the equation shown below.

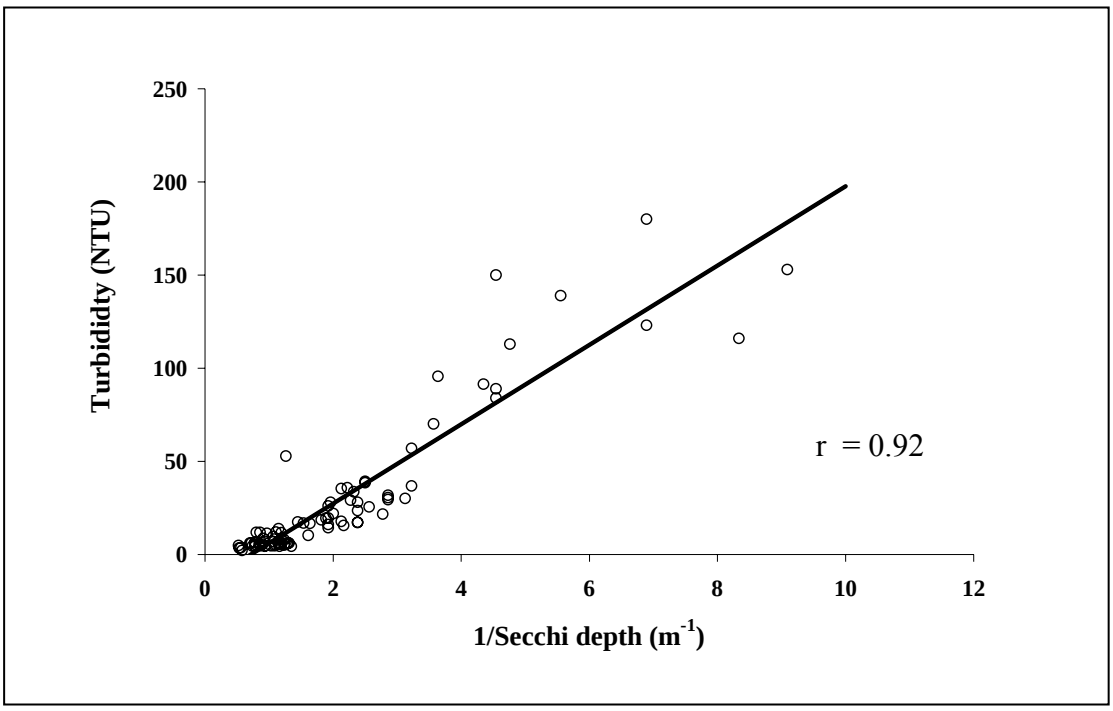

Figure 79 Relationships between 1/Secchi depth and turbidity

$$y = 21.299\ x - 15.28 \qquad (44)$$

where

x = 1/Secchi depth (m^{-1})

y = turbidity of water (NTU)

Relationships between these three parameters (turbidity, 1/Secchi depth, and SS concentration) have shown very well corresponding with very high statistical value of the correlation coefficient between 0.81 and 0.94. Since Secchi depth is the easiest water quality parameter to be measured and can be used to define SS concentration and turbidity of the lake and its tributaries, these equations can be later used to indicate light penetration that can be related to the suitability of the lake for living organism and its environment.

4.2 Results of water quality in Bung Boraphet using RMA2 and RMA11 models

As mention in the above section, sediment concentration happened to be only critical water quality parameter affecting the sustainability of the lake. The hydrodynamic model (RMA2) and the water quality model (RMA11) were then applied to identify the situation and to find the suitable control measures. To carry out these tasks, model calibration and model application for the RMA2 and RMA11 models are needed with the results of the study as shown in the followings.

4.2.1 Results of the RMA2 Model Calibration

In the process of model calibration for the hydrodynamic model (RMA2), the Manning's roughness coefficient and turbulence exchange coefficient, which are the model control parameters, have to be identified for the suitable values. This process can be carried out by comparing the results of flow velocities at different locations resulting from the model and the observed velocity data at the same location. The calibration process was carried out between 9th and 13th October 2004, when the lake water levels were above the weir crest and the water velocity values were high enough to be measured. To achieve the best fit between observed and calculated velocity values at different locations, model control parameters were then assigned with different values from one zone to another. Since there are four different physical characteristics that can be distinguished in the lake, model control parameters were therefore different at each zone. Roughness coefficient and turbulence exchange coefficient at each zone are concluded in Table 21.

Calculated and measured flow velocity at observation stations are shown in Figure 81. The correlation coefficient of all observation locations is 0.85. It can be seen from these results that calculated and measured flow velocities are acceptable with reasonable tendency.

Table 21 Roughness coefficient and turbulence exchange coefficient at each zone of the lake

Zone Number	Type	Manning's roughness	Turbulance coefficient (Pascal-sec)	
			x-direction	y-direction
1	Turbid Water	0.033	2000	2000
2	Open water	0.025	1800	1800
3	Lotus area	0.065	2500	2500
4	Flood plain	0.050	2400	2400

Note: Zone numbers are identified in Figure 80

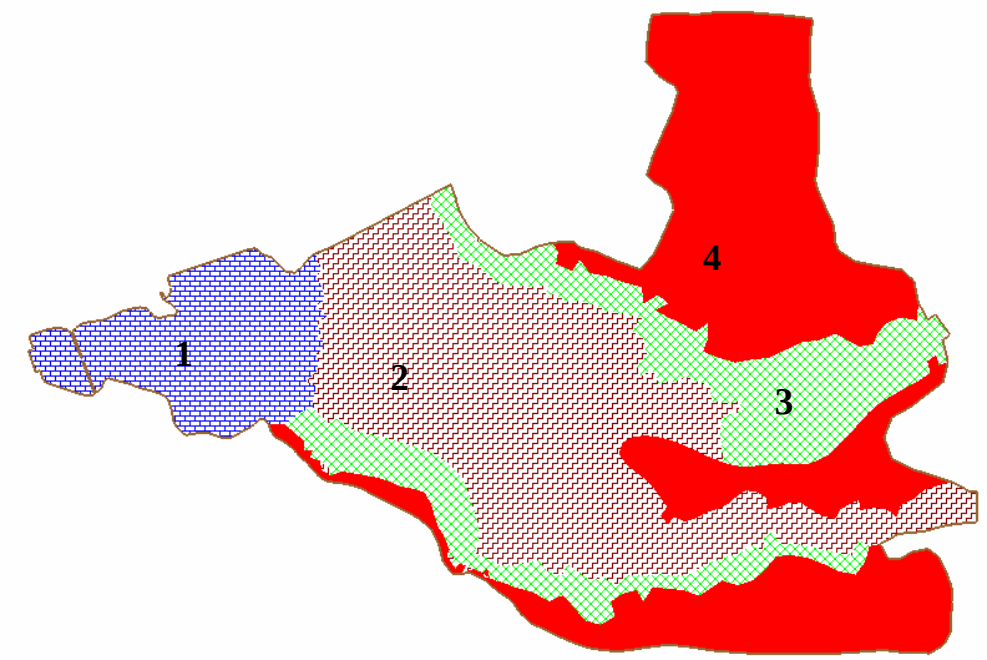

Figure 80 The category of finite element for the RMA2 Model calibration

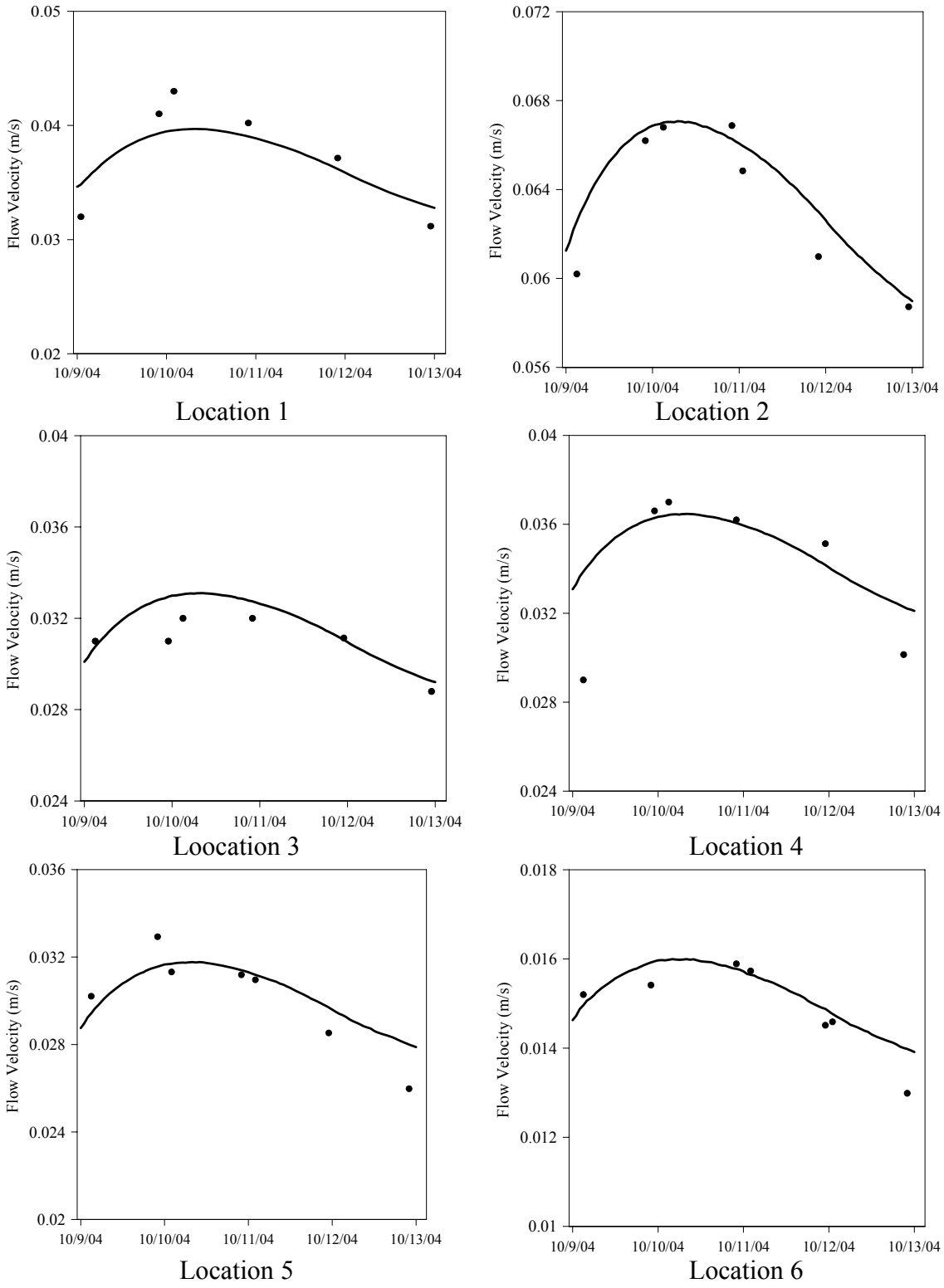

Figure 81 The comparison between the calculated and observed flow velocity

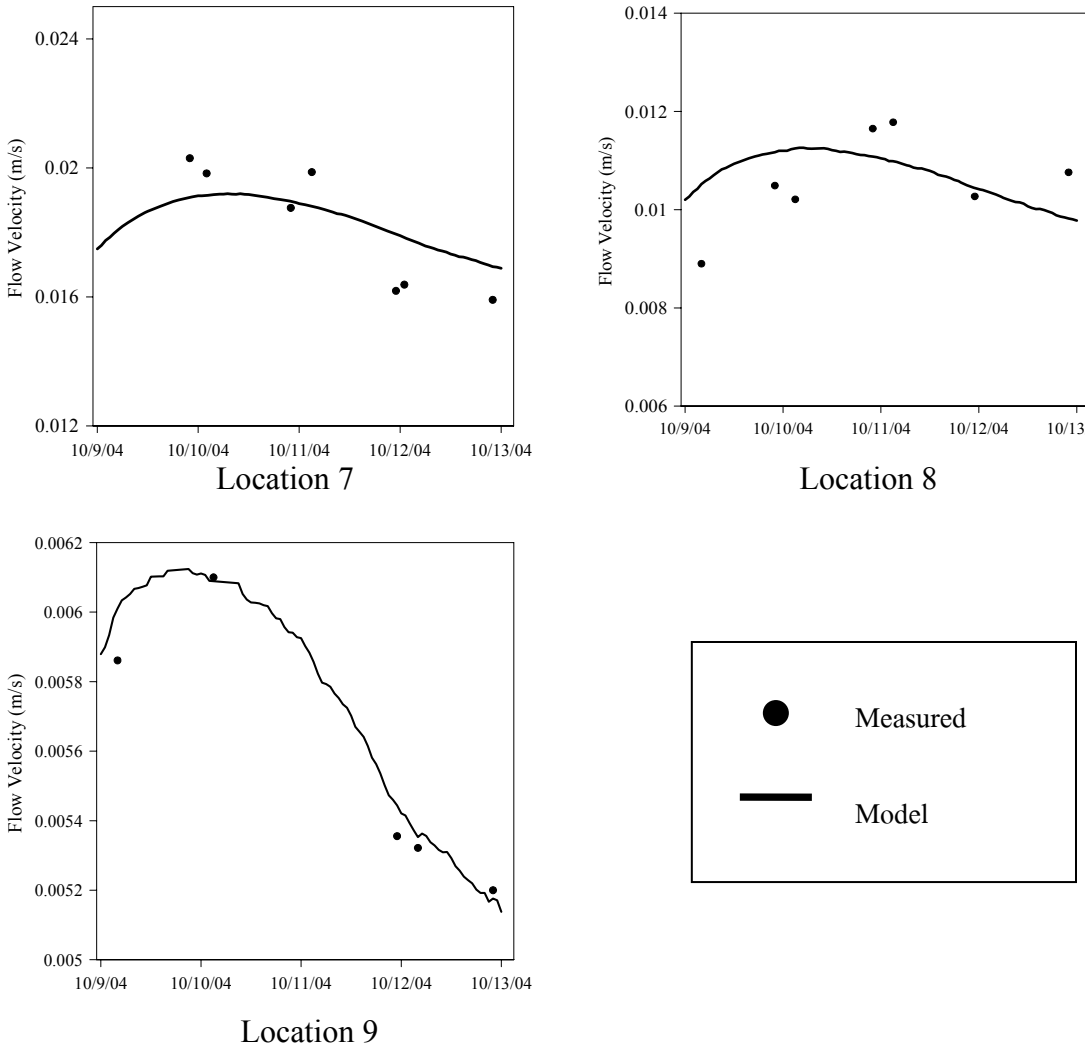

Figure 81 (Continued)

4.2.2 The results of the RMA2 Model Application

Since the RMA2 Model was calibrated by adjusting the control parameters and the results showed the best fit between observed and calculated flow velocities at the different locations in Bung Boraphet, it was then applied to evaluate the flow velocities and water depth between 10th February and 11th July 2003 for using as the in put data of the RMA11 Model. During this period, the lake water level was drawn down from +23.39 to 22.21 m (MSL) because of abstraction water from the tributaries and irrigation canals. The wet/dry checking algorithm provided in RMA2 was therefore applied to imitate the condition of wet/dry area of the model's

elemnts. According to wet/dry checking algorithm can limit the stability of the model (Stoscheck and Matheja, 2000), the boundary area was then re-generated by delineating along the contour line at +23.00 m (MSL) to reduce this unstable. The example of flow velocity vectors resulting of the RMA2 simulation during this period are shown Figure 82 and 83.

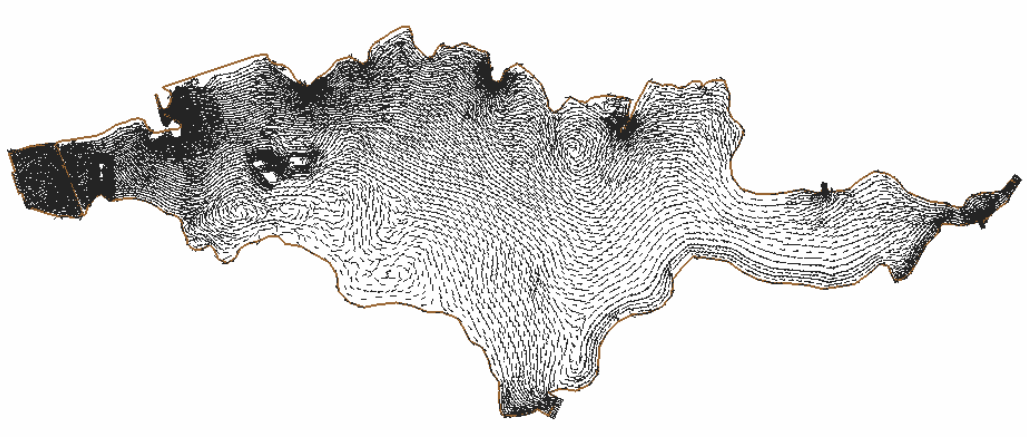

Figure 82 Flow velocity vectors resulting from RMA2 Model when the water level in Bung Boraphet was 23.39 m (MSL)

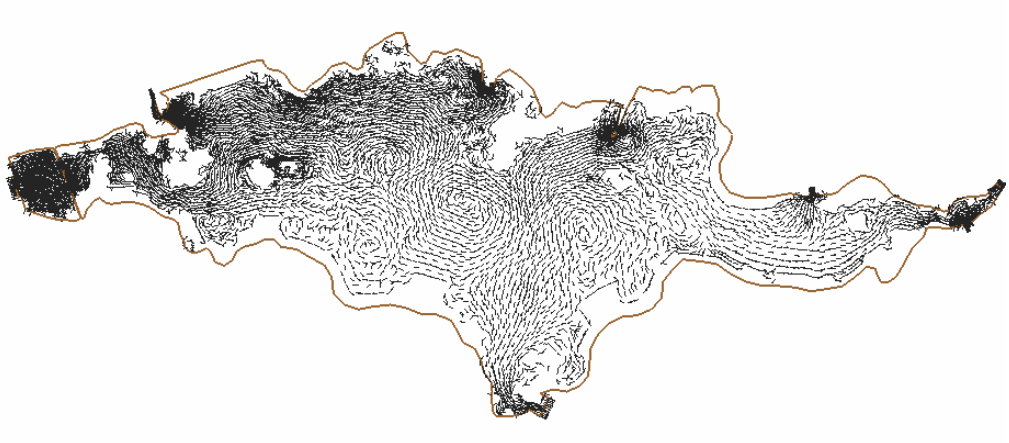

Figure 83 Flow velocity vectors resulting from RMA2 Model when the water level in Bung Boraphet was 22.21 m (MSL)

4.2.3 The results of the RMA11 Model Calibration

In the process of model calibration for the water quality model (RMA11), the model control parameters, which are dispersion coefficient, Von Karmanns constant, bed roughness height, critical shear stress for deposition of new layer, erosion rate constant for bottom layer, and setting velocity, have to be identified for the suitable values. This process can be carried out by comparing the results of SS concentration at different locations resulting from the model and the observed SS data at the same location.

The calibration process was carried out between 10th February and 11th July 2003, when the lake water levels were between 23.39 to 22.21 m (MSL). To achieve the best fit between observed and calculated SS concentration at different locations, dispersion coefficient were then assigned with different values from one zone to another. Since there are four different water quality characteristics that can be distinguished in the lake, model control parameters were therefore different at each zone. Dispersion coefficients at each zone are concluded in Table 22. While, the other control parameter values, which are showed in table 23, were assigned as only one value covering the entire element of the model.

Table 22 The dispersion coefficient for each element types

Zone Number	Type	Dispersion coefficient	
		x	Y
1	Turbid area	250	150
2	Clear water	200	200
3	Black water	200	180
4	Lotus area	250	200

Note: Zone numbers are identified in Figure 84

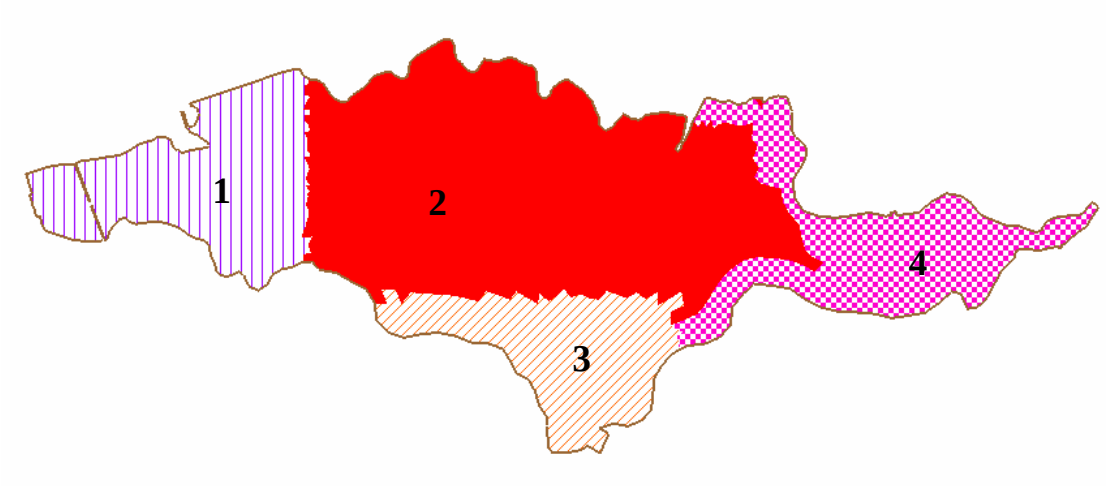

Figure 84 The category of finite element for the RMA11 Model calibration

Table 23 The value of control parameter used for SS calibration

Parameter Type	Parameter values	unit
Von Karmanns constant	0.5	-
bed roughness height	0.0031	m
critical shear stress for deposition of new layer	0.05	N/m^2
Erosion rate constant for bottom layer	0.0015	$Kg/(m^2.sec)$
setting velocity	1.8E-05	m/s
Critical shear stress for layer 1 (top layer)	0.08	N/m^2
Critical shear stress for layer 2 (bottom layer)	0.026	N/m^2

Furthermore, the properties of sediment, as shown in Table 24, including density of sediment material, bulk density of top and bottom layer were obtained from the study of AIT in 1982.

Table 24 The property of sediment in Bung Boraphet

Sediment Properties	Values (kg/m^3)
Density	2,355
Bulk density of top layer	1,025
Bulk density of bottom layer	563

Source: AIT (1982)

By using the trial and error method, an internal SS concentration originated from dredging operation was assigned as 276 mg/l/hr and occurred for eight hours on every working day during the calibration period. This SS concentration was applied at an element which represents the dredging location and was then converted to SS mass loading by multiplying with the volume of this element.

The comparisons between observed and calculated SS between the 11th of February 2002 and the 11th of July 2006 of observed location1, 8, 13 and 15 are shown in Figure 85-88. The goodness of fit between the observed and calculated SS were evaluated using three statistical measures which are the correlation coefficient. The correlation coefficient of all location is 0.79. It can be conclude that the calculated SS from RMA11 can be accepted and it can be used to evaluate the model's scenarios.

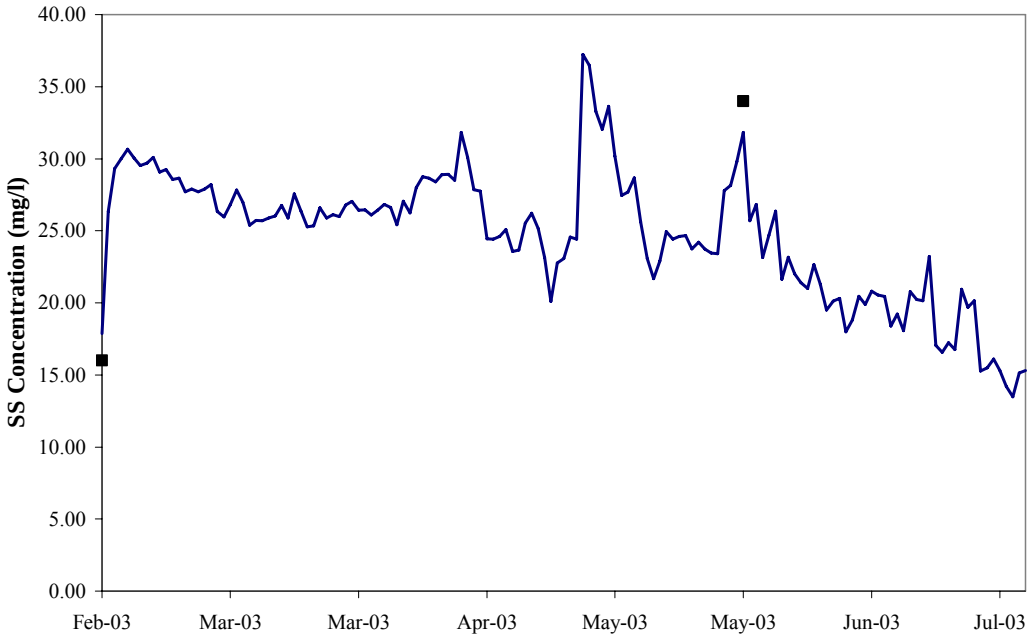

Figure 85 The comparisons between observed and calculated SS at location 1

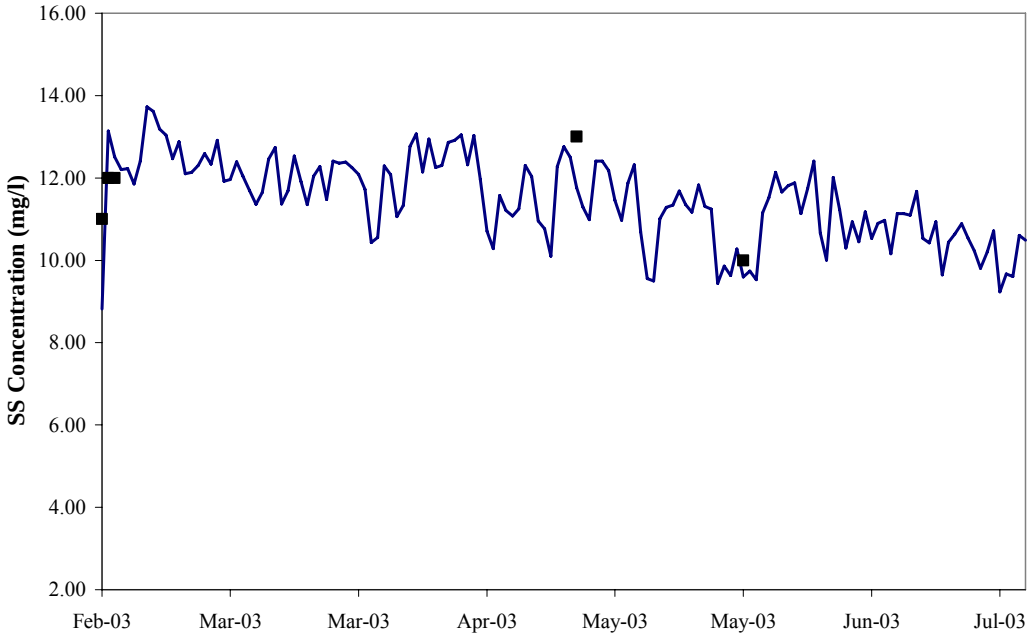

Figure 86 The comparisons between observed and calculated SS at location 8

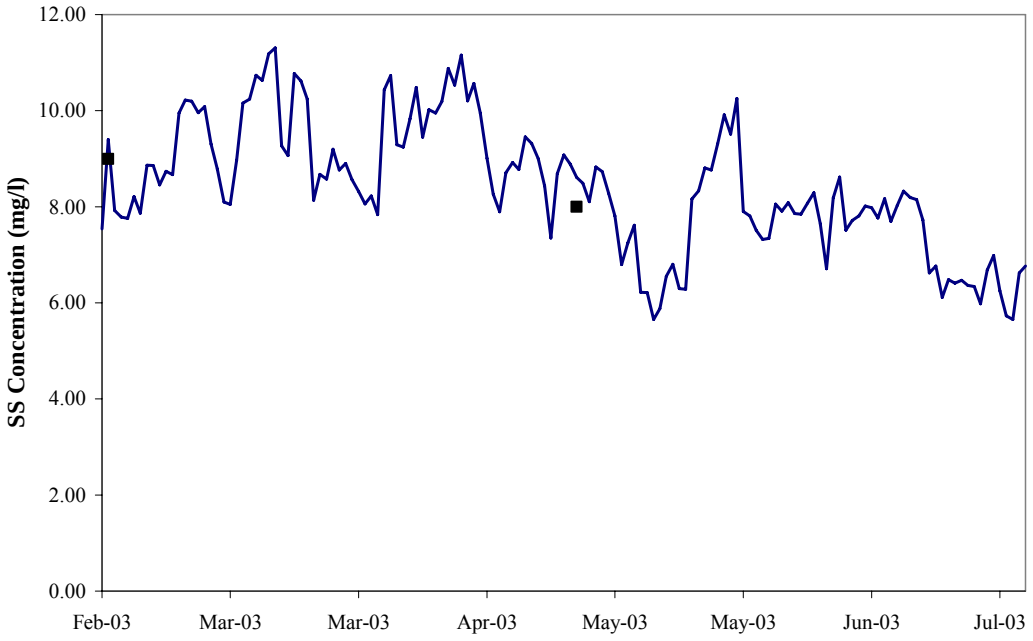

Figure 87 The comparisons between observed and calculated SS at location 13

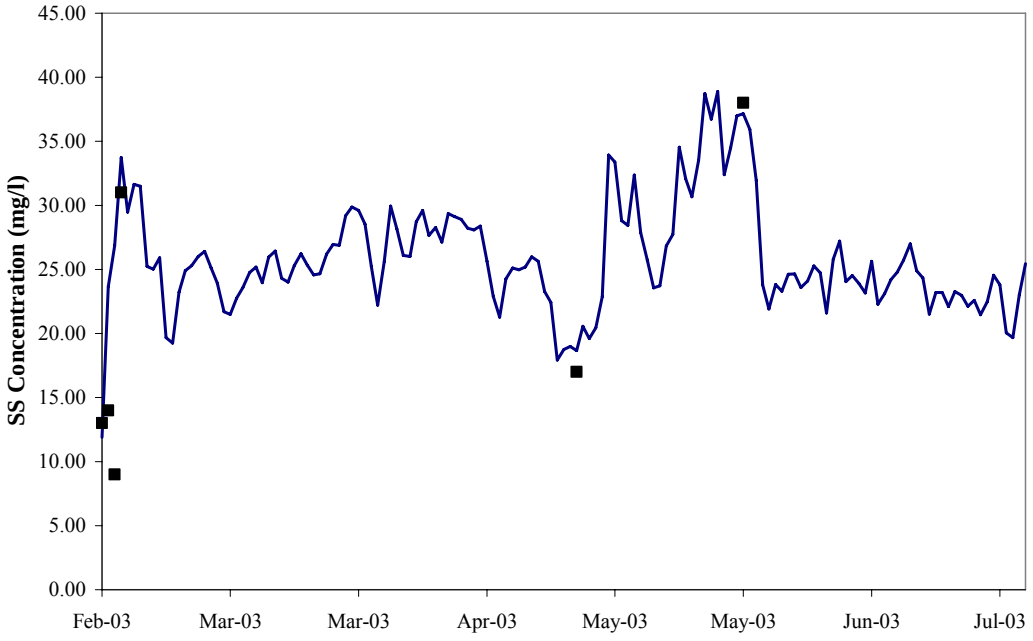

Figure 88 The comparisons between observed and calculated SS at location 15

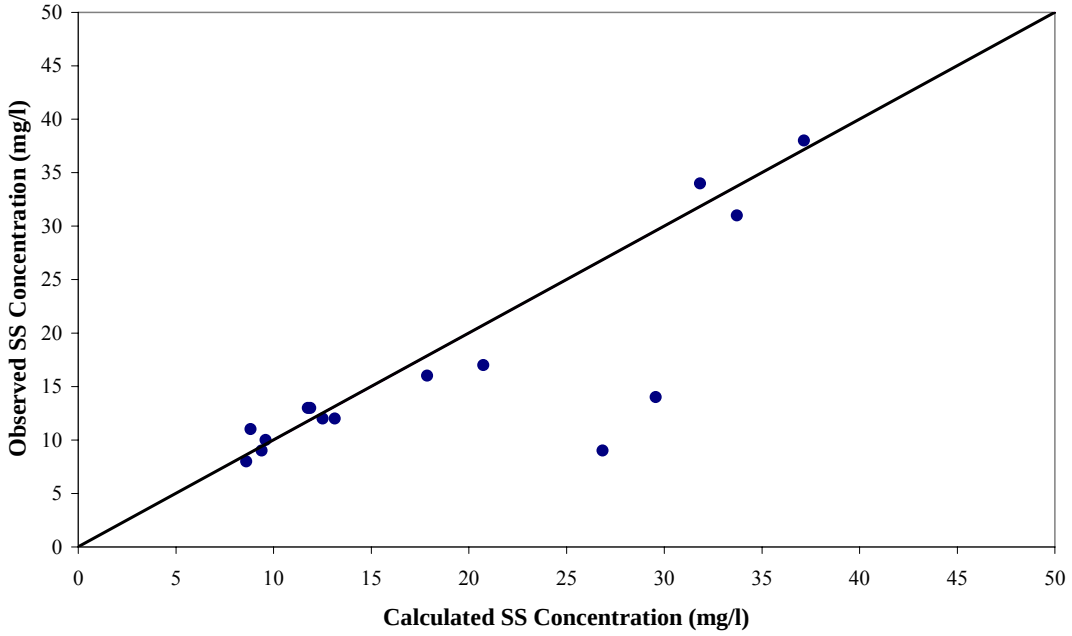

Figure 89 The comparison between calculated and observed SS for RMA11 calibration

4.2.4 The scenario of RMA11

For the RMA11 model scenario process, the input data and simulation period were also assigned as same as the calibration process. The RMA11 model was then used to analyze the changes of dredging operation in Bung Boraphet for 2 scenarios (Table 25 and Figure 90) in which increasing and reducing the SS concentration from the sediment mountain. The average value of SS concentration at the distance 0-0.5, 0.5-3, and more than 3 km away from the sediment mountain of each scenario were then compared.

Table 25 SS loading resulting from dredging operation for different scenarios

Scenario case	Percentage of SS loading compared with current situation	SS Concentation per day (mg/l/hr)
Current situation (Case0)	100	276
Case1	200	552
Case2	70	83

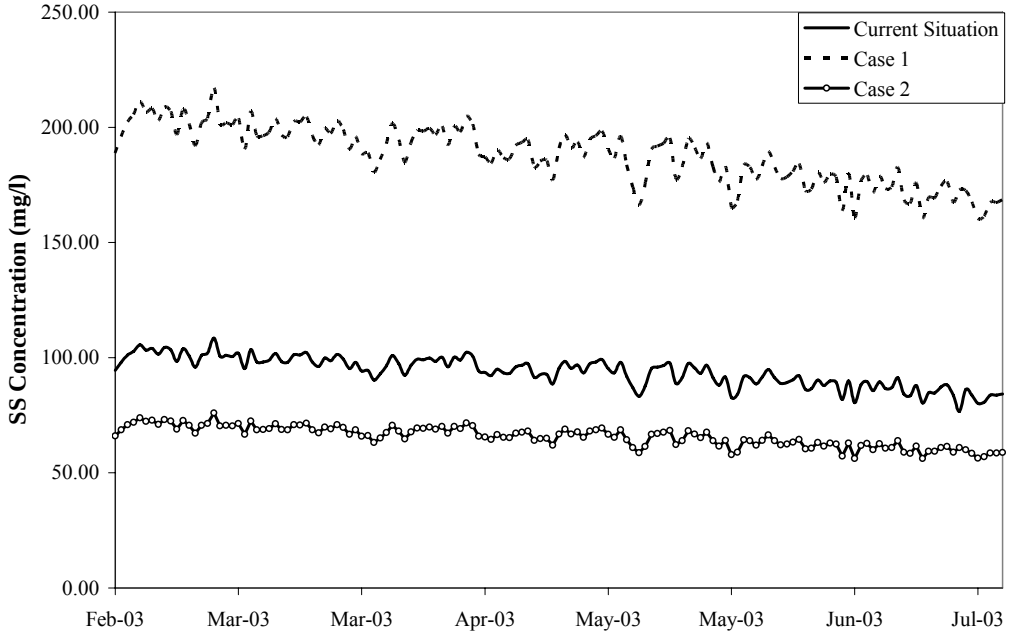

(a) 0-0.5 km

Figure 90 Scenario of average suspended sediment concentration for different distance away from Sediment mountain

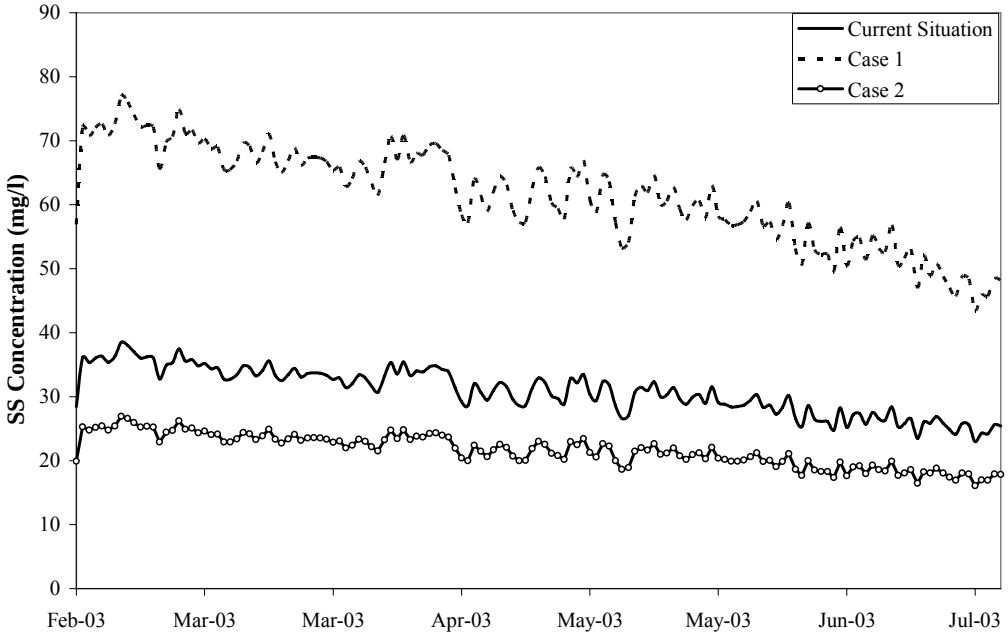

(b) 0.5 – 3.0 km

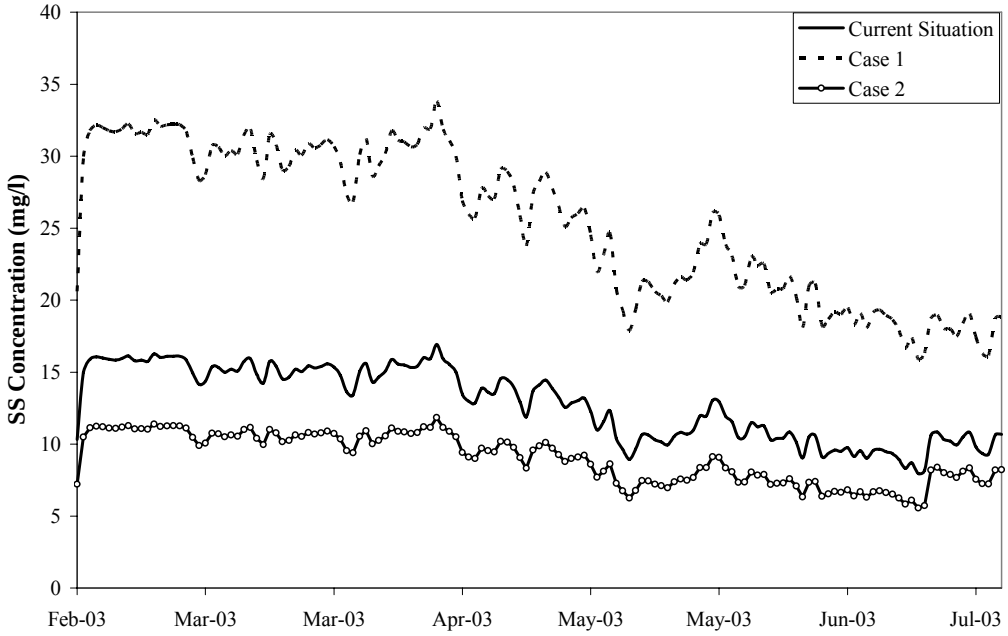

(c) More than 3 km

Figure 90 (Continued)

The results for the case of increasing sediment source by 100% showed that the value of SS concentration at the distance 0.5 and 3 km away from the sediment mountain for this period are 180.7 mg/l and 61.1 mg/l, respectively; while the average of SS outside the distance radius of 3 km away from the sediment mountain is 22.2 mg/l. By using the relationship between SS concentration and secchi depth as described in equation 43, It was found that an increasing of 100% in dredging operation would reduce the secchi depth which represents the light penetration by about 92, 59, and 24% of the current condition for distance 0.5, 3, and more than 3 km away from the sediment mountain, respectively. On the other hand, the results for the of deceasing sediment source by 30% showed that the average SS concentration at the distance 0.5 and 3 km away from the sediment mountain for this period are 63.2 mg/l and 19.1 mg/l, respectively; while the average of SS outside the distance radius of 3 km away from the sediment mountain is 10.1 mg/l. The reduction of 30% in dredging operation would increase light penetration by about 140, 41, and 8% of current condition for distance 0.5, 3, and more than 3 km away from the sediment mountain, respectively.

CONCLUSION AND RECOMMENDATION

Bung Boraphet is the largest feshwater wetland in Thailand. According to its significant biodiversity value, Bung Boraphet was therefore registered as an important international wetland for ecological system and biodiversity in 1999 (ONEP, 2002). However, natural resources of the lake are deteriorated dramatically by an increasing human exploitation of water resource. An understanding of the hydrologic budget components in the lake water budget would be useful to be used for managing the water resource of the lake more wisely. This dissertation was therefore investigated the daily water budget between December 2002 and May 2006. During that period, the calibration procedure for the daily water budget was carried out using the primary and secondary data which were continuously collected. The results showed that rainfall on the lake's water surface represented 28% of the total inflow on average. The runoff from the catchment was principally from the two main gauged catchment streams (Klong Tatako and Klong Bon). These delivered 49% and 20% of the average annual inflow, respectively. Although lake levels were consistently low and irrigation water was in high demand during the study period, the Nan River was only a minor source, representing less than 2% of the inflows. Evaporation and abstraction for irrigation were the two largest water loss terms, representing 42% and 55% of the average annual loss from the storage. Seepage represented less than 1% of the total discharge, whilst the discharges downstream through the weir and regulator were also minor terms during these low flood years (2002 -2006).

To demonstrate the value of the water budget analysis; it was therefore used to predict the lake water level during that period, with six different combinations of weir height, abstraction volumes, and diversion from Nan River (Scenario Analysis). These scenario results are compared with the current situation (Case 0; weir crest +24 m (MSL); daily abstraction set as 100%). In Cases 1-3, the weir crest is raised by 0.5 m. In Cases 0, 4 and 5, the weir level is unchanged but the abstraction rate is varied as a fixed percentage of the daily abstraction volume. If the weir crest had been 0.5m higher, and the abstraction rate is 65% of current (Case 2), the lake would have been

above the recommended level throughout. Abstraction at the current rate (Case 1), would have drawn the lake below the recommended level in 2 of the 4 years. A 20% increase in abstraction (Case 3) is similar to Case 1 but the drawdown in 2005 and 2006 is more extreme, matching the current situation (Case 0). When the weir height is not changed, an abstraction volume of only 38% of the current amount is needed to keep the lake above the recommended minimum level each year (Case 5). The worst case (Case 4) shows the impact of a 20% increase in abstraction with no increase in weir height. This produced a drawdown pattern similar to Case 0 in 3 of the 4 years, but in 2004 the drawdown is significantly lower and longer than Case 0. For Case 6, when the weir height and water abstraction are not changed, extra maximum flows of 132 MCM have to be diverted from the Nan River during the dry seasons in 2005 to maintain the recommended minimum level for fisheries. This activity would increase the water shortage problem that already exists downstream of the Nan River.

From the water budget analysis, it can be concluded that both proposals suggested by RID to raise the weir crest to increase the stored water volume and by DWR to divert extra flows from the Nan River during the dry seasons are not really practical. The measure of raising the weir crest would affect the overall environment of the lake, especially the biodiversity. Evaporation is an important loss factor in the water budget; so, increasing the stored volume by raising the height of the weir is an 'inefficient' way of storing water. Moreover, extra water volume (33 MCM) gained from increasing the weir crest would nearly be used up by increasing abstract water for rice farming of only 20%. The key point to solve the limited water resource of Bung Boraphet, which is under increasing pressure, is by limiting abstract water for their rice farming. Further falls in the minimum water level may cause irreparable damage to ecosystems and biodiversity.

Remote sensing technique was also applied in this dissertation to analyze the land use changes over time within and around the lake using the Landsat5 images between 1993 and 2003. These images were collected when the lake level was +23.00 m (MSL) for directly comparable and were then manipulated and interpreted for identifying physical feature in the study area. Results showed that the area of

irrigated rice surrounding the lake rose 100%, whilst the area of aquatic plants cover area (both submerged and emergent vegetation) declined by 50%. These evidences correspond to the results gained from the water balance and water quality studies.

In this dissertation, the filed data collections of eight observed water quality parameters (DO, BOD, TN, TKN, Nitrate, TP, Phosphate, and SS) were observed at 16 locations in Bung Boraphet, and at the outlet of four tributaries (Klong Bon, Klong Thatako, Irrigation Canal 1, and Irrigation Canal 2) for 12 events. Spatial and temporal variation of those parameters were plotted and were used to analyze the situation of those parameters that would affect the well being of flora and fauna living in the lake, as well as its environment. The results show that the concentrations of DO, BOD, and nutrients in the lake are in better condition than that of in the tributaries. All of the average values of DO and BOD are under the numbers recommended for fisheries. Even some of the maximum numbers are above the recommendation levels, their concentrations seem to be not persisted for a long time. It can be concluded that DO and BOD concentrations both in the lake and its tributaries are within acceptable levels. However, these concentrations still need awareness. For nutrients, since TP concentrations are a lot lower than the recommended level for preventing the algae bloom and lake's eutrophication, TN concentrations that are higher in some events cannot cause those effects (as explained by the Redfield ratio). The lake and its tributaries seem to be therefore affected only by the high concentration of SS that possibly affected by a dredging operation carried out by the FD as evidences shown earlier. SS concentration that tends to be increased requires the management control measures to keep the lake in a better environment for its biodiversity.

Since the analytical results showed that SS concentration is the critical parameter which has the effects on the water storages and biodiversity of the lake, profound investigations of suspended sediment was therefore needed. It can be carried out using the two dimensional depth averaged hydrodynamic and water quality models, which are the RMA2 and RMA11, respectively. In the calibration process of the RMA2 Model, the measured flow velocities between 9^{th} and 13^{th}

October 2004 were corresponded to the calculated flow velocities as shown by satisfied correlation coefficient of around 0.85. The control parameters resulting from model calibration are the roughness coefficient (the Manning's n) and the turbulence coefficient at each finite element mesh. The model results showed that the suitable Manning's n values were between 0.025 and 0.04; while the turbulence coefficient values were between 2500 and 3200 Pascal-sec. Control parameters resulting during the calibration period were then applied to the RMA2 Model for the flow event between 11th February and 11th July 2003. Flow velocities and flow depths at each mesh during that period were later input into the RMA11 Model for the model calibration. The calibration results of the RMA11 Model showed that the measured SS between 11th February and 11th July 2003 were corresponded to the calculated SS concentration as identified by quite satisfied correlation coefficient of around 0.79. The control parameter values resulting from model calibration consisting of: 1) the dispersion coefficients which are between 100 and 250 m^2/s, 2) the Von Karmans constant which is 0.5, 3) the bed roughness height which is 0.00031 m, 4) the critical shear stress for deposition which is 0.01 N/ m^2, 5) the erosion rate constant which is 0.0015 Kg/m/sec, and 6) the setting velocity which is 1.8E-05 m/s, and 7) the critical shear stress for layer top and bottom layers, which are 0.08 and 0.025 N/m^2, respectively.

The results of model calibration have shown that there are very high values of SS concentration within the radius close to the sediment mountain. The average values of SS concentration at the distances 0.5 and 3 km away from the sediment mountain for the calibration period are 93.9 and 30.8 mg/l, respectively; while the average value of SS outside the distance radius of 3 km away from the sediment mountain is 12.8 mg/l. It can be concluded that these high values around the sediment mountain were affected by dredging operation that has been carrying out by the FD for more than 25 years. To mitigate the consequences of dredging operation, these models were therefore used to find out the better ways for the management of dredging operation. In this study, the models were used to investigate changes of SS concentration affecting by increasing and reducing the sedimentation source from dredging operation by 100% and 30%, respectively. The results for the case of

increasing sediment source by 100% showed that the average values of SS concentration at the distances 0.5 and 3 km away from the sediment mountain for this period are 180.7 and 61.1 mg/l, respectively; while the average value of SS outside the distance radius of 3 km away from the sediment mountain is 22.2 mg/l. The results for the case of decreasing sediment source by 30% showed that the average SS concentration at the distances 0.5 and 3 km away from the sediment mountain for this period are 63.2 and 19.1 mg/l, respectively; while the average value of SS outside the distance radius of 3 km away from the sediment mountain is 10.1 mg/l. Since the FD had already proposed to have extra two boats to carry out more dredging in the lake, the first scenario of increasing 100% of sediment source would therefore possibly happen sooner or later. Once it really happens, light penetration especially within the first zone of fish conservation area (0.5-3.0 km away from the sediment mountain) would be reduced by 59%, therefore, the effects on biodiversity and finally on the sustainability of the lake would be so great. On the other hand, if dredging in the lake can be reduced by 30%, light penetration in this zone will be increase by 41%. Therefore, diversity of fish and plants in Bung Boraphet might be recovered.

The results carried out in this dissertation reveal that there are at least two main issues - an over-extraction of water for dry season rice and the sediment dredging operation - that need urgent policies from related government agencies and stakeholders to mitigate the consequences of mismanagement that would bring Bung Boraphet into its worst situation. The scientific tools and models investigated in this study were proved to be useful to identify the suitable operation and management of the lake. Different operation and management ideas can be explicitly reveal by easily applied the constructed daily water budget model, the RMA2 and RMA11 Models, together with the remote sensing technique. Closer collaboration between researchers, stakeholders including related government agencies, and visions of decision makers would be able to sustain the biodiversity of Bung Boraphet Wetland.

LITERATURE CITED

Chirananont, B. 1983. **Circulation of Depth-Average Flow in Open Channel**. M.S. Thesis, Asian Institute of Technology.

Chapra, S.C. and R. P. Canale. 2002. **Numerical Methods for Engineers**. McGraw-Hill Book Company, New York.

Chow,V.T. 1964. **Handbook of Applied Hydrology**. McGraw-Hill Book Company, New York.

Deas, M.L. 2003. **Assessment of Flow and Water Quality Alternatives in the Klamath River**. Available Source: http//www. my.engr.ucdavis.edu/~wreng/klamath.html, Auguest 23, 2003.

Department of Water Resources. 2006. **A Feasibility Study, Survey, and Design of the Water Network for Bung Boraphet, Nakhon Sawan Province**. Draft Final Rep.

Falcorner, R.A. and B.,Lin. 1997. Three-Dimesional Modelling of Water Quality in the Humber Esutary. **Water Research**. 31: 1092-1102.

Finnie John, Barbara Donnell, Joe Letter, and Robert S. Bernard4. 1999. Secondary Flow Correction for Depth-Average Flow Calculations. **Journal of Engineering Mechanics**. 125: 256-262.

Nakornsawan Inland Fisheries Development Center. 2001. **The Survey of Fish Population in Bung Boraphet.** Annual Rep. 2000.

Nakorn Sawan Inland Fisheries Development Center. 2005. **The Survey of Fish Population in Bung Boraphet**. Annual Rep. 2004.

King, I.P. 1996. **RMA11 –A Three Dimensional Finite Element Model for Water Quality in Estuaries and Streams Version 2.4.**, User manual.

Hansen, W. 1962. Hydrodynamic Methods Applied to Oceanographic Problems. **Proceedings of the Symposium on Mathematical-Hydrodynamical Methods of Physical Oceanography**. University Hamburg, Hamburg, West Germany.

Krause, P., D. P Boyle, and F. Base. 2005. Comparison of different efficiency criteria for hydrological model assessment. **Advances in Geosciences.** 5: 89–97.

Lance, F. and W. Lesack. 1995. Seepage exchange in an Amazon floodplain lake. **Limnol Oceanogr**. 40(3): 598-609.

Leendertse, J.J. 1967. **Aspects of a Computational Model for Long Period Water-Wave Propagation, California.** The Rand Corporation.

Liengcharernsit, W., 1979. **Mathematical Models for Hydrodynamic Circulation and Dispersions of Selected Water Quality Constituents with Applications to the Upper of Thailand**. D. Eng Thesis, Asian Institute of Technology.

Lillesand, T.M and R.W., Kiefer. 2000. **Remote Sensing and Image Interpretation.** 4th ed John Wiley & Sons, New York.

Madsen, H. 2000. Automatic Calibration and Uncertainty Assessment in Rainfall-Runoff Modelling. **Joint Conference on Water Resources Engineering and Water Resources Planning & Management**. Hyatt Agency Mineapolis, USA.

Mutreja, K.N. 1986. **Applied Hydrology**. 3rd ed. Tata McG raw-Hill, New Delhi.

Nash, J.E. and J.V. Sutcliffe. 1970. River flow forecasting through conceptual models, part 1 – A discussion of principles. **Journal of Hydrology**, 10: 282-290.

National Park, Wildlife, and Plants Conservation Department. 2005. **Survey of Wildlife in Bung Boraphet**. Annual Research Rep. 2004.

Office of National Economic and Social Development Board. 1983. **The Re-Habitation and Development of Bung Boraped.** Final Report.

Office of Natural Resources and Environmental Policy and Planning. 2002. **The Biodiversity in Bung Boraphet Wetland.** Final Report.

Pinthong, K. 1998. T**he Development of Mathematical Model for Predicting the Distribution of Salinity and Water Quality Parameter in Shallow Lake with Tidal Inlets**. M.S.Thesis, King Mongkut's University of Technology Thonburi.

Ponce, V.M. and S.S. Yabusaki. 1981. Modelling Circulation in Depth-Average Flow. **Journal of the Hydraulics Division ASCE**. 107: 1501-1507.

Popitak, K. 1970. **The Study of Consuming Deposition of Important Fish Species in Bung Boraphet by Investigation the Composition of Food in Fish's Stomach.** Annual Rep. 1969.

Promprot, V. 1983. **Studies on Plankton Composition and Water Qualities in Bung Boraped Reservoir, Nakorn Sawan Province**. M.S.Thesis, Kasetsart University.

Royal Irrigation Department. 2003. **The Study of Bung Boraphet Development Project.** Final Report.

Srithongsom, S. 2003. **Study of Two Dimensional Depth Averaged Hydrodynamic and Water Quality Model for the Case Study of Bung Boraped.** M.S.Thesis, Kasetsart University.

Stoschek O. and Matheja A. 2000. Sensitivity Analysis of Numerical Solving Techniques for Modeling Sediment Transport under Tidal Conditions. **4th Int. Conf. on Hydroinformatics**. Iowa City, USA.

Nakorn Sawan Meteorological Office. 2001. **Summary of Recorded Climate Data of Nakorn Sawan Province between 1981-2000.** Annual Rep. 2000

US Army Crop of Engineer. 1997. **User Guide to RMA2 WES Version 1997**.

APPENDIX